

Evaluating alternative routes of using algal biomass for energy production

Xinyu Wei

A thesis submitted in partial fulfilment
of the requirements for the degree of

Doctor of Philosophy

in

Biochemical Engineering

The Advanced Centre for Biochemical Engineering
Department of Biochemical Engineering
University College London

2020

Declaration

I, Xinyu Wei, confirm that the work presented in this thesis is my own. Where information has been derived from other sources, I confirm that this has been indicated in the thesis.

Signature: _____

Date: _____

Acknowledgement

First and foremost, and without reservation, I would like to express my sincerest gratitude to my parents for their unwavering support, genuine encouragement and boundless love. Thank you for believing in me and being patient with me.

Equally, I would like to express my sincere gratitude to my supervisors, Dr. Frank Baganz and Dr. Paul Hellier, for their guidance and support during the past four years. To Dr. Baganz, I am forever indebted for this opportunity to pursue a PhD degree at UCL. It is also with his selfless guidance in the project and all the time and effort he put in every meeting and thesis correction that I have managed to pull through the process. To Dr Hellier, I have the utmost respect for his patience, technical expertise, practical assistance and wise support in the mechanical field. I have learnt so much from his detailed instructions and scientific advice and I am very grateful for his efforts in manuscript preparation and thesis correction.

I would also like to express my deep appreciation to Dr. Gareth Mannall, Dr. Mike Sulu and Dr. Brian O'Sullivan and thank them for their generous help and technical support in ACBE. I am grateful to other departmental members and staff who helped me overcome so many difficulties during the research. Special thanks to my cousin Bingying Han and his colleague Prof. Yajun Li for providing material for my research.

Finally, my joy knows no bounds in extending my thanks to all my friends for their endless love and affection allowing me to keep an optimistic attitude in my research life.

Publication

Wei, X., P. Hellier and F. Baganz, *Impact on performance and emissions of the aspiration of algal biomass suspensions in the intake air of a direct injection diesel engine*. Energy Conversion and Management, 2020. 205: p. 112347.

Abstract

Biomass is an excellent renewable energy source for alleviating the energy crisis and reducing the GHG emissions from the combustion of fossil fuels. Since the microalgae can accumulate lipids in the cell, the concept of using algal biomass for biodiesel production has attracted significant attention in recent years. The advantages of using microalgae as a biofuel source are that these organisms have a high growth rate, high lipid content and low requirement for nutrition compared to oil-producing plants. The most important property is that they can absorb CO₂ from the atmosphere thus contributing to an overall reduction of GHG emissions. The existing downstream processes of biodiesel production are complex and costly, which makes the product not compatible with other bioenergy sources. Therefore, it is important to develop alternative routes of utilising algal biomass for energy production.

This study mainly developed a novel method to deliver algal biomass through the air intake into a diesel engine for energy production and evaluated the environmental impact of the processes. A correlation between engine work produced during aspiration and combustion of algae biomass suspension was found. At constant flowrate and greater than 5% of biomass concentrations, a contribution to energy release during combustion from the aspirated algae could be observed. However, the aspiration of low concentration biomass suspension produced a negative impact on engine performance relative to water-only aspiration. From the perspective of the impact on the environment, the increase of biomass concentration and aspiration flowrates in the life cycle impact assessment of the whole process show a proportional increase in GWP, NO_x and water consumption. Contribution analysis indicates that changing the biomass concentration has a greater impact on the environment than changing the aspiration

flowrate and the proportion of total impact of the DSP steps increase with the increase of biomass concentration. Moreover, as an alternative way of using algae/diesel emulsion for energy generation, the results of the investigation on stability and viscosity of algae/diesel emulsion show the maximum stable time is 8.5 hours with the relative low viscosity of 49.9 mPa·s. However, the engine test of the stable emulsion was not successful due to the injector failure caused by phase separation of the emulsion under high pressure in the modern diesel engine.

Overall, these findings demonstrate the feasibility of utilising the energy content of algal biomass in combustion without lipid extraction, with added benefits of reducing NO_x emissions. It therefore gives a foundation for further exploration and development of algal biomass-derived bioenergy production.

Impact statement

This research has demonstrated and proved the feasibility of utilising microalgal biomass directly in a diesel engine for energy production. It serves as a solid foundation of using algal biomass as a potential energy source without complete dewatering and the additional steps of the biodiesel production process. It is not only benefiting the field of algal biofuel production, but also in the industrial sphere to have a new approach of energy production from microalgae.

In academia, this is the first study to demonstrate the possibility of delivering algal biomass directly to a diesel engine for energy production to date. This approach has been presented on the international stage at the Algal Biomass, Biofuels & Bioproducts 2019 conference. The work presented in Chapter 2 of this thesis has been published as a research paper in the Energy Conversion and Management Journal. Besides, the concept of using water/diesel and algae/diesel emulsions for alternative engine fuel has attracted more attention in recent years. To alleviate the energy crisis and reduce negative impact of fossil fuel combustion, future research can be designed and carried out to explore the suitable utilisation method of algal/diesel emulsions for energy production.

The findings of this research in the aspiration of algal biomass at optimum concentration results in the increasing of the engine output and the reduction of total environmental impact relative to small scale of algal biodiesel production. It could have potential benefits for the industrial plant. The microalgae can be cultivated for wastewater treatment, where the produced algal biomass have value for energy production. Therefore, with the positive results in this work, it has potential to create an industrial symbiosis and circular economy between two industries, where the algae cultivated in the wastewater from one plant is then used

to generate energy to support other industrial facilities. This model will firstly avoid costly and complexity of the downstream process for algal biodiesel production; secondly relatively reduce the environmental impact for both of the industrial processes.

In general, further development is essential before the new process can be used in reality; however, this work has indicated a solid foundation.

Table of content

Declaration	2
Acknowledgement.....	3
Publication	4
Abstract	5
Impact statement	7
Table of content.....	9
List of tables.....	13
List of figures	15
Abbreviations and nomenclature.....	20
Chapter 1 Introduction	22
1.1 Context of the research.....	22
1.2 Algal Biomass Production	24
1.2.1 Algae strains.....	24
1.2.2 Cultivation type.....	25
1.2.3 Cultivation systems	27
1.2.4 Cultivation conditions	33
1.3 Biomass harvesting techniques	36
1.3.1 Centrifugation	36
1.3.2 Flocculation.....	36
1.3.3 Flotation	37
1.3.4 Filtration.....	38
1.3.5 Electricity assisted techniques	38
1.4 Biodiesel production process	39
1.4.1 Microalgal cell disruption methods.....	39

1.4.2 Lipid extraction	42
1.4.3 Transesterification.....	44
1.5 Challenges and prospects for the commercialisation of algal biofuels ...	45
1.6 Diesel engine	46
1.6.1 Operation of diesel engine	47
1.6.2 Direct injection fuel system	48
1.6.3 Exhaust emissions from diesel engines.....	49
1.7 Research aims and objectives.....	52
Chapter 2 Aspiration of algal biomass suspensions in the intake air of a direct injection diesel engine.....	53
2.1 Introduction	53
2.2 Experimental Methods	57
2.2.1 Preparation of algal biomass slurry.....	57
2.2.2 Apparatus	57
2.2.3 Experimental conditions.....	60
2.3 Results and Discussion.....	62
2.3.1 Effects of algal biomass concentration in aspirated suspensions on combustion and emissions	62
2.3.2 Effects of algal biomass injection flowrates in aspirated suspensions on combustion and emissions	71
2.4 Conclusion	81
Chapter 3 Algae biomass production and development of algae/diesel emulsion	83
3.1 Introduction	83

3.1.1 Water/oil emulsions	83
3.1.2 Algae/diesel emulsion	86
3.2 Material and methods	87
3.2.1 Algae characteristic and cultivation	87
3.2.2 Algal biomass harvesting and determination of biomass.....	90
3.2.3 Preparation of algae/diesel emulsion	94
3.2.4 Combustion of algae/diesel emulsion	96
3.3 Results and discussion	98
3.3.1 Biomass production of <i>C. sorokiniana</i>	98
3.3.2 Characterisation of <i>C. sorokiniana</i>	100
3.3.3 Preparation of stable algae/diesel emulsion	103
3.3.4 Combustion of algae/diesel emulsion	116
3.4 Conclusion	118
Chapter 4 Life Cycle Assessment	120
4.1 Introduction	120
4.2 Goals and scoping	122
4.2.1 Impact assessment method.....	122
4.2.2 System boundaries	123
4.2.3 System description	123
4.3 Data sources	125
4.3.1 Dry algal biomass powder production data.....	125
4.3.2 Combustion and exhaust emissions data.....	126
4.4 Life cycle inventory	128

4.5 Life cycle impact assessment and discussion.....	132
4.5.1 Scenario with varying biomass concentrations	132
4.5.2 Scenario with varying biomass aspiration flowrate	135
4.6 Conclusion	138
Chapter 5 Conclusion and future work	140
5.1 General conclusion.....	140
5.2 Future work	144
5.2.1 Short-term experiments	144
5.2.2 Long-term prospect	145
Reference.....	147
Appendix A	158
A.1 Evaluation of algal growth	158
A.2 Determination of lipid production.....	159
Appendix B	160
B.1 Assumptions for the LCA study	160
B.2 Calculations and data in combustion process	162
B.2.1 Calculations of injection flowrate of fossil diesel	162
B.2.2 Calculations of the power out from the combustion process	163
B.3 Adjustment of exhaust emissions data from combustion process	164
B.3.1 The combustion equation:	164
B.3.2 Balancing the atoms in the combustion equation	164
B.3.3 Calculation of the molar fraction of atoms	165
Appendix C	169

List of tables

Table 2.1 Engine specification.....	59
Table 2.2 Summary of the engine test conditions.....	60
Table 3.1 Physiochemical properties of Span 80, Tween 80, Triton x-100 surfactant.....	85
Table 3.2 Basic medium composition of TAP, 10%N TAP medium and TAP + Glucose medium.....	88
Table 3.3 Dilution rate for growth standard curve.....	91
Table 3.4 Dilution made for triolein standard curve.....	93
Table 3.5 Specific growth rate, cell doubling time and maximum biomass concentration of biomass cultured in TAP and 10% N TAP and TAP + glucose medium.....	99
Table 3.6 Percentage of the elemental composition in <i>C. sorokiniana</i>	102
Table 3.7 Higher and lower heating value of algal biomass cultured in TAP, 10% TAP and TAP+ glucose medium.....	102
Table 3.8 Optimization of the ratio of each chemical composition in the surfactant mixture Yellow: surfactant mixtures tested; Green: Surfactant mixtures formed stable emulsions after 24 hours settling.....	106
Table 3.9 Stability of algae/diesel emulsions with 2% (v/v) of Triton X-100...	110
Table 3.10 Viscosity of W/O and algae/diesel emulsions with 20% and 30% of water content and 2% of Triton X-100.....	111
Table 3.11 The viscosity of emulsions containing 30% water and 2.5% algae and 2% surfactant Triton X-100.....	113
Table 4.1 Impact categories considered in the analysis.....	123
Table 4.2 Input data of algae culture broth and biomass concentration.....	125
Table 4.3 Properties of dry algae powder.....	126

Table 4.4 Specifications of fossil diesel with no FAME content.....	126
Table 4.5 Injection duration and flowrate of fossil diesel in combustion tests..	127
Table 4.6 Data input of air exhaust gases in the aspiration combustion process.	127
Table 4.7 Life cycle inventory data.....	129
Table B.1 General assumptions.	160
Table B.2 Molar mass of elements.....	161
Table B.3 Injection duration and injection flowrate of fossil diesel for the reference diesel only condition.	162
Table B.4 IMEP measured in the combustion process.	163
Table B.5 Original exhaust emission data on a dry basis.	167
Table B.6 Adjusted exhaust emission data on a wet basis.	168

List of figures

Figure 1.1 (a) Schematic diagram of a raceway pond (Chisti, 2007); (b) Outdoor algae raceway pond systems (EERE, 2019).....	28
Figure 1.2 A design and picture of horizontal tubular photobioreactor (Singh et al., 2012).	30
Figure 1.3 Schematic diagram for (A) airlift photobioreactor and (B) bubble column photobioreactor (Krichnavaruk et al., 2005).	31
Figure 1.4 (a) Schematic diagram of a stirred tank photobioreactor (Concas et al., 2012); (b) a picture of a stirred tank photobioreactor with external lighting (ReskiLab, 2019).....	32
Figure 1.5 (a) Schematic diagram of a flat panel photobioreactor (Singh and Sharma, 2012); a picture of flat panel photobioreactors (Entwistle, 2015).	33
Figure 1.6 Direct injection system (DieselHub, 2019).	48
Figure 2.1 Schematic showing operation of the algal biomass aspiration system and test engine set-up. The engine was operated at steady state conditions with direct injection of fossil diesel while the algal biomass suspension was delivered via a spray gun through the air intake and combusted with direct injected diesel.	58
Figure 2.2 Delivery system of algal biomass suspension. (a) A picture of whole system; (b) A picture of the spray gun.	61
Figure 2.3 In-cylinder pressure with aspirated algal biomass suspensions of varying mass concentration.....	62
Figure 2.4 Apparent net heat release rate with aspirated algal biomass suspensions of varying concentration.	63
Figure 2.5 Engine IMEP with aspirated algal biomass suspensions of varying concentration. The error bars presented show plus and minus the standard deviation from the mean value.	64

Figure 2.6 Ignition delay duration with aspirated algal biomass suspensions of varying concentration. The error bars present show plus and minus the standard deviation from the mean value.	65
Figure 2.7 Peak heat release rate with aspirated algal biomass suspensions of varying concentration. The error bars present show plus and minus the standard deviation from the mean value.	66
Figure 2.8 NO _x exhaust emission level with aspirated algal biomass suspensions of varying concentration. The error bars present show plus and minus the standard deviation from the mean value.	67
Figure 2.9. CO exhaust emission level with aspirated algal biomass suspensions of varying concentration. The error bars present show plus and minus the standard deviation from the mean value.	68
Figure 2.10 CO ₂ exhaust emission level with aspirated algal biomass suspensions of varying concentration. The error bars present show plus and minus the standard deviation from the mean value.	69
Figure 2.11 Thermal efficiency of diesel engine and extra output work relative to water only with aspirated algal biomass suspensions of varying concentration. .	70
Figure 2.12 In-cylinder pressure with aspirated algae biomass suspensions and water of varying flowrate.	71
Figure 2.13 Apparent net heat release rate with aspirated algae biomass suspensions and water of varying injection flowrate.	72
Figure 2.14 Engine IMEP with aspirated algae biomass suspensions and water of varying injection flowrate. The error bars present show plus and minus the standard deviation from the mean value.	73
Figure 2.15 Ignition delay duration with aspirated algae biomass suspensions and water of varying injection flowrate. The error bars present show plus and minus the standard deviation from the mean value.	74
Figure 2.16 Peak heat release rate with aspirated algae biomass suspensions and water of varying injection flowrate. The error bars present show plus and minus the standard deviation from the mean value.	75

Figure 2.17 NO _x exhaust emission level with aspirated algae biomass suspensions and water of varying injection flowrate. The error bars present show plus and minus the standard deviation from the mean value.	76
Figure 2.18 CO exhaust emission level with aspirated algae biomass suspensions and water of varying injection flowrate. The error bars present show plus and minus the standard deviation from the mean value.....	77
Figure 2.19 (a) CO ₂ exhaust emission level with aspirated algae biomass suspensions and water of varying injection flowrate (b) CO ₂ exhaust emission level normalized with respect to the engine IMEP. The error bars present show plus and minus the standard deviation from the mean value.	78
Figure 2.20 Thermal efficiency of diesel engine and extra output work with aspirated algae biomass suspensions of varying injection flowrate.....	79
Figure 3.1 Schematic diagram of two-phase water-in-oil and oil-in-water emulsions (Yahaya Khan et al., 2014).	84
Figure 3.2 A sketch of the high pressure low volume fuel system in schematic form (Talibi, 2015).....	96
Figure 3.3 A solenoid valve fuel injector (functional principle). 1 Fuel return; 2 Solenoid coil; 3 Overlift spring; 4 Solenoid armature; 5 Valve ball; 6 Valve control chamber; 7 Nozzle spring; 8 Nozzle needle pressure shoulder; 9 Chamber volume; 10 Spray hole; 11 Solenoid valve spring; 12 Outlet throttle; 13 High pressure port; 14 Inlet throttle; 15 Valve piston (control piston); 16 Nozzle needle (Terentyev, 2019).	97
Figure 3.4 Dry cell weight of <i>C. sorokiniana</i> during cultivation in TAP medium, 10% N TAP medium and TAP + glucose medium.	98
Figure 3.5 Average cell diameter of <i>C. sorokiniana</i> measured by Smartsizer 3000.....	100
Figure 3.6 Comparison of the four tested surfactants for water/diesel blending (Span 80, Triton X-100, Tween 80 and CTAB, left to right).	103
Figure 3.7 Use of Span 80 to prepare algal slurry/diesel emulsion. Pictures were taken right after mixing, after 10-minute, 1-hour and 24-hour settling (left to right).....	104

Figure 3.8 Three combinations of surfactant mixtures (Span 80/CTAB, Span 80/Tween 80, Span 80/Triton X-100) for preparing algal slurry/diesel emulsion. Pictures were taken after 1 hour settling.	105
Figure 3.9 Algae/diesel emulsions prepared with highlighted surfactant mixtures after 24 hours settling. (a) 0.3 mL Span 80 + 0.6 mL Triton X-100; (b) 0.3 mL Span 80 + 0.8 mL Triton X-100 (c) 0.4 mL Span 80 + 0.6 mL Triton X-100 (d) 0.4 mL Span 80 + 0.8 mL Triton X-100.	106
Figure 3.10 Water/diesel emulsion of 10% (v/v) water and 0.2% (v/v) Triton X-100 content. Picture was taken 5 minutes after mixing.	107
Figure 3.11 Photos of algae/diesel emulsions taken directly after mixing and containing (a) 1% (b) 2.5% and (c) 5% v/v biomass with 10% water concentration and 0.2% Triton X-100.....	109
Figure 3.12 Algae/diesel emulsion with 20% water content and (a) 1% (b) 2.5% (c) 5% algal biomass concentration after 2 hours settling period.	110
Figure 3.13 Diesel mixtures with 5%, 10% and 20% (v/v) FAME concentration.	112
Figure 3.14 The diesel viscosity with varying FAME concentration.	113
Figure 3.15 Microscopic observations of stable emulsions. With 30% (v/v) water content and (a) 1% (w/v) algal biomass content; (b) 2.5% (w/v) algal biomass content; (c) 5% (w/v) algal biomass content. With 30% (v/v) water content, 2.5% (w/v) algal biomass content and (d) algae/FAME 5 diesel; (e) algae/FAME 10 diesel; (f) algae/FAME 20 diesel. The white bars show the 200 μ m of actual scale in the image. Circles represent algae cells (green), air bubble (red), water (blue) and diesel (yellow).....	115
Figure 3.16 In-cylinder pressures during direct injection of algae/diesel emulsion at 500 bar.....	117
Figure 3.17 Maximum in-cylinder pressures achieved during direct injection of algae/diesel emulsion at 500 bar. Red crosses indicated no combustion was taken place.	117
Figure 4.1 System boundaries depicting the unit processes considered in the LCA study.	124

Figure 4.2 Comparison of three impact categories: (a) GWP; (b) NO _x ; (c) water consumption of algal biomass suspension combusted using different biomass concentrations per functional unit (1MJ of energy released in the diesel engine).	133
Figure 4.3 Contribution analysis of the main process of algal biomass preparation and combustion using different biomass concentrations per functional unit (1MJ of energy released in the diesel engine).	134
Figure 4.4 Comparison of three impact categories: (a) GWP; (b) NO _x ; (c) water consumption of algal biomass suspension combusted using different aspiration flowrate per functional unit (1MJ of energy released in the diesel engine).	136
Figure 4.5 Contribution analysis of the main process of algal biomass preparation and combustion using different aspiration flowrate per functional unit (1MJ of energy released in the diesel engine).	137
Figure A.1 The biomass concentration (g/L) in wet weight versus optical density (OD _{750nm}).	158
Figure A.2 The biomass concentration (g/L) in dry weight versus optical density (OD _{750nm}).	159
Figure A.3 The calibration curve of Nile Red test.	159
Figure C.1 Certificate of analysis for the fossil diesel fuel used in the experiments presented in this thesis (page 1 of 2).	169
Figure C.2 Certificate of analysis for the fossil diesel fuel used in the experiments presented in this thesis (page 2 of 2).	170
Figure C.3 Certificate of analysis for the FAME used in the experiments presented in this thesis (page 1 of 2).	171
Figure C.4 Certificate of analysis for the FAME used in the experiments presented in this thesis (page 2 of 2).	172

Abbreviations and nomenclature

BDC	bottom dead centre
BTDC	before-top-dead-centre
CAD	crack angle degree
CATAS	Chinese Academy of Tropical Agricultural Sciences
CDS	coal diesel slurry
CI	compression ignition
CO	carbon monoxide
CO ₂	carbon dioxide
CR	common rail
CTAB	cetyltrimethylammonium bromide
CWS	coal water slurry
DI	direct injection
EDC	Electronic Diesel Control
ELCD	European Life Cycle Database
FAME	fatty acid methyl esters
GHG	greenhouse gas
GWP	global warming potential
HCl	hydrochloric acid
HCN	hydrogen cyanide
HHV	higher heating value
HLB	hydrophilic-lipophilic balance
HPH	high pressure homogenisation
HPLVFS	high pressure low volume fuel system
HRR	heat release rate
IC	internal combustion
ICE	internal combustion engine
IMEP	indicated mean effective pressure
IPCC	Intergovernmental Panel on Climate Change
LCA	Life Cycle Assessment
LCI	Life Cycle Inventory
LHV	lower heating value
NER	net energy ratio
NO	nitric oxide

NO ₂	nitrogen dioxide
NO _x	nitrogen oxides
O/W	oil-in-water
OD	optical density
PHRR	peak heat release rates
PM	particulate matter
RO	Reverse Osmosis
SOC	start of combustion
SOF	soluble organic fraction
SOI	start of ignition
Span80	sorbitan monooleate
TAP	Tris Acetate Phosphate
TDC	top dead centre
TICS	Thermal Ignition Combustion System
TM	total moisture
Tris-MIN	tris minimal
Triton X-100	polyethylene glycol tertoctylphenyl ether
Tween80	polyoxyethylene sorbitan mono-oleate
USLCI	U.S. Life Cycle Inventory
W/D	water/diesel
W/O	water-in-oil
μ	growth rate
T _d	doubling time

Chapter 1 Introduction

1.1 Context of the research

Fossil fuels have been used for centuries and played a crucial role in human development. However, with greatly increasing consumption of fossil fuel, many issues are beginning to affect sustainable economic development and national energy security. The two most serious issues are the potential energy crisis and the effects of global warming. In 2018, the global primary energy consumption was 13864.9 million tonnes of oil equivalent, of which fossil fuels was the primary energy source accounting for 84.7%, with oil (33.6% share), coal (27.2%) and natural gas (23.9%) (BP Statistical Review of World Energy, 2019). To control this situation, it is not enough to only reduce the greenhouse gas (GHG) emissions, but also optimise efficiency in terms of energy consumption. Therefore, the development of new renewable energy sources and the reduction of carbon emissions are of key importance.

Biomass is a diverse source of renewable energy. Its development and utilisation can not only help alleviate the increasing depletion of energy resources but can also reduce emissions of fossil diesel carbon dioxide (CO₂), the main produced GHG. Combustion of solid, liquid and gaseous biomass fuels to generate electricity and steam/heat via high-efficiency and low-emission conversion processes has been developed successfully (IFC, 2017). Recently, microalgae have gained increased attention from researchers and policymakers as it is considered one of the most promising sources of biofuels for total substitution of fossil fuels. Compared with other sources of biodiesel such as soybean, rapeseed, corn and sunflower seed, microalgae has several advantages. These organisms have a high growth rate, high lipid content and low requirement for nutrition. Meanwhile, the cultivation of microalgae does not compete with food production and also can

absorb CO₂ from the atmosphere thus contributing to an overall reduction of GHG emissions (Sayre, 2010).

As the most feasible feedstock for third generation of biodiesel, microalgae has been investigated for the biodiesel production. The existing conventional process consists of many steps from the cultivation and harvesting of algae to the oil extraction and conversion of algal lipids into biodiesel. The processes of converting biomass to biodiesel comprise almost 60% of the total cost of producing biofuel from microalgae and hence it is crucial to reduce this cost (Mata et al., 2010). Harvesting contributes over 20% to the total cost but this is dependent on the type of harvesting technology used and the density of the microalgal broth (Mata et al., 2010). By using cell rupturing techniques and treatment with organic solvents, oil extraction costs can be reduced. However, mechanical methods are not recommended since microalgal cell walls are too thick to allow efficient oil extraction (Lam et al., 2012). Also, if the oil is extracted, using methanol and an acidic or alkaline catalyst in the transesterification reaction also creates obstacles such as toxic chemicals in future solvent recovery process.

There is a tremendous potential to improve the economics of producing microalgae-based biofuels as the downstream process is the largest contributor to the high cost of production. By overcoming the high cost associated with the commercial downstream processing of algal biomass to biodiesel, it has the potential to become a very sustainable form of energy source.

1.2 Algal Biomass Production

1.2.1 Algae strains

Microalgae are a large and highly diverse group of organism which has more than 40,000 different types and contain 20% to 50% of lipid content from their total biomass (Zhu, 2015). In order for microalgae to be a sustainable and feasible feedstock of the third-generation biodiesel, selection of certain algae strains with high lipid content in biomass and other growth characteristics plays a key role in the economical production of biofuel.

Algae strains with high biomass productivity and lipid content directly increase the biodiesel yield in the industries and should be considered first (Chia et al., 2018). The growth rate of microalgae varies among different species and also significantly depends on the cultivation systems and conditions. Generally, algae cells cultured under mixotrophic condition in photobioreactor systems gives higher biomass productivity compared with the cells under phototrophic condition in open ponds. Meanwhile, algae strains with high lipid content can reduce the labour cost for lipid extraction and purification process, which enhance the process yield coefficient and result in the reduction of the cost of production (Borowitzka, 1992).

Another consideration of algae strain is the tolerance ability towards extreme environmental conditions. Most of the algae species can produce higher cellular lipid content under stressed growth conditions such as nitrogen or silicon starvation. Meanwhile, a large range of salinity and temperature tolerance is required for strain selection because the evaporation of water from culture medium may cause increases in salinity and temperature during large scale outdoor

cultivation (Lim et al., 2017). Moreover, due to the constant agitation in the reactor, the algae cells should be able to survive in the high shear stress condition.

In fact, considering all the criteria, there has yet to be any species that has met all the requirement for large scale production. However, some species come close, for example, majority of *Chlorella*, *Botryococcus*, *Scenedesmus*, *Haematococcus* and *Nannochloropsis* are suitable for biodiesel production (Kilian et al., 2011).

1.2.2 Cultivation type

Microalgae can shift cell metabolism according to the environmental conditions and the growth of algae cells in different conditions significantly affect the lipid content and biomass productivities (Mata et al., 2010). Meanwhile, the algae with high lipid producing ability is usually at the expense of reducing biomass productivity. Therefore, an appropriate culture environment should be optimised for maximising the algae oil production. The four main environment types are photoautotrophic cultivation, heterotrophic cultivation, mixotrophic cultivation and photoheterotrophic cultivation (Che et al., 2016).

Phototrophic cultivation

Phototrophic cultivation is a method that using light as an energy source and inorganic carbon such as carbon dioxide as a carbon source to generate chemical energy through photosynthesis (Huang et al., 2010). As the most commonly used cultivation method, the lipid content of algae cells cultivated under phototrophic condition can be produced in the range of 5 - 68% depending on the species (Chen et al., 2011). Due to the algae consuming CO₂ directly from the atmosphere during the algae growth, phototrophic cultivation makes great contribution to global CO₂ reduction. This is also advantageous for large scale biomass productions as CO₂ can be directly channelled from external source (e.g. power plant) into the growth

media for algae cultivation. Moreover, large scale outdoor cultivation system such as raceway pond usually use phototrophic cultivation condition because of the lower chance of contamination compared to other conditions. However, the concentration of algal biomass cultivated under this condition is relatively low, which results in higher cost in the biomass harvesting process (Cheirsilp et al., 2012).

Heterotrophic cultivation

Heterotrophic cultivation uses organic carbon such as acetate and glucose as the source of both energy and carbon for cell growth (Chojnacka et al., 2004). The presence of extra carbon source allows for fast cell growth leading to a high biomass production rate and enhancing lipid productivity. Xu et al. (2006) reported a 40% increase of lipid content with high biomass production (2g/L/day) in the *Chlorella protothecoides* by changing the cultivation type from phototropic to heterotrophic. A group has attempted the use of heterotrophic microalgae for the production of biodiesel which was reported to be promising, although the high cost of carbon source required for the cultivation is one of the drawbacks (Chi et al., 2011). Meanwhile, the contamination risk of sugar-based culture medium is severe in heterotrophic cultivation and thus a close system such as bioreactors are more suitable for this type.

Mixotrophic cultivation

Mixotrophic cultivation involves organic and inorganic (CO₂) compounds as energy sources and being simultaneously used to induce cell growth under adequate light conditions through photosynthesis (Mata et al., 2010). Microalgae species cultivated in mixotrophic condition can live under either phototropic or heterotrophic or both conditions and they will release CO₂ via respiration and also absorb CO₂ and reuse it when the light is available (Mata et al., 2010). Hence, this

cultivation type can contribute to the global dioxide reduction due to the consumption of CO₂ during the algae biomass production. Moreover, microalgae grown under mixotrophic condition often have a higher lipid concentration and specific growth rate relative to heterotrophic cultivation (Shu et al., 2016). A photobioreactor is commonly used for this condition because the contamination risk of using sugar-based nutrient is high and the light source can reduce the chances of getting contamination to a certain extent.

Photoheterotrophic cultivation

In photoheterotrophic cultivation, microalgae require light as energy source while using organic compounds as carbon source. The principal difference between photoheterotrophic and mixotrophic cultivation is that the light has to be present all the time as the only energy source during photoheterotrophic growth while mixotrophic cultivation can use organic compounds as the energy source for the cell growth (Chew et al., 2018). Similar to the mixotrophic cultivation, this method is limited by the risk of contamination and the presence of light may require a special design of photobioreactor, resulting in high capital and operation cost of cultivation (Suali et al., 2012).

1.2.3 Cultivation systems

There are various techniques for microalgae cultivation and the selection of these cultivation systems mainly depend on the algae strain, type of nutrient source and the investment cost. Generally, there are two types of cultivation systems commonly applied for algae growth, which are open system (open pond or raceway pond) and close system (photobioreactors).

Open system (open pond)

The open pond system for the cultivation of microalgae has been well developed and used for a long time around the world since 1950s (Brennan et al., 2010). The most commonly used system of open pond is the raceway pond, which is usually designed to a depth in a range of 0.2 m to 0.5 m to ensure high growth rate of algal biomass. The pond is typically made of concrete and lined with a plastic liner and also constructed with a paddlewheel to provide better mixing of the algae cells and nutrients (Brennan and Owende, 2010). A schematic diagram of a representative raceway pond and a picture of algae raceway ponds are shown in Figure 1.1.

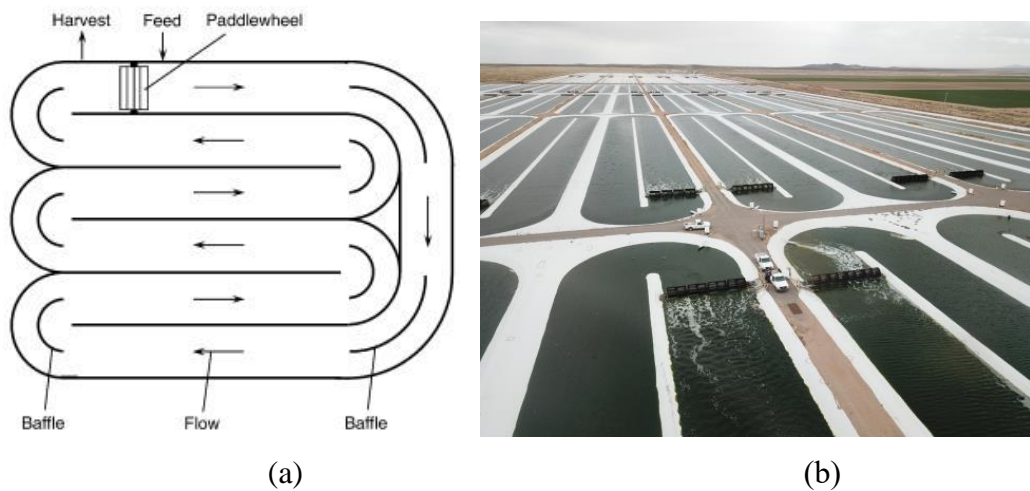


Figure 1.1 (a) Schematic diagram of a raceway pond (Chisti, 2007); (b) Outdoor algae raceway pond systems (EERE, 2019).

Compared with close photobioreactors, the open pond is more cost effective and easier to operate. A similar conclusion was drawn by Sheehan et al. (1998) that the open pond cultivation was the only feasible method for large scale algal biofuel cultivation, and until now, it is still the cheapest method for commercial algae production processes. The biomass yield of open pond system cultivation in US and China was reported in average of 0.5 g/L (Dragone et al., 2010). Meanwhile, a major disadvantage of this system is the contamination of competitive microorganisms and predators, which will consume algae cells and reduce the

biomass yield (Venkata Subhash et al., 2019). In addition, the constant evaporation of water will also reduce the efficiency of CO₂ utilisation by algae cells and result in the reduction of biomass production. Therefore, the current improvement of open pond design is to cover it by a greenhouse, which can prevent water loss, predators and rainfall.

Close system (photobioreactors)

A photobioreactor is a reactor which utilises light as energy source to cultivate phototropic microorganisms (Mata et al., 2010). In microalgae cultivation, a photobioreactor can provide a well monitored and controlled environment for algal cell growth. Comparing with open system cultivation, photobioreactors allow monoculture of microalgae for a long time with low risk of contamination (Brennan and Owende, 2010). However, from the perspective of economics, photobioreactors have much higher capital costs as compared with open pond and it is not ideal for commercial scale algal biomass production. According to the geometric shape of photobioreactors, they can be classified into tubular photobioreactors, column photobioreactors, stirred tank photobioreactors and flat panel photobioreactors.

1) Tubular photobioreactors

Tubular reactor is the first closed construction model for microalgae cultivation, which consists of straight transparent glass or plastic pipes (solar collector), a reservoir and an airlifting pump as shown in Figure 1.2. This setup requires large land area because of the high surface area demand of solar collector. In order to obtain sufficient light penetration to the culture medium, the diameter of the tubes should be less than 0.1 m (Tan et al., 2018). During microalgae cultivation, the culture medium is circulated in the tubes with receiving light source (sunlight or artificial light) and cycled back to the reservoir driven by the airlifting pump. This

process can deliver the exchange of carbon dioxide and oxygen in the culture medium and improve the mixing process. Meanwhile, it is important to avoid flocculation of algae cells, which can be prevented by maintaining the highly turbulent flow regime in the system (Klinthong et al., 2015).

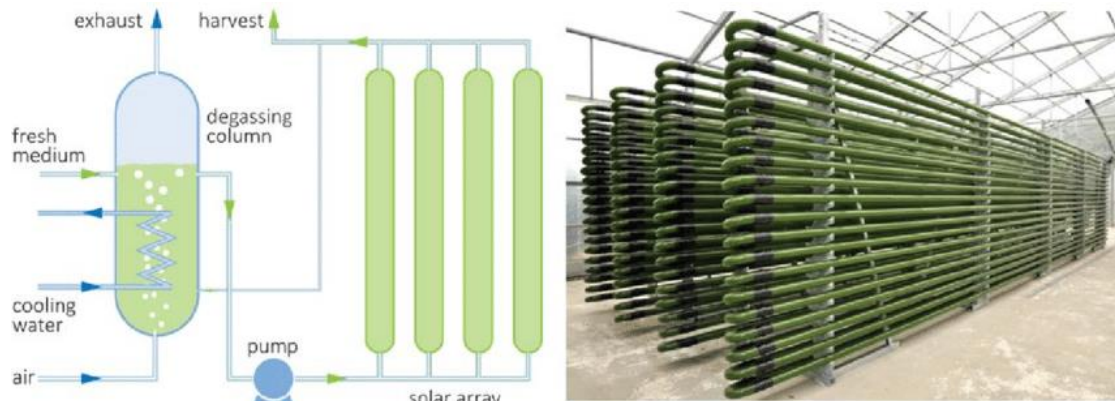


Figure 1.2 A design and picture of horizontal tubular photobioreactor (Singh et al., 2012).

2) Column photobioreactors

A column photobioreactor is a vertical tube photobioreactor design, which resembles a cylindrical shape vessel with no internal structure as shown in Figure 1.3. This type of reactor provides efficient mixing and satisfactory liquid-gas mass transfer due to the vertical gas flow. The small gas bubbles are released from the air spargers at the bottom and increase the surface area of the water to gas phase, which helps to increase the gas-liquid exchange and further increase algal biomass yield. Moreover, the fluid pattern flow in the bubble column is driven by the air bubbles. This will enhance the mixing of culture and together with shifting algae cells from illuminated areas to axial dark zone, there will be an overall improvement of photosynthesis efficiency (Chew et al., 2018). An improved design of the bubble column is airlift column, which added a draft tube in the column to increase axial mixing throughout the whole reactor by reducing bubble coalescence (Duan et al., 2014). Although the column photobioreactor has high

volumetric productivity and it is a good choice for large scale algal biomass production, the capital cost is relatively high. Therefore, a compromise between productive efficiency and total cost should also be considered in the future design.

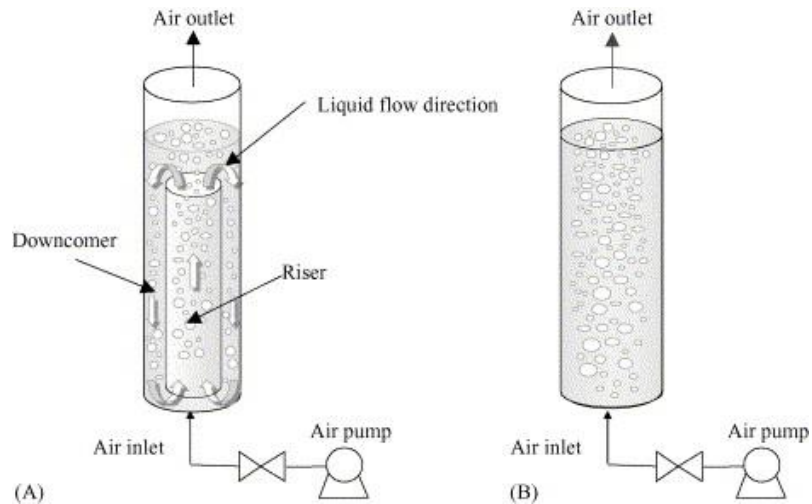


Figure 1.3 Schematic diagram for (A) airlift photobioreactor and (B) bubble column photobioreactor (Krichnavaruk et al., 2005).

3) Stirred tank photobioreactor

Typically, the stirred tank photobioreactor applied for microalgae cultivation is developed from the fermentation tank. Based on the requirement of algae growth, an additional external light source is added to the fermenter tank and adjusted to support the cell photosynthesis. In this type of reactor, the agitation is provided by the mechanical movement of the impeller to achieve the mixing of the culture medium and achieve optimal heat and mass transfer. However, compared with a column photobioreactor, stirred bioreactors cause more mechanical damage to algae cells and the relative low surface area to volume ratio leads to reduction of photosynthetic efficiency of microalgae. Due to the insufficient illumination for the large bioreactor, stirred tank photobioreactor is currently used on the laboratory scale only. The schematic diagram and picture of stirred tank photobioreactor is shown in Figure 1.4.

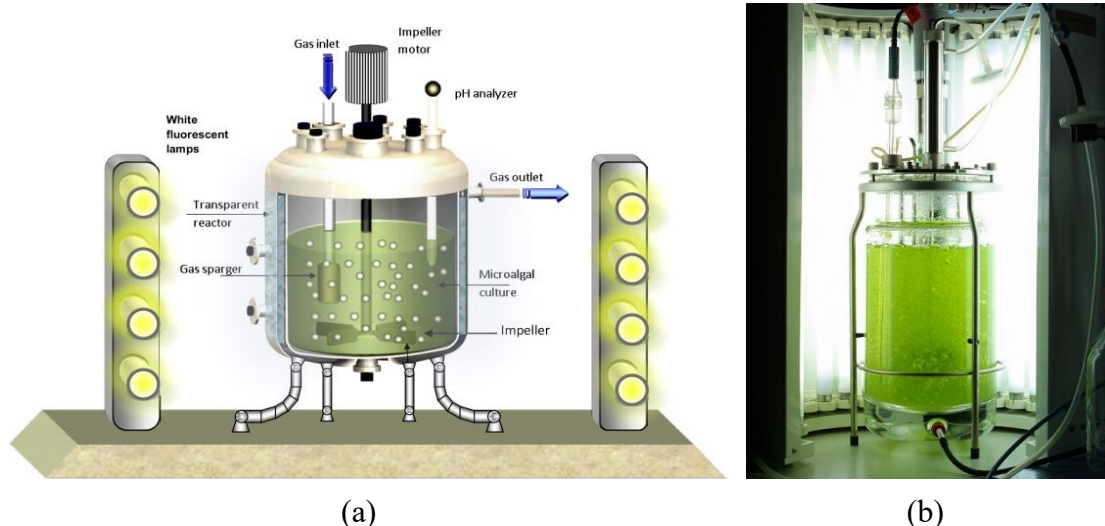


Figure 1.4 (a) Schematic diagram of a stirred tank photobioreactor (Concas et al., 2012); (b) a picture of a stirred tank photobioreactor with external lighting (ReskiLab, 2019).

4) Flat panel photobioreactors

Flat panel photobioreactor is the reactor consisting of two transparent or semi-transparent glass sheets and assembled as a rectangular box as shown in Figure 1.5. This type of photobioreactor provides high surface area for illumination and can be placed vertically or inclined at certain angles to maximize the absorption of light energy (Ting et al., 2017). The transparent glasses are also made in small thickness to enable easy penetration of the light through algae cells. The air bubbles generated by the sparger help in achieving better mixing and circulating of the culture medium. Moreover, the flat panel photobioreactor has lower amount of dissolved oxygen accumulation and higher photosynthetic efficiency relative to tubular photobioreactor (Brennan and Owende, 2010). However, a few drawbacks of this design such as aeration may cause hydrodynamic stress and create biofouling at the surface (Chew et al., 2018). Meanwhile, the scale up of this photobioreactor requires many support materials, which will significantly increase the capital cost.

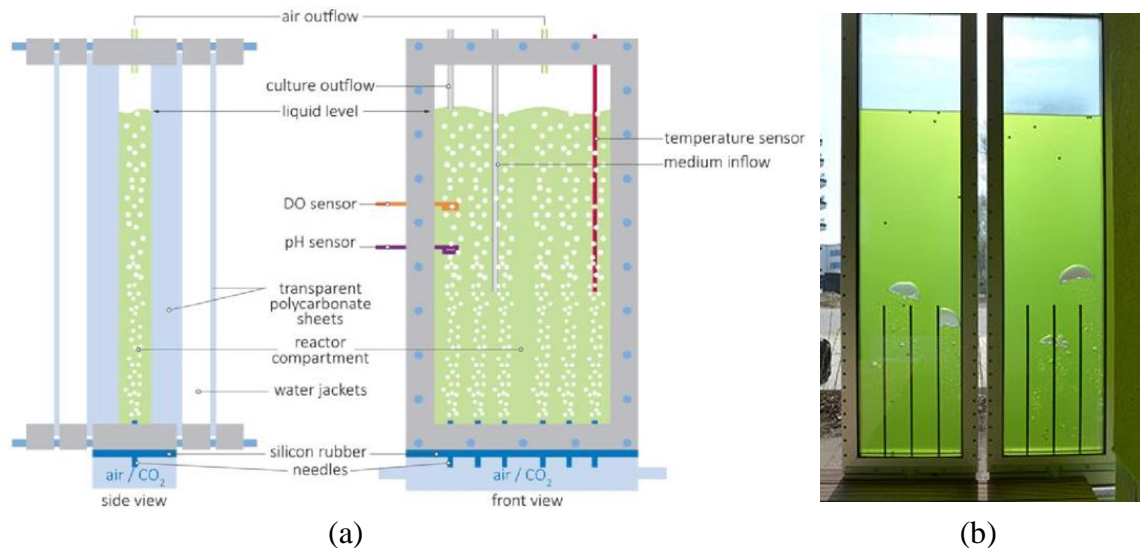


Figure 1.5 (a) Schematic diagram of a flat panel photobioreactor (Singh and Sharma, 2012); a picture of flat panel photobioreactors (Entwistle, 2015).

1.2.4 Cultivation conditions

To make the algal biomass production more environmentally friendly, feasible and economical viable, it is necessary to develop and optimise the culturing condition for different algae species. Generally, the cultivation of microalgae is affected by factors such as light intensity, temperature, nutrient availability (N, P, K, etc.), pH, inorganic carbon, oxygen and carbon dioxide (Mata et al., 2010). The following factors have significant impact on the biomass yield and bioproduction of microalgae.

Light

Light intensity is one of the major parameters in algae cultivation, which supplies the energy to algae cells for photosynthesis and directly affects the composition of microalgae and biomass production (Krzemińska et al., 2014). For different algae species, light requirement can be varied to achieve the maximum growth and biomass accumulation. Under too low or too high light intensities, microalgae will reduce the growth rate and productivity due to reduction of photosynthesis or the effect of photoinhibition (Ren, 2014). Most researchers reported that the most

suitable light condition for algae growth is around 16 hours light/8 hours dark (Khan et al., 2018). Mata et al. (2010) found that the microalgae cultured under the 12 hours daylight with 12,000 Lux intensity reached the highest biomass yield, and it was decreased by reducing the light intensity. Daliry et al. (2017) recently reported that *Chlorella vulgaris* achieved the maximum growth rate and lipid content at light intensities of 5000 ~ 7000 Lux.

Temperature

Temperature is another important parameter that directly affects the growth of microalgae. In order to achieve ideal efficiency of biomass accumulation, an optimal growth temperature should be maintained at around 20 to 30 °C for most of microalgae species (Singh et al., 2015). The cultivation at low temperature will reduce the carbon assimilation activity and thus affect the photosynthesis of algae cells. On the contrary, too high a temperature will inactivate the photosynthetic protein and also lead to the reduction of photosynthesis (Khan et al., 2018). Hence, a temperature beyond the optimal point will significantly reduce and/or even stop the algae growth and activity resulting in biomass decreasing (Béchet et al., 2017).

Nutrients

Although the exact requirements of nutrients may vary for different microalgae species, the basic nutrients including nitrogen, phosphorus and carbon are the fundamental source for the formation of all microalgae species (Juneja et al., 2013). For commercial production of algal biomass, it is critical to provide proper nutrients for rapid algal growth. In fact, the quantities of nutrients strongly affect the cell growth. Aslan et al. (2006) observed a decrease of the cell growth rate of *Chlorella* after reducing the concentrations of nitrogen and phosphorus from 31.5 and 10.5 mg/L respectively. Meanwhile, the limited nitrogen source in the culture medium can increase the lipid production of microalgae but it reduces the growth

and biomass accumulation to some extent. The micronutrients such as Fe, K, Co, Mg, etc. have significant impact on microalgae growth even if the requirements are small. This is due to the fact that the trace elements can support the activities of enzymes in the algae cell and keep them healthy (Khan et al., 2018). Carbon source is a partial energy source for algae cultivation and organic carbon sources such as acetate and glucose are usually applied to increase the biomass production. However, for large scale cultivation of microalgae, the CO₂ from the environment will be the major carbon source. It is not only for reducing the total cost, but also for the contribution of CO₂ mitigation.

pH and salinity

In the cultivation process of microalgae, pH is another factor affecting the cell growth. The pH of different culture media depends on the source requirements of algae species. Usually, the most well grown range of pH for microalgae is between 6 to 8 (Tan et al., 2018). Although most algae species are sensitive to pH, few of them have good tolerance abilities that allow them to survive in large range of pH environments. Daliry et al. (2017) reported that *C. vulgaris* can survive in the environment with broad range of pH and the maximum growth rate and biomass productivity can be achieved at pH 9 to 10. Moreover, the increasing salinity of the culture medium is harmful for algae cells. Liu (2006) found that the microalgae growth will be inhibited when the salinity increased.

1.3 Biomass harvesting techniques

After cultivation the microalgal biomass needs to be recovered from the culture medium, which requires harvesting to reduce the water content for the further downstream processes. There are several biomass-concentrating techniques that have been applied with their unique features. Generally, all of these techniques have high energy consumption and high capital cost (Wang et al., 2015).

1.3.1 Centrifugation

Centrifugation is commonly used for microalgae bulk harvesting, which is utilising centrifugal force to separate the algal biomass and culture medium without any chemical solvents. During the operation, the biomass solids are moved through the liquid and concentrated near the walls under centrifugal force. This technique effectively prevents the risk of chemical contamination (Laamanen et al., 2016). Meanwhile, the biomass recovery performance of centrifugation process can be achieved up to 95% under optimal conditions. However, due to the high cost of process operation and maintenance of machines, this technique is not ideal for large scale production. Moreover, the high shear and heat generated inside the centrifuge may cause damage to algae cells and results in product loss during the process (Goh et al., 2019).

1.3.2 Flocculation

Flocculation is a cost-effective technique for removing particles from certain suspensions in the industry such as wastewater treatment and biomass recovery. Typically, flocculation can be carried out with chemical, magnetic and biological methods. The most commonly used flocculants such as ferric chloride (FeCl_3), aluminium sulphate ($\text{Al}_2(\text{SO}_4)_3$) and ferric sulphate ($\text{Fe}_2(\text{SO}_4)_3$) can dissolve in the suspension and the metal ions will hydrolyse and precipitate (Vandamme et al.,

2013). The major problem of using this method is that once the chemicals are added into the production system, the metals will remain in the final product and affect the product quality.

The magnetic method for harvesting algal biomass is based on the negative charges on the algae cell surface. Therefore, positive charged magnetic adsorbents such as magnetite (Fe_2O_3) nanoparticles can be introduced into the microalgae suspension to form large cell aggregates for sufficient sedimentation. However, it would be costly to separate these magnetic adsorbents from the residue after the harvesting process.

Bio-flocculation has also been used for biomass dewatering. Oh et al. (2001) studied using bacteria to induce flocculation in the culture of *Chlorella vulgaris* and the recovery efficiency of more than 80% can be achieved. However, the cultivation of bacteria requires additional cost and there would be a safety issue if the algal biomass is used for food production.

1.3.3 Flotation

Flotation was first used in the mining industry for removal of solids from liquid phase. The principle of this technique for algal biomass recovery is that with adding additional surfactants, the generated air bubble can attach on the hydrophobic surface of algae cells and carry them to the liquid surface (Garg et al., 2015). Based on the size of air bubbles, flotation can be classified into dissolved air flotation and dispersed air flotation. The dissolved air flotation generates small bubbles at average diameters of 40 micrometres (μm) by saturating suspensions in high pressures and then releasing them in low pressures. Although it is an effective method for biomass harvesting, the generation of high pressure is energy intensive and expensive (Shah et al., 2014). Dispersed air flotation can also achieve the

separation of algae cells and culture medium with lifting air bubbles, which is generated through porous material. Compared with dissolved air flotation, this method requires less energy input for generation of microbubbles. However, the larger air bubbles reduce the air/liquid surface area and thus reduce the efficiency of biomass recovery.

1.3.4 Filtration

Filtration is a conventional method for separation of solid and liquid, which is normally applied after flocculation to improve the harvesting efficiency. During the process, the algae suspension is forced to flow through a filtration membrane and thereby achieve the algae cells recovery (Barros et al., 2015). However, the resultant filter cake that built up on the membrane will cause the increase of flow resistance and results in membrane clogging. Therefore, the membrane replacement is required to maintain the harvesting efficiency, which also increases the operation cost. Moreover, the crossflow filtration is invented to solve this problem by using tangential flow to remove the filter cakes. Researches (Petruševski et al., 1995) reported that *Stephanodiscus hantzschii*, *S. Astraea*, *Cyclotella sp.*, and *Rhodomonas minuta* could be recovered with efficiencies of 70% to 89%. Compared with other filtration techniques, crossflow filtration requires longer duration in the algal biomass dewatering process.

1.3.5 Electricity assisted techniques

Electricity has also been applied in the harvesting processes to increase the efficiency of biomass recovery. As an environmentally friendly approach, it can be used for the microalgae separation without adding any chemical due the negative charge of algae cells. Meanwhile, a combination of electricity with flocculation and flotation can significantly increase the harvesting efficiency. In the electro-flocculation process, algal cells are coagulated in the anode area by

charge neutralisation while hydrogen is produced from the cathode compartment (Shi et al., 2017). The electro-flotation can generate fine microbubbles at the cathode that float the algal flocs to achieve better microalgae separation. However, these methods have high energy cost and thus it is difficult to scale up for commercial production.

1.4 Biodiesel production process

1.4.1 Microalgal cell disruption methods

After harvesting of algal biomass, pre-treatment of microalgae cells must be considered for the further lipid extraction due to the cell wall structure, which is a thick and rigid layer composed of complex carbohydrates and glycoproteins with high mechanical strength and chemical resistance. Therefore, in order to break the microalgae cell walls and allow the lipids been released into extraction solvent, efficient cell disruption methods are required and these can be classified into three types: mechanical, chemical and biological methods.

Mechanical methods

Microalgae cell wall can be disrupted by physical force directly based on mechanical methods. Mechanical methods are suitable for cell disruption to keep the components intact, as chemical or enzymatic methods can lead to degradation of molecules. The following mechanical methods based on different mechanisms are commonly applied for biodiesel production.

1) Microwave

Microwave is a kind of electromagnetic wave where the frequency of the wave ranges from 300 MHz to 300 GHz. For microalgae cell disruption, a microwave with approximately 2450 MHz is applied to break the –OH bonds in water or

alcohols (Dejoye et al., 2011). During the process, cell walls can be disrupted rapidly due to the microwave radiation moving quickly into the algal biomass and generate heat to vaporise water in the algae cells. This technique has many advantages such as short operation time, high disruption efficiency for all cell species and low operating cost. However, the requirement for an efficient cooling system is a limitation for large scale application (Ranjith Kumar et al., 2015).

2) Ultrasonication

Ultrasonication technique is based on the cavitation effect that caused by pressure fluctuation from an ultrasound in a liquid. The movement of liquid molecules forms microbubbles as vacant regions, which break microalgae cells by creating pressures on the cell walls (Chen et al., 2018). Zhang et al. (2016) investigated the ultrasonic performance on the biodiesel production of *Trichosporon oleaginosus* sludge and observed a 95% production yield with an operating duration shortened by 23 hours compared to the process without ultrasonic treatment. Moreover, the efficiency of ultrasonication is affected by the temperature and liquid viscosity of the medium and thus a continuous cooling system is required to maintain the process productivity. Compared to the microwave disruption technique, this method is only suitable for microalgae species with rigid cell walls such as *Chlorella sp.* and difficult to scale up due to cavitation effect that can only occur in small regions near the ultrasonic probe (Natarajan et al., 2014).

3) Bead beating

Bead beating is a simple method of breaking the cells with a bead mill or a ball mill. The cells are disrupted by friction or collision between cells and fine beads in the mill. There are two types of beat mills usually applied for algae cell disruption: shaking vessels and agitation beads (Lee et al., 2012). Shaking vessel

consisting of multiple containers or well-plates filled with cells and beads on a vibration platform. The algae cells can be broken up during the platform vibration with certain speed. This type is normally employed for a lab scale process due to the limited sample space on the platform. Meanwhile, the agitation system gives better cell disruption efficiency by providing agitation in a fixed vessel filled with cell culture and beads. Although bead beating is an effective disruption technique, it is still limited for a large scale operation as there is a limitation of the high temperatures caused by the immense friction that may lead to reduction of product quality (Kim et al., 2013).

4) High pressure homogenisation (HPH)

High pressure homogenisation can be used for breaking cell walls by generating hydraulic shear forces by spraying of a high-pressure slurry through a narrow tube. The advantage of HPH is low heat consumption and low possibility of thermal degradation, which is suitable for processing large volumes (Spiden et al., 2013). Halim et al. (2012b) reported a 73.8% yield of cell disruption achieved with *Chlorococcum sp.* using cell homogenization, which is higher than bead beating and ultrasonication. However, HPH requires relative long time for treatment and consumes large amount of energy.

Chemical methods

Since the concentration of the outer solution affects the permeability of cells, chemicals have been used for the disruption of cell walls. It has been verified that the chemical linkages on microalgal cell envelope can be degraded after chemical treatments with acids (HCl and H₂SO₄), alkalis (NaOH) and surfactants, which results in the breakup of cell walls (Chen et al., 2018). Meanwhile, Park et al. (2014) reported an increase of the disruption efficiency of *C. vulgaris* via acid chemicals treatment under higher temperature. Comparatively, the performance of chemical

treatment is outstanding while having low energy requirement for the cell disruption. However, the continuous consumption of chemicals may cause environmental damage and must be researched carefully before applying to large scale production (Kim et al., 2013).

Biological methods

Enzymes has been intensively studied as biological treatments for algae cell walls disruption. The structural cell components can be degraded via pretreatment with specific enzymes, thus improving the release of desired intracellular compounds (Zuorro et al., 2016). Compared with chemical methods, enzymes are biological material as more environmentally friendly and easier to control since they only react with specific chemical linkages without affecting other target products such as lipids. Moreover, enzymatic disruption combined with other methods is usually considered for improving economic process and disruption performance. Liang et al. (2012) found that the lipid extraction efficiency of algal biomass can be improved with a combination of enzyme and sonication disruption treatments. On the other hand, the high cost of purchasing or producing enzymes and the different combination of enzymes required in any reaction may cause difficulties in the commercial production processes (Kim et al., 2013).

1.4.2 Lipid extraction

The lipid extraction is the subsequent process after cell disruption and used for separating fatty acids and neutral lipids from cellular matrix and water. In the biodiesel production process, solvent extraction and supercritical fluid extraction are the common techniques for lipid extraction from algal biomass (Halim et al., 2012a).

The technique of conventional organic solvents extraction was developed by Bligh et al. (1959), which used a combination of chloroform and methanol as the organic solvents. During the process, organic solvents first penetrate through cell membranes and interact with lipid to form a solvent-lipids complex in the cytoplasm. Then, the complex flows out through cell membrane by diffusion effect and finally be released into bulk organic solvent (Chen et al., 2018). Nonpolar organic solvents such as hexane, benzene, toluene, diethyl ether, ethyl acetate, and chloroform are commonly used in this process, but the selection of them may vary due to the different cell wall and lipid properties of microalgae species. Moreover, this technique is not ideal for large scale operation as it requires large quantity of volatile organic solvents and may cause environmental impact and safety concerns (Li et al., 2014).

Supercritical fluid extraction is an alternative technique for lipid extraction, which can potentially displace the use of conventional solvent extraction due to the short extraction time, high selectivity and non-toxic solvents. In the process of CO₂ supercritical extraction, the CO₂ is condensed to liquid form and heated up to a supercritical state. Then, the CO₂ fluid is pumped into the extraction vessel, acting as the main solvent under well-controlled conditions. Finally, the extracted lipids are cooled and collected after extraction process. Halim et al. (2011) obtained 7.1 wt% lipid yield from a wet *Chlorococum sp.* paste by using supercritical fluid extraction at a temperature of 60 °C and a pressure of 30 MPa. Although many advantages of this technique exist, the maintenance of supercritical conditions like high temperature (100 °C) and pressure (41 MPa) are potential hazards and limits industrial scale application (Liau et al., 2010).

1.4.3 Transesterification

Transesterification reaction is the final step to produce biodiesel, in which triglycerides from algal lipids are converted to fatty acid methyl esters (FAME) when reacted with alcohol, usually in the presence of a catalyst. This process lowers the molecular weight of the components from oil lipids and significantly reduces the viscosity of algae oil that makes it available for direct engine combustion (Rawat et al., 2011).

Generally, the selection of catalyst of transesterification reaction depends on the nature and type of feedstock and it can be acid, base or enzyme. Base catalysts such as NaOH and KOH are the most commonly used for lipid transesterification and have up to 98% of biodiesel conversion efficiency under low temperature and pressure conditions (Taher et al., 2011). However, in cases where the lipid oil contains high concentration of free fatty acids (2% to 5%) and upon reaction with base catalyst, saponification will occur instead of transesterification (Banani et al., 2015). Therefore, acid catalyst can be applied in this situation but requires high temperature and pressure to achieve high biodiesel yield. Chemical catalysed processes have some limitations such as requirement of high energy input and the catalyst is not easily removed from the product. This may cause issues on the commercial scale. Enzymes has been investigated for biodiesel production over the last ten years. The advantages of using enzymes in transesterification reaction include high specificity of product, insensitivity to free fatty acids, available of reusability and less energy requirement (Lam et al., 2010). However, it is still not feasible for large scale operation due to the high cost of enzymes production and maintenance.

In recent years, many researchers have studied the direct biodiesel synthesis of microalgal biomass, which is a single step combining lipid extraction and

transesterification. In this process, alcohol acts as the extraction solvent and the reactant in the transesterification reaction (Zhu et al., 2017). Compared with conventional processes, direct biodiesel synthesis converts all the algal biomass into biodiesel without any loss of cell lipid and thus improving the process efficiency. Lemões et al. (2016) studied direct biodiesel synthesis with *Chlorella sp.* and found that the process had higher ethyl and methyl esters yields than the conventional multi-step biodiesel production process. However, due to the large requirement of catalyst during the reaction, this process has not yet been established in industry.

1.5 Challenges and prospects for the commercialisation of algal biofuels

Development of third generation biodiesel derived from microalgae has shown good progress in recent years and an increasing number of companies and countries are turning their attention to improving the industrial production of biodiesel. The use of microalgae as a biodiesel feedstock has many promising advantages such as rapid biomass growth, avoidance of the use of agriculture land and CO₂ fixation for reduction of GHG. However, the whole process from algal biomass cultivation to biodiesel production is either cost intensive or vulnerable to external influences, and thus no successful industrialisation approach has been reported.

In order to achieve sufficient productivity of algal biofuel in the commercial scale as well as the price competitiveness against other energy sources, each part of the whole production process needs to be further developed and optimised. Firstly, the selection of species should consider several factors such as environmental tolerance, high growth rate and high lipid content (Islam et al., 2017). Generally

modified microalgae have the potential to meet these characteristics but these efforts are still at the research stage. Meanwhile, the scale up of biomass cultivation is limited by the large requirement of nutrients and light sources for increasing the biomass productivity. A concept of co-cultivation has been developed that the microalgae cultivated in wastewater or seawater can utilise the energy source without using fertilisers and also can be used for wastewater remediation (Komolafe et al., 2014). Furthermore, the processes of biomass harvesting and biodiesel production are not economically feasible at the moment. These require further optimisation to reduce the high operating cost. Besides technical challenges, there are also wider problems such as the lack of proper policy to support efficient commercialisation in different countries. For instance, China is the second highest oil consumer, but only produces 15% of its biodiesel need due to the lack of policies and regulations that encourage the use of biodiesel (Xu et al., 2016a).

With the development of the global economy, energy consumption will continue to increase in the next few decades. At the same time, under the dual pressures of energy crisis and carbon dioxide emission reduction, algae biodiesel is getting more attention from global society. Although there are many existing challenges for the industrial biodiesel production processes, with continuous in-depth research, technological advancement, and strong support of governments in policy, it will become an indispensable part of the global energy.

1.6 Diesel engine

The diesel engine, also known as a compression ignition (CI) engine, is an internal combustion engine, first invented by Rudolf Diesel in 1892 and widely used for over hundred years (Kamimoto et al., 1991). With continuous study and development, the diesel engine has obtained many advanced features such as the

highest thermal efficiency of all combustion engines, reliable fuel autoignition without a high voltage electrical ignition system, and the most important, the ability to utilise a variety of fuels. Based on these advantages, many researchers are using diesel engines as a tool to investigate the possibility of energy production from sustainable energy sources.

1.6.1 Operation of diesel engine

The diesel engine differs from a spark ignition engine by using compressed hot air rather than a spark plug for ignition of the fuel air mixture. Generally, most diesel engines are four-stroke cycle engines in which the piston makes four separate strokes (two revolutions) to complete one operating cycle.

The first stroke is the intake stroke, where the piston moves from top dead centre (TDC) to bottom dead centre (BDC). The intake valve is open during this period and air is sucked into the cylinder by the vacuum pressure created from the piston movement. Then, the compression stroke starts from BDC with the piston moving upward until it reaches TDC. In this stroke the intake and exhaust valve are closed, while the air is compressed with a high compression ratio (typically between 15:1 to 23:1). This massively increases the air temperature and pressure inside the cylinder, thus creating conditions suitable for the spontaneous ignition of diesel fuel. Near TDC, the fuel is injected via a injector and atomised into the air. As autoignition occurs and the combustion process proceeds, the expanding air drives the piston downwards to BDC, supplying power to the crankshaft to produce mechanical work. In the final stroke, the exhaust valve opens while the piston returns from BDC to TDC by inertia to force the exhaust gases out of the cylinder. At this point, one operating cycle has been completed (Stone, 1999).

1.6.2 Direct injection fuel system

Direct injection (DI) fuel systems are a technology that allows an engine to burn fuel more efficiently and has been commonly used in modern diesel engines. After the air is compressed in the cylinder, diesel fuel is directly injected onto the top of the piston, which usually has a combustion bowl or cup for fuel spraying, and as can be seen in Figure 1.6, showing in schematic form, a typical direct injection combustion chamber arrangement. Due to the high injection pressure (e.g. 500 to 2000 bar), more complete fuel atomisation occurs before combustion and thus there is no requirement of a pre-chamber for proper diffusion of the fuel into the air. Compared with other injection techniques, the direct injection process gives precise control of the amount of fuel delivered and also the time of injection, typically resulting in more power, cleaner emissions, and increased fuel economy.

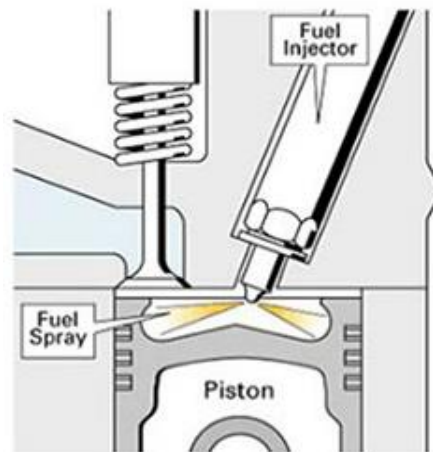


Figure 1.6 Direct injection system (DieselHub, 2019).

A common rail (CR) direct injection system is an advanced injection system that has been developed for better fuel efficiency, and also the reduction of noise and emissions from diesel engines. This system consists of a high-pressure pump, common rail, fuel injectors, engine control unit and various sensors. The high-pressure injection pump compresses the fuel through a plunger to a high-pressure

meeting the requirement of fuel injection. The common rail is used to store compressed fuel while inhibiting the pressure fluctuations caused by a high-pressure pump and fuel injection to maintain the system pressure stability. It also allows anytime fuel injection, even multiple injections within a single cycle, in a very short amount of time. The Electronic Diesel Control unit (EDC) is a management system to determine rail pressure and injections based on engine parameters. The injection timing and duration of the CR injector are accurately calculated by the EDC unit to give a control signal, which is then actuated by a solenoid valve within the injector. Newer CR injectors use piezoelectric actuator derived plungers, which allow more injections in a very short period of time. Furthermore, another difference between older and modern CR systems is the injection pressure utilised, with the latter able to produce 140 MPa to 270 MPa of fuel pressure.

1.6.3 Exhaust emissions from diesel engines

Diesel exhaust emissions include gaseous and particulate species formed during combustion. The composition of these depends on the type of engine, the temperature during combustion and the speed of engine operation. The three major components which have the greatest impact on global pollution and which have received significant research attention are: nitrogen oxides (NO_x), carbon monoxide (CO) and particulate matter (PM). Due to the harmful impact of exhaust gases on human health and the global environment, it is crucial to further investigate the emission measurement when the engine is fuelled by a biofuel (or algae suspensions).

Nitrogen Oxides (NO_x)

NO_x generally includes nitric oxide (NO) and nitrogen dioxide (NO_2), with NO dominating the composition of NO_x from diesel combustion. The main source of

NO is the oxidation of the atmospheric nitrogen, referred to as thermal NO_x. Due to the high combustion temperature, the triple bond of nitrogen is broken down and the atomic N reacts with oxygen to form thermal NO_x (Inagaki et al., 2006). With the combustion of fuel containing nitrogen, NO_x formation can occur at low temperature, however, current diesel fuels do not contain appreciable amounts of nitrogen. The prompt mechanism is another chemical reaction able to produce NO_x, where the hydrocarbon radicals react with atmospheric nitrogen to produce hydrogen cyanide (HCN) and eventually form NO_x after several gas-phase reactions. The amount of NO_x produced via this process is much lower than that produced by thermal oxidation and fuel NO_x. (Annamalai et al., 2006)

Generally, the local oxygen concentration, in-cylinder temperature, air surplus coefficient and residence time all affect the formation of NO_x. Therefore, NO_x can be generated both in the flame front and post flame gases (Heywood, 1988). The high combustion pressure is created in the flame reaction zone with short residence time under the extremely thin space of the flame front, which enhances NO_x production. Nevertheless, NO_x will start forming as long as sufficiently high temperature and pressure are achieved during combustion (Imtenan et al., 2014).

Carbon Monoxide (CO)

The formation of carbon monoxide is mainly from the incomplete oxidation of fuel. This situation normally takes place at the time of starting the engine or instantaneous acceleration where more fuel is required and the air fuel ratio becomes rich. During incomplete combustion, carbon cannot fully convert to carbon dioxide as there is insufficient air to support the full chemical reaction. However, a small amount of CO can still be produced under air-rich conditions due to chemical kinetic effects (Asif Faiz, 1996). Diesel engines generally have

high air-fuel ratios as they are lean combustion engines, and thus the CO formation is minimal in diesel engines. However, if the droplets injected are too large (local deficiency in oxygen) or insufficient turbulence is generated (poor mixing) in the combustion chamber, CO can still be produced (Reşitoğlu et al., 2015).

Particulate matter (PM)

PM is a highly complex mixture of soot and aerosols such as ash particulates, wear metals, fuel-derived sulfate and hydrocarbon soluble organic fraction (SOF), which are significantly emitted by CI engines. The size distribution of PMs has three modes, which are nucleation mode particles (3 to 30 nm), accumulation mode particles (30 to 500 nm) and coarse particles (above 1 µm). The size of soot particles in their initial states is normally 1-2 nm, but they can increase to 100 – 1000 nm after coagulation and clustering caused by collision (Annamalai and Puri, 2006). Soot is not only harmful to human respiratory system, but also potentially contains sulfur dioxide and carcinogenic polycyclic aromatic hydrocarbons in the pores of soot particles.

PM can be produced from incomplete combustion of fuel hydrocarbons, present in the rich combustion zones with higher equivalence ratio. Soot is generally formed in a diesel combustion environment with temperatures higher than 1800K. However, the majority of soot particles formed during early on in combustion are oxidised as fuel air mixing proceeds. As with the formation of NO_x, the formation and oxidation of soot are both highly dependent on the combustion temperature (Bittle et al., 2010).

1.7 Research aims and objectives

The downstream processes of algae-derived biodiesel production, especially in lipid extraction and transesterification, are energy intensive and have several limitations for commercial scaling up. In order to utilise the energy from algal biomass more effectively and environmentally friendly, it is necessary to have further development and optimisation of the current processes. Hence, the objective of this study is to develop alternative routes for energy production from algal biomass.

The project aims to explore alternative routes of biomass use for biofuels. Specifically, the project will include:

- An investigation on combustion test with aspiration of the algal biomass suspensions to the air intake of a diesel engine. It would also be beneficial to find out its efficiency and compare with the diesel blending approach. (Chapter 2)
- Investigation of the emulsion properties of algae/diesel mixtures and combustion characteristics of fuel blends with algal biomass or biodiesel. (Chapter 3)
- Integration of all the processes from algal biomass harvesting to its combustion as aspirated suspension in the diesel engine (see Chapter 2) and evaluating their environmental impact via a life cycle assessment study. (Chapter 4)

Chapter 2 Aspiration of algal biomass suspensions in the intake air of a direct injection diesel engine

2.1 Introduction

Due to a need for the integration of multiple steps of processing including harvesting, extraction and conversion of biomass to biodiesel, the high cost associated with algae biofuel production has meant that its economic viability remains uncompetitive relative to petroleum or bioethanol. Therefore, to improve the economics of producing microalgae-based biofuels, the greatest challenge to overcome is the downstream process. There is potential therefore in developing alternative approaches to utilising algal biomass in internal combustion (IC) engines which avoid conventional routes of downstream processing.

Utilising algal biomass with less processing intensity will inevitably result in the use of wet biomass or slurries with a significant water content. The concept of introducing water into the air fuel mixture of IC engines can be traced back to the early 20th century, and has been used for the reduction of combustion temperatures and control of NO_x emissions (Dryer, 1977). The easiest way to inject water into an engine is inlet air water injection (WI), also known as intake air humidification or fumigation (Zhu et al., 2019). Samec et al. (2000) investigated the effect of water injection into the intake air of a boosted diesel engine and the results indicated that both water injection locations, at the manifold port and upstream of the compressor, resulted in similar levels of NO_x reduction as compared to a direct injection of a water/fuel emulsion with a 40% v/v water in diesel mixing ratio. Although the results of water injection have found to be promising in the reduction of NO_x emission, it is important to avoid water condensation and accumulation in the intake manifold, and also corrosion problems in the cylinder.

The use of solid fuel dusts, for example coal, in diesel engines has a long history of use, dating back to the 19th century. Rudolf Diesel first investigated the use of dry coal dust in a CI engine in 1892 but stopped due to the difficulty in handling of powdered fuel and subsequent piston blockage (Piriou et al., 2013). Rudolf Pawlikowski then improved the engine feed system by adding a co-chamber, which can pre-ignite the solid fuel before injecting it into the combustion chamber (Soehngen, 1976). Several German companies developed low speed engines utilising solid fuel dusts, operating between 100 to 1000 rpm due to the slow burning rate of coal dust (Piriou et al., 2013). However, in all cases it was found that the flowrate of direct injection coal dust limited the engine speed and resulted in high engine wear. Therefore, to overcome these issues, later work focused on the use of coal slurries, which mix the coal powder with fossil fuel, known as coal diesel slurry (CDS) or water (coal water slurry) (Caton et al., 1983). This allowed the conventional diesel injection systems to be used during experiments and reduce the cost of engine modification.

A coal/diesel slurry was first tested by Hanse, who investigated the combustion of a mixture of 20/80%wt coal/diesel slurry with a coal particle size of 45 – 75 microns and 124 bars injection pressure in a four-stroke Hill engine (model 4R) at 1200 rpm. Due to the employment of a commercial injection system, the blockage of the injector needle was significant (Caton and Rosegay, 1983). Tracy reported on the use of a 30/70%wt coal/diesel slurry with less than 20 microns particle size tested in a single cylinder four-stroke diesel engine. While the reduced particle size improved the coal slurry injection rate and engine operation, the wear of the engine was still 35 times higher than when operated with conventional fossil diesel (Tracy Jr, 1957). Considering the high NO_x and particulates level in exhaust emissions and significant wear of engine of using CDS (Piriou et al., 2013), recent researches have mostly focused on coal-water based slurry (CWS) in IC engine.

Tataiah and Wood performed experiments on a four-cylinder Mercedes diesel engine with CWS in 1980. The results showed that the engine efficiency decreased at high speed and load, and higher emissions of CO and particulates, but lower NO_x, were obtained when compared with pure diesel operation (Tataiah et al., 1980). Dunlay et al. conducted tests with CWS (34% coal) on a 2-stroke Sulzer Bros crosshead diesel engine (model 1RSA76) and found out that the thermal efficiency is close to the results of pure diesel. However, the injector wear was significant due to slurry accumulation during the cold start of the engine (Belousov, 2006). In 2004, Wilson (2007) from TIAX LLC company ran a Colt Pielstick PC2.6 two cylinder engine with a Kentucky coal-based CWS for one hour with no major problems. As an alternative to using coal slurry, Soloiu et al. (2011) studied the use of a 10 µm charcoal slurry (25% by weight) on a Yanmar Nf-19 engine and found engine performance very similar to that with diesel, and net heat release even higher than in the case of pure diesel operation.

During the same period, the intake air aspiration of coal dust into a CI engine, with continued direct injection of diesel fuel, has also been investigated. Marshall and Shelton operated a 1400cc Nordberg diesel engine at 1750 rpm with coal dust intake aspiration for 45 hours, and the results showed several issues, including significant wear, crankcase oil contamination and an efficiency drop (Caton and Rosegay, 1983). Rich and Walker continued this study but at a lower speed of 1000 rpm and found thermal efficiency to drop from 27% (pure diesel) to 11% (diesel and coal dust) (Caton and Rosegay, 1983). Between 1989 and 1994, Adiabatics Incorporated company tested dry coal dust and coal slurry with a Thermal Ignition Combustion System (TICS), which was developed by Kamo et al. (1988) to enable better control of the engine speed, load through more precise delivery of the coal dust and lower the injection pressure and nozzle wear. The tests saw the 100% engine performance with powder (with pilot diesel injection)/slurry (without pilot

diesel injection) fed into the intake manifold, and then injected to the combustion chamber through the TICS chamber.

The physical similarities in the particle size of the coal dust and algae powder makes it a suitable candidate as a source of fuel for combustion engine. However, there is no report on the approach of using algal biomass in engines. This chapter presents a novel method of utilising algal biomass directly as a second fuel source with diesel for an IC engine, through the engine testing of intake air aspirated algae slurry with a variety of biomass concentrations and injection flowrates. Part of this work has been previously published.

2.2 Experimental Methods

2.2.1 Preparation of algal biomass slurry

The biomass (wild type strain of *Chlorella sorokiniana*) was obtained from the Chinese Academy of Tropical Agricultural Sciences. Algae cells were cultivated in Tris Acetate Phosphate (TAP) medium and spray dried (200 °C inlet and 82 °C outlet) to remove all the water content in and outside of the cells. The biomass suspension was blended with Reverse Osmosis (RO) water and prepared in four concentrations: 5%, 7.5%, 10% and 20% (w/v). All the suspensions were properly mixed in 1L beakers on a magnetic stirrer and then transferred into 1L Duran bottle.

2.2.2 Apparatus

The single cylinder direct injection diesel engine used for all experiments was based on a 2L Ford Duratorq head, with the original combustion chamber geometry preserved and a compression ratio of 15.8:1. The specification of the research engine and associated system has been described previously in further detail (Hellier et al., 2012b). The engine was operated naturally aspirated and the intake pipe modified to mount a liquid spray gun 250 mm upstream of the engine intake valve and deliver the water and biomass slurry into the engine intake manifold.

A schematic of the algae aspiration system is shown in Figure 2.1. The spray gun was utilised with a supply of compressed air at 1.2 bar, and was gravity fed, necessitating that two reservoirs for RO water and algae suspensions respectively were installed 200mm above the spray gun, isolated with two independent control valves. This allowed the injection system to be flushed with RO water between every test run. The spray nozzle was modified to produce a circular spray pattern. Further details of the engine and control apparatus are given in Table 2.1.

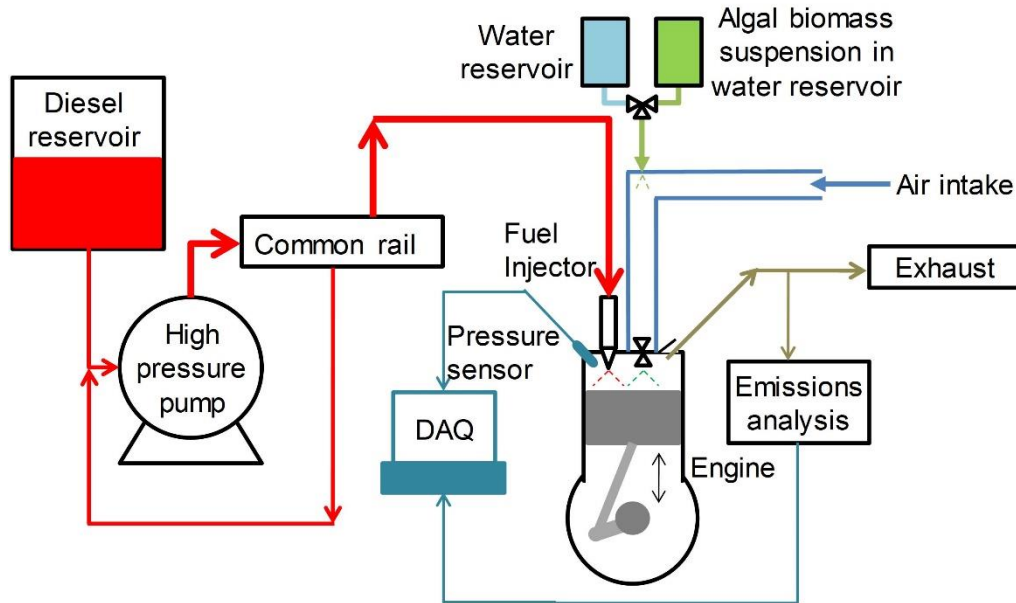


Figure 2.1 Schematic showing operation of the algal biomass aspiration system and test engine set-up. The engine was operated at steady state conditions with direct injection of fossil diesel while the algal biomass suspension was delivered via a spray gun through the air intake and combusted with direct injected diesel.

During the experiments, several parameters were controlled and recorded by a PC data acquisition system (National Instruments). A piezoelectric pressure transducer (Kistler 6056AU38) with charge amplifier (Kistler 5011) was used for measuring and logging the gas pressure in the engine cylinder at every 0.2 crank angle degree (CAD). A piezoresistive pressure transducer (Druck PTX 7517-3257) was installed in the intake manifold (at 160 mm upstream of the intake valves) to measure the in-cylinder pressure at bottom-dead-centre of every combustion cycle. The same PC data acquisition system was utilised for logging in-cylinder pressure was also used to measure various control and experiment temperatures using K-type thermocouples. The net apparent heat release rate was derived from the in-cylinder pressure (MATLAB) measured during post-processing, using a one-dimensional and one-zone model assuming homogeneity and ideal gas behaviour of the cylinder contents.

Exhaust gas sampling occurred 180 mm downstream of the exhaust valves to determine concentrations of gaseous species. Gaseous species (CO, CO₂ and NO_x) sampled via a heated line, were measured by an automotive gas analyser system (Horiba MEXA 9100 HEGR).

Table 2.1 Engine specification

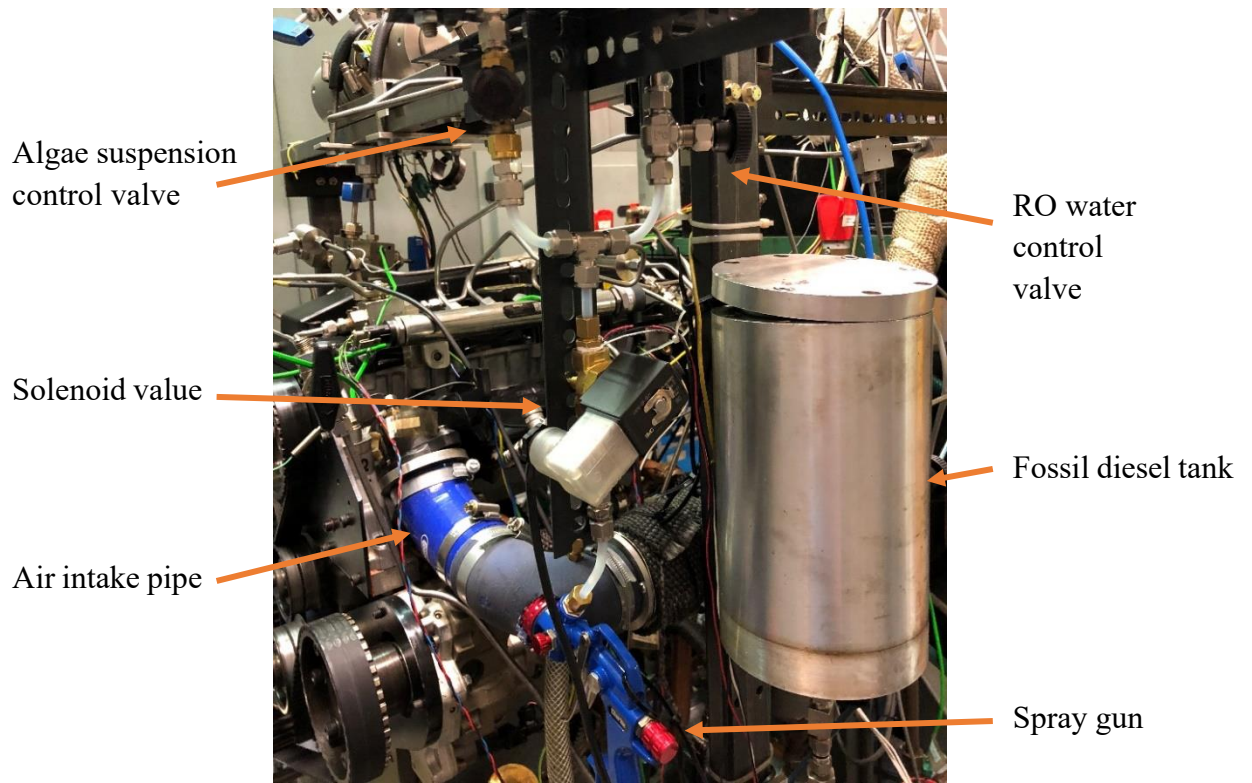
Parameters	Values
Engine head model	Ford Duratorq
Engine bottom end model	Richardo Hydra
Number of cylinders	1
Cylinder bore	86mm
Crankshaft stroke	86mm
Swept volume	499.56cc
Compression ratio	15.8:1
Maximum cylinder pressure	150 bar
Peak motoring pressure at test conditions	45 bar
Piston design	Central ω -bowl in piston
Oil temperature	80 \pm 2.5 °C
Water temperature	80 \pm 2.5 °C
Fuel injection pump	Single-cam radial-piston pump (BOSCH CP3)
Injectors	6-hole solenoid controlled (DELPHI DF1 1.3)
Electronic fuel injection system	1 μ s accuracy (EMTRONIX EC-GEN 500)
Shaft encoder	0.2 CAD resolution

2.2.3 Experimental conditions

Due to the changing viscosity of the water and algae suspension with varying biomass content, and in order to maintain a constant injection volumetric flowrate for all experiments, the spray gun was calibrated by adjusting the release valve and measuring the actual volumes of water and biomass suspension sprayed out during 1 minute (Figure 2.2). This calibration procedure was conducted before every test. The water and algae suspensions were delivered into the engine intake air with flowrates of 40, 49.2, 56 mL/min. During the tests, the engine was set to a constant speed of 1200 rpm and constant start of diesel fuel direct injection of 5 CAD BTDC (before-top-dead-centre). The injection duration was varied as necessary to maintain a constant engine indicated mean effective pressure (IMEP) of 4 bars when operated with a reference RO water only aspiration at an injection flowrate of 40, 49.2, 56 mL/min. Water only tests were used to establish a baseline to investigate the effect of aspirating algae suspension on engine performance and emissions. The summary of the test conditions is shown in Table 2.2.

Table 2.2 Summary of the engine test conditions.

Test No.	Aspiration flowrate (mL/min)	Biomass concentration (w/v)	Biomass flowrate (g/min)	Diesel injection flowrate (mL/min)	Energy supplied from biomass (kW)	Energy supplied from diesel (kW)
1		5	2	13.34	0.75	8.02
2	40	7.5	3	13.4	1.12	8.05
3		10	4	13.72	1.5	8.24
4		20	8	13.28	2.99	7.98
5		40		2	13.34	0.75
6	49.2	5	2.46	16.88	0.92	10.14
7	56		2.8	17.1	1.05	10.27



(a)



(b)

Figure 2.2 Delivery system of algal biomass suspension. (a) A picture of whole system; (b) A picture of the spray gun.

2.3 Results and Discussion

2.3.1 Effects of algal biomass concentration in aspirated suspensions on combustion and emissions

In order to investigate the impact of the aspirating algae cells directly into the air intake on the efficiency of combustion and emissions levels in a diesel engine (Section 2.2), dry algae powder (*C. sorokiniana*) was utilised to form an algal suspension with RO water containing 5% w/v, 7.5% w/v, 10% w/v and 20% w/v dry algal biomass. A reference RO water was also prepared with no biomass content.

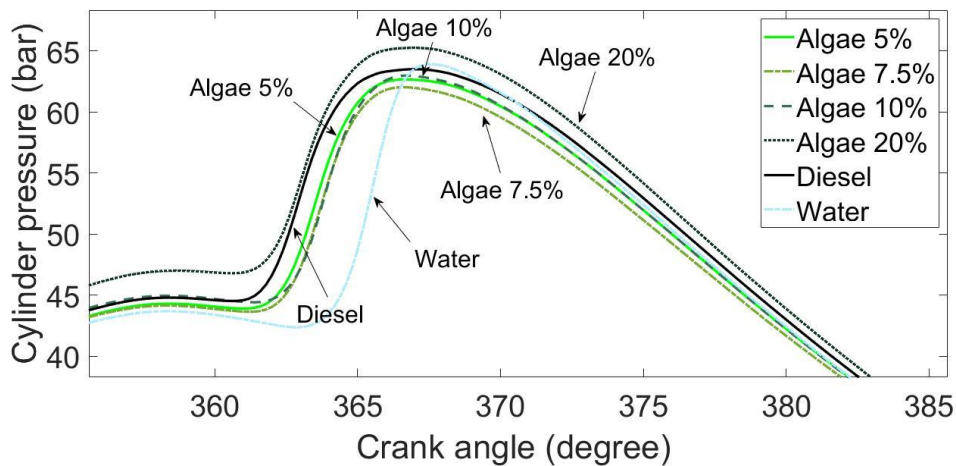


Figure 2.3 In-cylinder pressure with aspirated algal biomass suspensions of varying mass concentration.

Figure 2.3 shows the in-cylinder pressure during direct injection diesel operation with intake air aspiration of varying concentrations of algal biomass water suspensions and direct injection diesel operation without any water or suspension aspiration into the air intake at constant injection timing. It can be seen that the in-cylinder pressure rises due only to compression, and before the start of combustion, it is somewhat higher in the case of the aspiration of the algal biomass suspension with 20% biomass concentration. The manifold temperature reduced from an average of 37 °C for all other tests to 19 °C, suggesting the increased compression

pressure to be likely attributable to an increased density of the intake air. In the case of water only aspiration, peak in-cylinder pressure occurs much later than diesel only and all the algae suspensions conditions result in lower peak in-cylinder pressure than fossil diesel only.

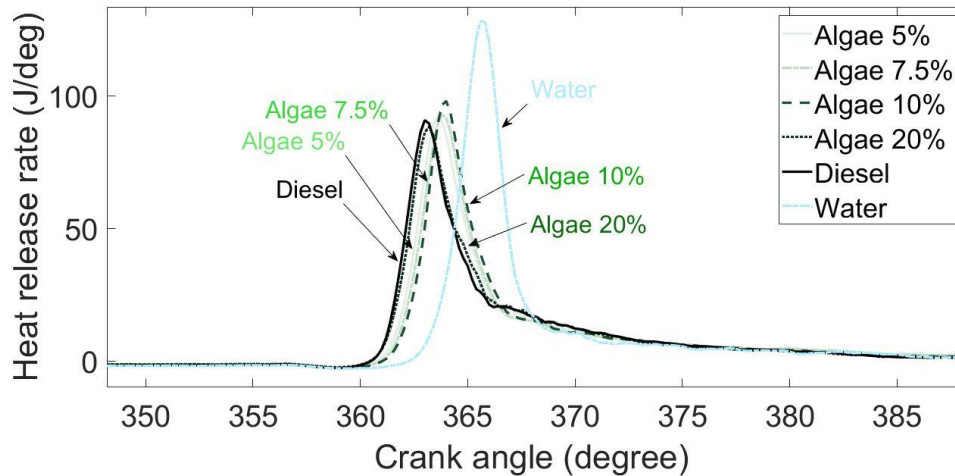


Figure 2.4 Apparent net heat release rate with aspirated algal biomass suspensions of varying concentration.

Figure 2.4 shows the apparent net heat release rate (HRR) of varying algal biomass concentration suspensions aspiration and also fossil diesel only. It can be seen that at all conditions, combustion was predominate premixed, especially apparent in the case of water only aspiration. Meanwhile, following peak heat release rates during the premixed combustion phase, HRR in the case of aspiration of 20% algal biomass suspension has the trace most similar to diesel only and it also drops fast in the water only condition relative to other cases. It is likely due to the large number of algae cells in the suspension helped to maintain the premixed burn fraction and results in a similar diffusion-controlled combustion and HRR as diesel only.

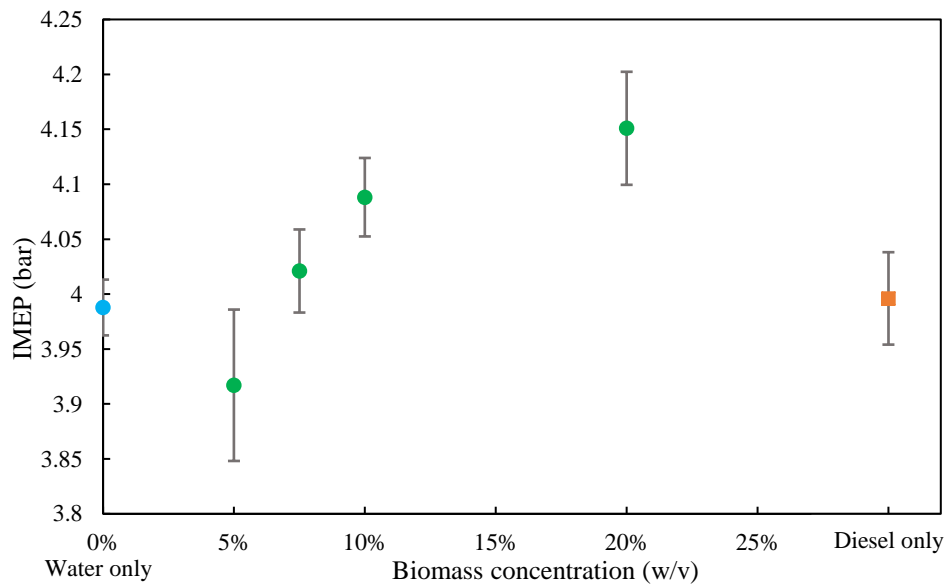


Figure 2.5 Engine IMEP with aspirated algal biomass suspensions of varying concentration. The error bars presented show plus and minus the standard deviation from the mean value.

Figure 2.5 shows the effect of varying the algal biomass concentration of the intake aspiration suspensions while maintaining a constant duration of fossil diesel direct injection on engine IMEP, and also reference fossil diesel without any water or suspension aspiration and where the diesel fuel injection duration was adjusted to achieve an engine load of 4 bar IMEP. Immediately apparent in Figure 2.5 is an increase in engine IMEP with the biomass concentration of the aspirated suspensions. It can be seen that the 20% algae suspension resulted in the highest engine IMEP, and that from a biomass concentration of 5% to 20%, there is a linear increase in the engine IMEP with an increase of biomass content. However, also apparent is a decrease in IMEP at 5% algae content relative to water only (0%) aspiration. Notwithstanding this decrease with a 5% biomass concentration suspension, this cautiously suggests that an increase in the concentration algal cells results in more useful energy towards the engine output.

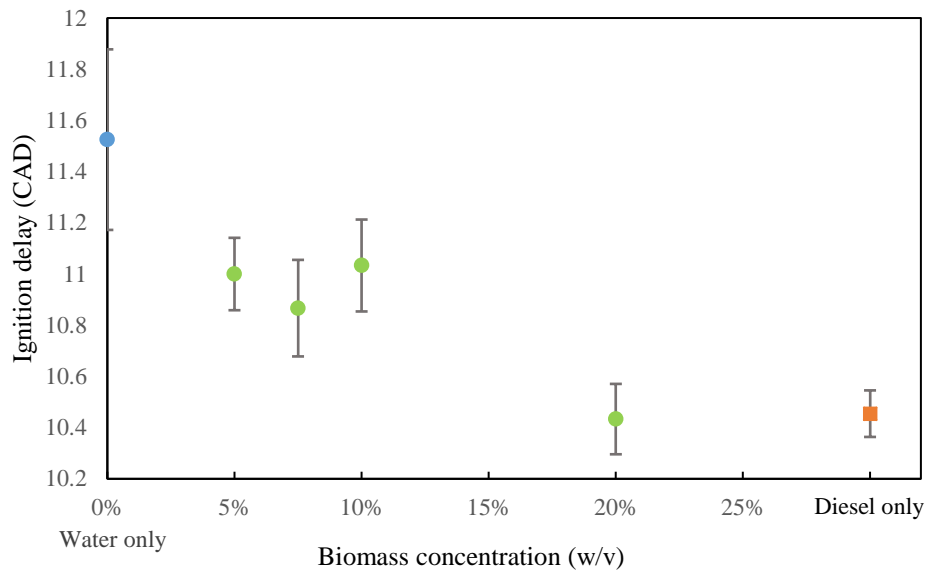


Figure 2.6 Ignition delay duration with aspirated algal biomass suspensions of varying concentration. The error bars present show plus and minus the standard deviation from the mean value.

Figure 2.6 shows the ignition delay during combustion with the aspiration of algae water suspension of varying biomass concentration into the engine intake air, and also that of reference diesel direct injection without water or suspension aspiration. The ignition delay is defined as the time between start of ignition (SOI) and start of combustion (SOC), where SOC is the incidence of positive heat release observed after SOI. It can be seen in Figure 2.6 that aspiration of all of the suspensions into the engine, except that with 20% algae content resulted in a longer duration of ignition delay relative to diesel only. This is likely attributable to the water present in the algae suspension, which absorbs heat from the in-cylinder charge on evaporation and results in a higher specific heating value, reducing temperatures at TDC and slowing the rates of diesel low temperature branching reactions which culminate in fuel autoignition (Westbrook, 2000). Notwithstanding the range of error present, it is interesting to note that an increase in the biomass suspension concentration appears to result in a reduction in the

duration of ignition delay. It is anticipated that potential energy release from the aspirated biomass would only occur following autoignition of the fossil diesel, and so it is tentatively suggested that this effect of the aspirated biomass may in fact be through changes in local temperature distribution and heat transfer.

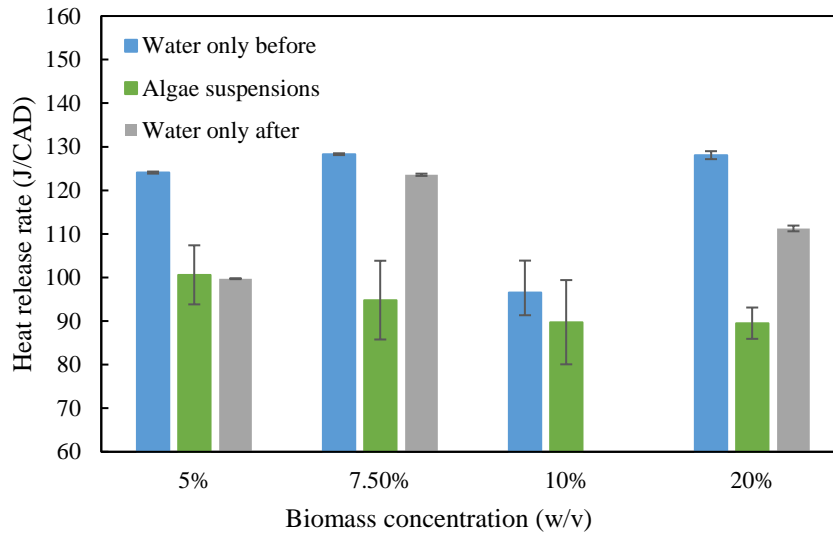


Figure 2.7 Peak heat release rate with aspirated algal biomass suspensions of varying concentration. The error bars present show plus and minus the standard deviation from the mean value.

Figure 2.7 shows the impact of varying the biomass concentration aspirated through the air intake on peak heat release rates, and also that from water only aspiration immediately before and after each test of algae suspension. In the case of 10% algal biomass aspiration, the water only test result after algae test could not be recorded due to the biomass accumulated inside the engine after a long period of running and abnormal noise was detected during the operation. To ensure that the experimental conditions were consistent during each biomass aspiration test, the engine was operated with direct injection diesel only for several minutes after water only tests until the IMEP stabilised at 4 bar with the same diesel fuel injection duration as previously observed. Apparent in most instances in Figure 2.7, is a reduction in peak heat release rate with aspiration of the algal biomass

suspensions relative to water only, likely attributable to a smaller premixed burn fraction where a reduced duration of ignition delay (Figure 2.6) decreased the time available for fuel and air mixing prior to the start of combustion. Meanwhile, in the case of all biomass concentrations, results of water only tests before algae aspiration are always higher than those immediately after, which is suggestive of a possible accumulation of algal biomass in the engine intake system during aspiration as the manifold was only been cleaned after each change of algae concentration. Additionally, aspiration of water only will also cause a side effect on the engine, but it was eliminated by running with fossil diesel only for at least ten minutes. This is to allow the IMEP to recover with the same injection duration.

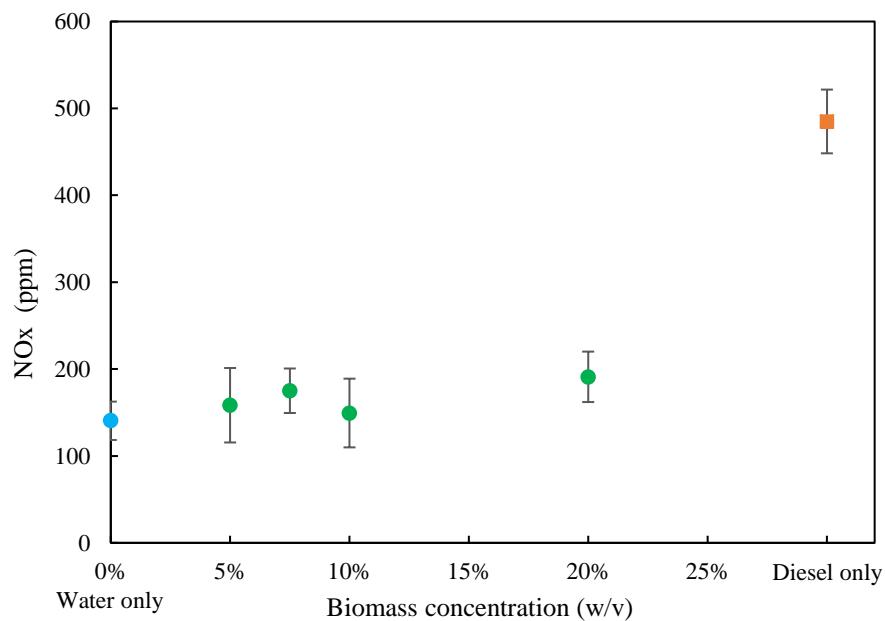


Figure 2.8 NO_x exhaust emission level with aspirated algal biomass suspensions of varying concentration. The error bars present show plus and minus the standard deviation from the mean value.

Figure 2.8 shows the effect of varying algal biomass concentration on levels of NO_x in the exhaust gas. It is clear to see that water only has the lowest NO_x exhaust level and that there is a small increase with increasing biomass concentration. In

all cases of intake aspiration, the level of NO_x is much lower compared to diesel only. The formation of NO_x during combustion in a diesel engine is related to the rates of thermal oxidation of nitrogen and has a strong positive correlation with in-cylinder temperature and peak heat release rates (PHRR) (Hellier et al., 2012a). However, in Figure 2.3, it can be seen that in most cases intake aspiration resulted in a higher PHRR than the reference fossil diesel only, which exhibited the highest NO_x exhaust level. Therefore, it is suggested the higher rates of heat release were insufficient to overcome the significantly lower in-cylinder temperatures as a result of the water evaporation and higher specific heat capacity of the in-cylinder charge (Tesfa et al., 2012).

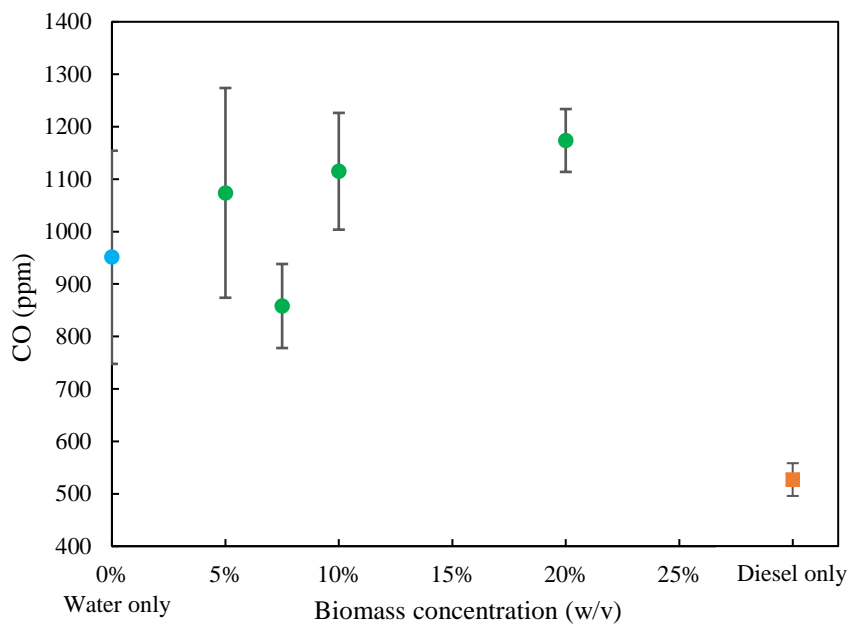


Figure 2.9. CO exhaust emission level with aspirated algal biomass suspensions of varying concentration. The error bars present show plus and minus the standard deviation from the mean value.

Figure 2.9 shows the effect of varying algae content suspensions aspirated via the air intake on exhaust gas levels of CO. Notwithstanding, the range of error shown, Figure 2.9 shows that with aspiration of water or algae suspensions, CO levels

increased significantly relative to diesel only. This is likely attributable to the lower in-cylinder temperatures during water or suspension aspiration, as indicated by reduced levels of NO_x emissions (Figure 2.8), resulting in higher levels of incomplete combustion.

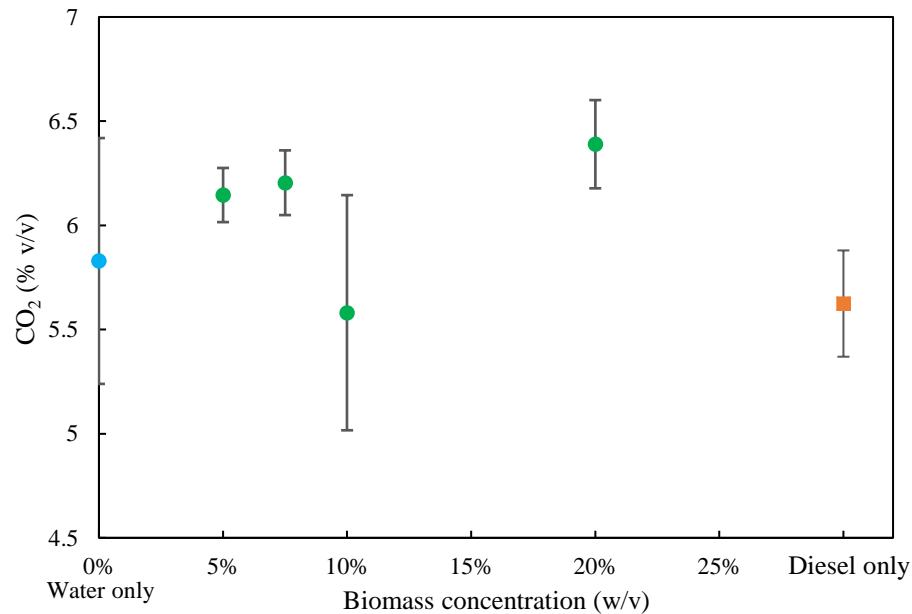


Figure 2.10 CO₂ exhaust emission level with aspirated algal biomass suspensions of varying concentration. The error bars present show plus and minus the standard deviation from the mean value.

Figure 2.10 shows the level of CO₂ in the exhaust gas with the aspiration of varying biomass concentration suspensions into the engine intake air. In order to maintain a constant load of 4 IMEP, a longer injection duration under the water only condition relative to diesel only combustion was required, and a concurrent increase in CO₂ levels can be seen in Figure 2.10. Notwithstanding the values of CO₂ recorded in the case of the 10% w/v algae suspension, it is tentatively suggested that levels of CO₂ increased with biomass suspension concentration, in agreement with increasing IMEP (Figure 2.3), possibly attributable to greater combustion efficiency or the presence of more algal biomass available for combustion.

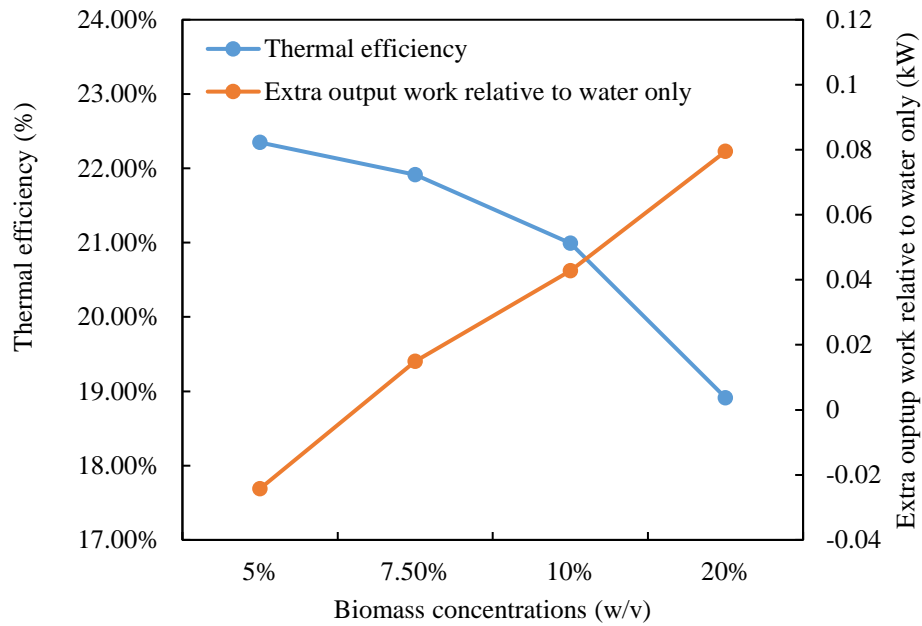


Figure 2.11 Thermal efficiency of diesel engine and extra output work relative to water only with aspirated algal biomass suspensions of varying concentration.

Figure 2.11 shows the impact of aspirated concentration of algal biomass suspensions on the thermal efficiency of diesel engine and extra output work compared with water only condition. It can be seen that a reduction of thermo efficiency occurred with an increasing of the biomass concentration. With the increasing of CO emission relative to water only test (Figure 2.9), it suggests that more incomplete combustion occurred and decrease of the combustion efficiency during the algae combustion. Meanwhile, the extra output work from algal biomass was increased by increasing the biomass concentration and reached 0.08 kW relative to water only with 20% biomass concentration. However, 5% biomass concentration gave a negative impact on total engine output and the energy inputs from 7.5%, 10% and 20% algal biomass were 1.12, 1.5, and 2.99 kW (assuming 5% lost during combustion), which the extra outputs were only equivalent to 1.33%, 2.86% and 2.65% respectively of additional energy provided from algae.

2.3.2 Effects of algal biomass injection flowrates in aspirated suspensions on combustion and emissions

Following the engine tests of aspirated algal biomass suspensions with varying concentration, experiments investigating the aspiration of algal biomass suspension with varying injection flowrate (40, 49.2, 56 mL/min) were conducted with a constant biomass concentration of 5% w/v. Reference tests of water only and diesel only were also conducted.

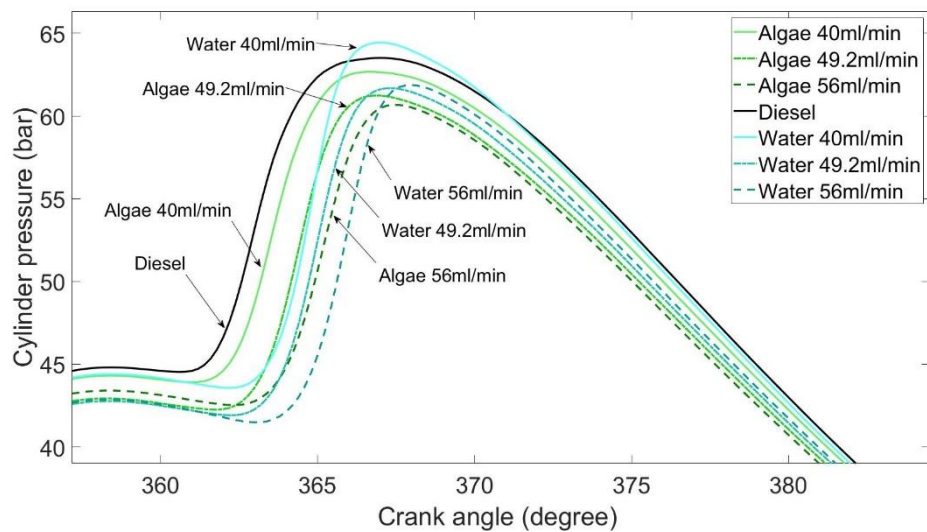


Figure 2.12 In-cylinder pressure with aspirated algae biomass suspensions and water of varying flowrate.

Figure 2.12 shows the in-cylinder pressure of varying injection flowrate of aspirated algae suspension at 5% biomass concentration, and water only, at constant fuel direct injection duration. Except in the case of 40 mL/min water only, peak in-cylinder pressure occurs much later and is lower relative to diesel only. A flowrate of 56 mL/min algae suspension gives the lowest peak in-cylinder pressure, suggesting that the engine output was reduced due to the lower compression pressure achieved caused by the high flowrate of algal biomass aspiration.

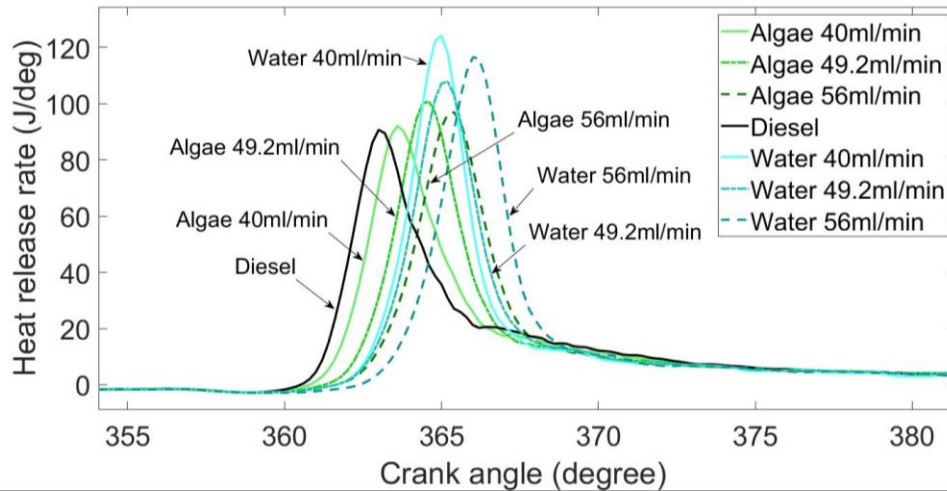


Figure 2.13 Apparent net heat release rate with aspirated algae biomass suspensions and water of varying injection flowrate.

Figure 2.13 shows the apparent heat release rates of water and 5% biomass content suspensions aspiration at variable injection flowrates, and fossil diesel only. It can be seen from Figure 2.13 that premixed combustion dominates in all cases and algae suspension. In the case of 40 mL/min algae biomass aspiration, HRR reduces more slowly after reaching a peak heat release rate relative to algal biomass suspensions at higher flowrates, and water only. This suggests that an increase in water flowrate increases the premixed burn fraction, and thus there is a much smaller diffusion-controlled combustion and so a more abrupt decrease in HRR.

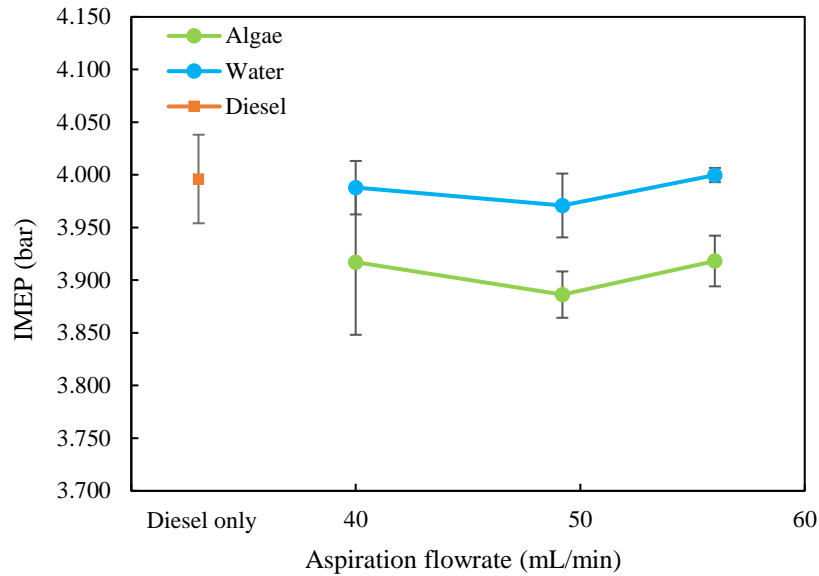


Figure 2.14 Engine IMEP with aspirated algae biomass suspensions and water of varying injection flowrate. The error bars present show plus and minus the standard deviation from the mean value.

Figure 2.14 shows the effect of varying the algae biomass and water injection flowrate of the intake aspiration suspensions while maintaining a constant duration of fossil diesel direct injection on engine IMEP. It can be seen that for the water only condition, the duration of the diesel injection duration was increased to remain at 4 IMEP, and so there was no apparent effect of changing the flowrate of water only aspiration. Meanwhile, the aspiration of 5% algal biomass consistently reduced IMEP relative to diesel and water only cases, where the duration of diesel injection was kept constant. In addition, the exhaust gas temperatures in the cases with algae present had an average 15°C increase relative to the water only case, which indicates that with 5% algal biomass content, combustion of the algal suspensions resulted in a greater amount of energy lost in the exhaust. However, no clear effect of increasing injection flowrate under constant algal biomass concentration condition could be seen, despite an anticipated change in the levels of suspensions present per combustion cycle.

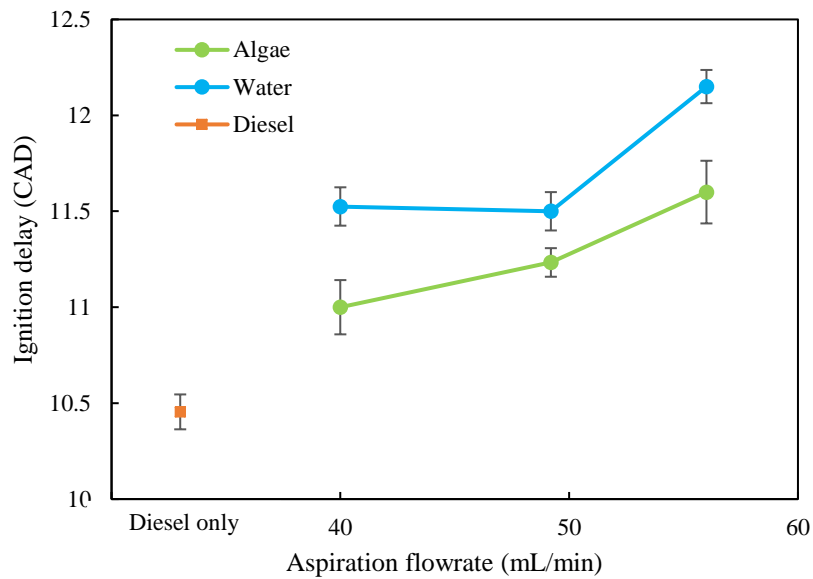


Figure 2.15 Ignition delay duration with aspirated algae biomass suspensions and water of varying injection flowrate. The error bars present show plus and minus the standard deviation from the mean value.

Figure 2.15 shows the ignition delay during combustion with the aspiration of algae suspension and water only of varying injection flowrate into the engine intake air. It can be seen from Figure 2.15 that aspiration of the algal biomass suspension and water both resulted in an increase in ignition delay relative to diesel only. Furthermore, an increase in the flowrate of either further increased the ignition delay; this is to be expected as a higher flowrate of water or suspension would increase the level of in-cylinder cooling. However, at a constant injection flowrate, water only results in longer ignition delay than algae suspension. This is due to the algae cells displacing water and increasing the suspension density relative to water only, so the level of water present in-cylinder is relatively less than water only condition and therefore resulted in reduction of ignition delay.

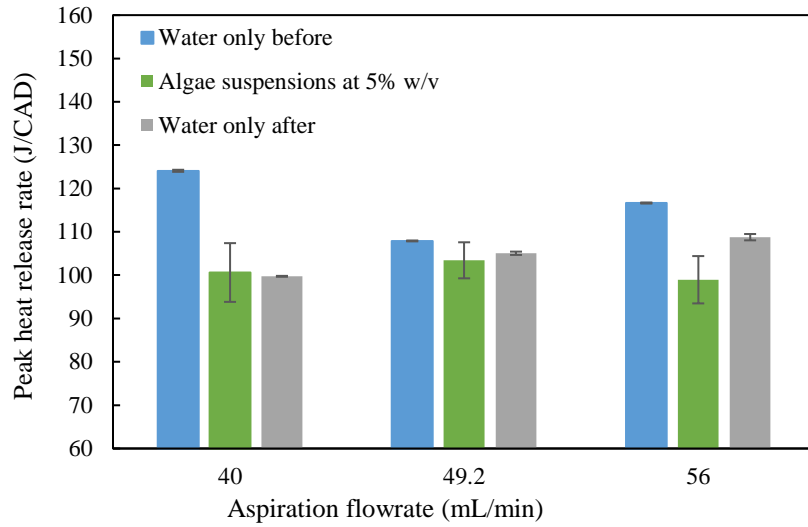


Figure 2.16 Peak heat release rate with aspirated algae biomass suspensions and water of varying injection flowrate. The error bars present show plus and minus the standard deviation from the mean value.

Figure 2.16 shows the impact of variable flowrate of algal biomass and water immediately before and after algae combustion test on peak heat release rate. In all the flowrate conditions, the results of water only after algae test has lower PHRR than the one before algae test, which suggest that there is a memory effect after combustion of algae suspension due to accumulation of algal biomass or water in the engine. This memory effect was eliminated as explained in Section 2.3.1. It can be seen in Figure 2.16 that the changes of algae aspiration flowrate do not have a clear impact on PHRR of the suspensions or of the subsequent water only tests, outside of the range of experiment variability shown.

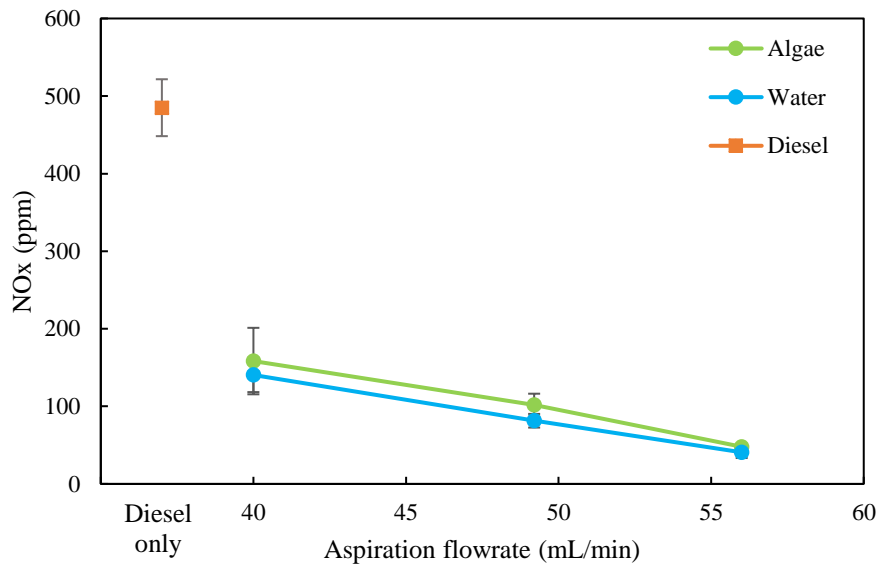


Figure 2.17 NO_x exhaust emission level with aspirated algae biomass suspensions and water of varying injection flowrate. The error bars present show plus and minus the standard deviation from the mean value.

Figure 2.17 shows the effect of varying algae biomass and water injection flowrate on levels of NO_x in the exhaust gas. It can be seen from Figure 2.17 that there is a linear decrease in NO_x emission levels with increasing injection flowrate for water only and algae suspension. It is also clear to see that the tests with algae suspension or water have much lower NO_x level in the exhaust gas relative to diesel only. Delivering more water into the engine per cycle would increase the total amount of water vapour and be expected to further reduce in-cylinder temperature, and thus decrease NO_x production. Furthermore, under the condition of constant aspiration flowrate, algae suspension give higher NO_x level than water only. According to the previous ignition delay results (Figure 2.15), aspiration of water only resulted in a higher ignition delay and lower NO_x emission level relative to algae suspension, which suggests that the in-cylinder temperature in water only condition is lower than in the case of the algae suspension aspiration at all flowrates tested.

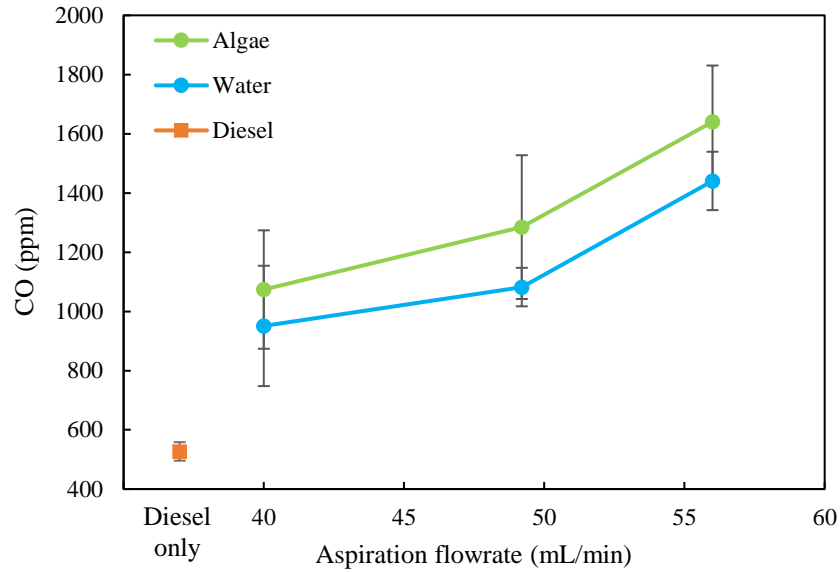
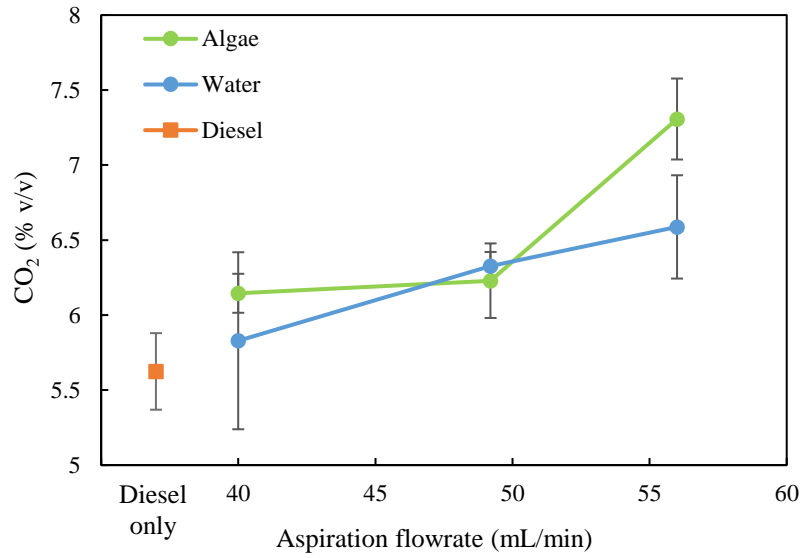
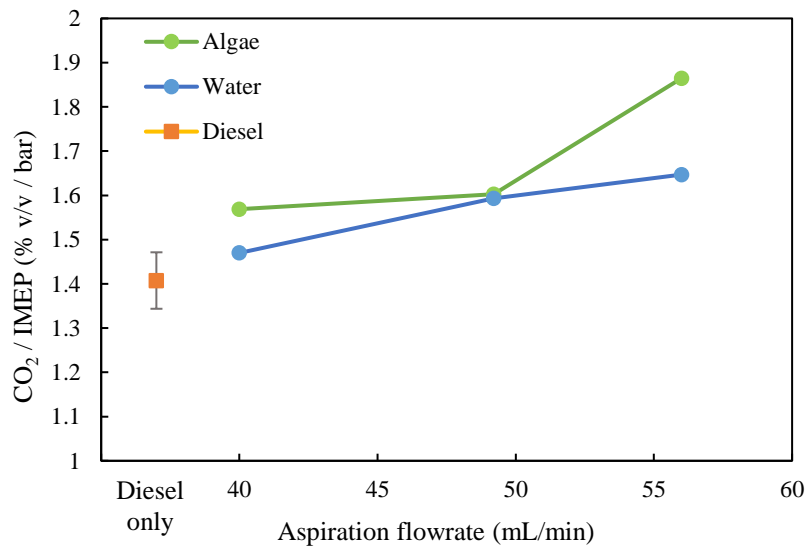


Figure 2.18 CO exhaust emission level with aspirated algae biomass suspensions and water of varying injection flowrate. The error bars present show plus and minus the standard deviation from the mean value.

Figure 2.18 shows the effect of varying algae suspension and water injection flowrate aspirated via the air intake on exhaust gas levels of CO. It can be seen from Figure 2.18 that all the conditions of algae and water aspiration have higher CO emission levels relative to diesel only, and that there is increase in these with increasing aspiration flowrate. This observation is in agreement with previous studies where the water content of the combustion chamber reduced the in-cylinder temperature and resulted in more incomplete combustion, which will increase CO formation (Tree et al., 2007). Meanwhile, at constant flowrate, combustion of the algae suspension produces more CO than water only. It is plausible that the size of aggregated algae cells (50 ~ 100 μm) are much bigger than the size of diesel droplets (10 ~ 20 μm) (Arai, 2012) and the presence of algae cells inhibits the air mixing with fuel, thereby causing incomplete combustion of the cells and producing more exhaust CO.



(a)



(b)

Figure 2.19 (a) CO₂ exhaust emission level with aspirated algae biomass suspensions and water of varying injection flowrate (b) CO₂ exhaust emission level normalized with respect to the engine IMEP. The error bars present show plus and minus the standard deviation from the mean value.

Figure 2.19 shows the effect of variable injection flowrate of algae suspension and water at constant biomass concentration on CO₂ emission levels in the exhaust gas. It can be seen that the algae test under 56 mL/min injection flowrate gives the

highest CO₂ level. Notwithstanding the extent of the error bars shown, with the flowrate increasing, all the CO₂ levels in algae suspension and water aspiration test increase relative to diesel only (Figure 2.19 a). It is likely due to the extension of fuel injection duration to maintain the IMEP at 4 bars and combustion of more algae biomass delivered into the engine produce more CO₂ emission. However, in Figure 2.19 (b) it can be seen that CO₂ emission during aspiration of water only and the algae suspensions remain higher than that during diesel only combustion when normalised with respect to engine IMEP, suggesting a decrease in the thermal efficiency of the engine under these conditions. However, it should be noted, that as the level of water in the exhaust increases, the levels of CO₂ on a volumetric percentage basis might increase because the analyser removes the water prior to measurement, even if the CO₂ levels remain constant on an absolute basis.

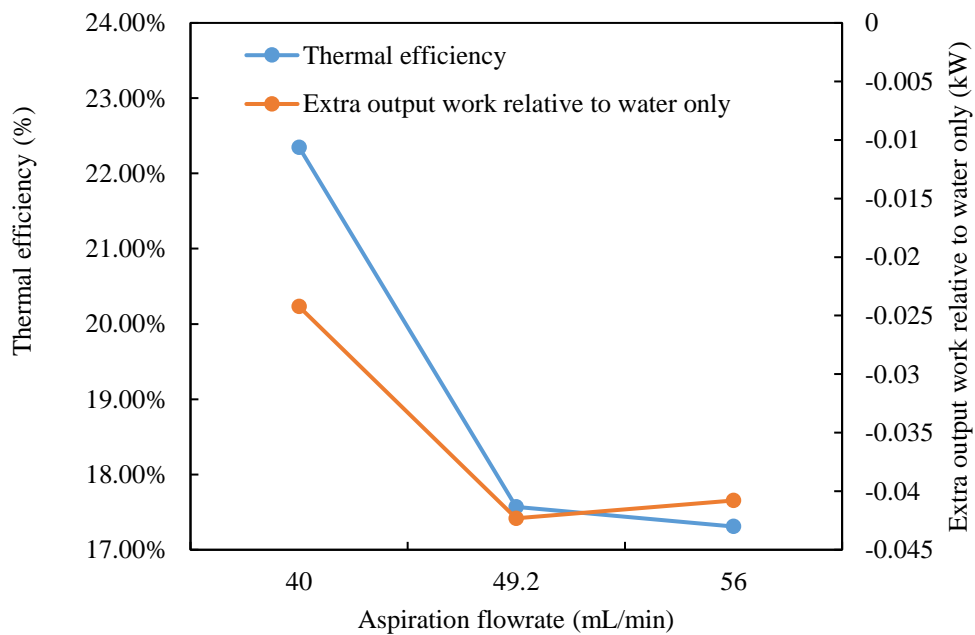


Figure 2.20 Thermal efficiency of diesel engine and extra output work with aspirated algae biomass suspensions of varying injection flowrate.

Figure 2.20 shows the effect of varying injection flowrate of algal biomass aspirated via the air intake on thermal efficiency of diesel engine and the extra output work relative to water only. In all flowrate conditions, there were less extra output work of diesel engine than water only, which suggest that the algal biomass has negative impact on the engine combustion under low biomass concentration and results in reduction of total engine output. Meanwhile, a decreasing of thermal efficiency was observed with increasing of aspiration flowrate. Along with the increasing level of CO emission (Figure 2.18), it indicates that increasing aspiration flowrate significantly affects the combustion quality and produced more incomplete combustion during engine operation.

2.4 Conclusion

The direct aspiration of algal biomass slurry in the air intake of a diesel engine was investigated as an alternative route of utilising the energy content of microalgae without a complete dewatering process to lower the cost and energy input of algae biofuel production. From the research of combustion and emissions characterisation of algae slurry in a modern compression ignition engine, the results can be summarised in the following conclusions:

1. At algal biomass suspension concentrations of more than 7.5% w/v, an increase in IMEP was observed, suggesting a positive contribution of the aspirated algae biomass to useful work output.
2. However, at 5% w/v algal biomass concentrations, the presence of the algal cells resulted in a reduced IMEP relative to an equivalent aspiration flowrate of water only. It was possibly due to the greater degree of energy lost in the exhaust during the combustion of algae suspension.
3. All the engine combustion with the aspiration of water (with and without algae) reduced NO_x emission levels relative to reference diesel. With increase of biomass concentration, NO_x levels increased. However, increasing aspiration flowrate resulted in a reduction of NO_x emission.
4. Both CO and CO₂ emissions levels increased in all cases, which indicates that the presents of algae cells contribute additional carbon source to increase the CO₂ emission level. Meanwhile, the presence of the algae increases levels of incomplete combustion.
5. There is a potential of build-up of biomass residues in the engine after

aspiration, which may affect the engine operation and decrease combustion efficiency.

The experimental results proved the possibility of increasing the total engine output by aspirating algal biomass into the engine; however, it decreased the thermal efficiency of the engine combustion. In order to receive better result of delivering algal biomass into IC engine, the air intake should be redesigned to avoid any blind angle between the biomass injection point and combustion chamber. It also suggests examining the aspiration of algae suspension in a smaller engine with large surface area to volume ratio to achieve better combustion efficiency. Moreover, it is not ideal to transport significant volumes of algae suspension over long distance due to the sedimentation of algae cells. Therefore, it is suggested that rather it could be used for stationary power generation nearby the algae cultivation.

Chapter 3 Algae biomass production and development of algae/diesel emulsion

3.1 Introduction

Considering the high-energy consumption in the algal biodiesel production processes, direct utilisation of algal biomass in the IC engine was developed in recent years. Although the diameter of algae cells is in the range of 3 ~ 10 micrometres (μm) and it is much smaller than the pore size of the fuel injector, previous work suggested that dried algae biomass was not suitable for mixing with liquid fuel (Scragg et al., 2003). Therefore, to deliver algal biomass into the engine for energy production, stable water/diesel emulsions are required as a carrier for algae cells. Comparing with the novel approach described in Chapter 2, this method does not require an additional set up for introducing algal biomass into the diesel engine and it has potential to reduce the water content compared to using aspirated algal biomass and thereby increase the energy efficiency of the engine.

3.1.1 Water/oil emulsions

The emulsion is defined as a mixture of two incomplete immiscible liquids, with dispersion of one liquid (small spherical droplets) into another (Fingas et al., 2004). To generate a stable emulsion, high-energy methods, such as mechanical agitation and high-pressure homogenizers, and emulsifier are required (Kapadia et al., 2019). There are two different forms of two-phase emulsion: water-in-oil (W/O) and oil-in-water (O/W). The former type of emulsion contains water as a dispersed phase in oil phase and the latter contains oil as a dispersed phase in aqueous phase. The schematic diagram of W/O and O/W emulsions is shown in Figure 3.1.

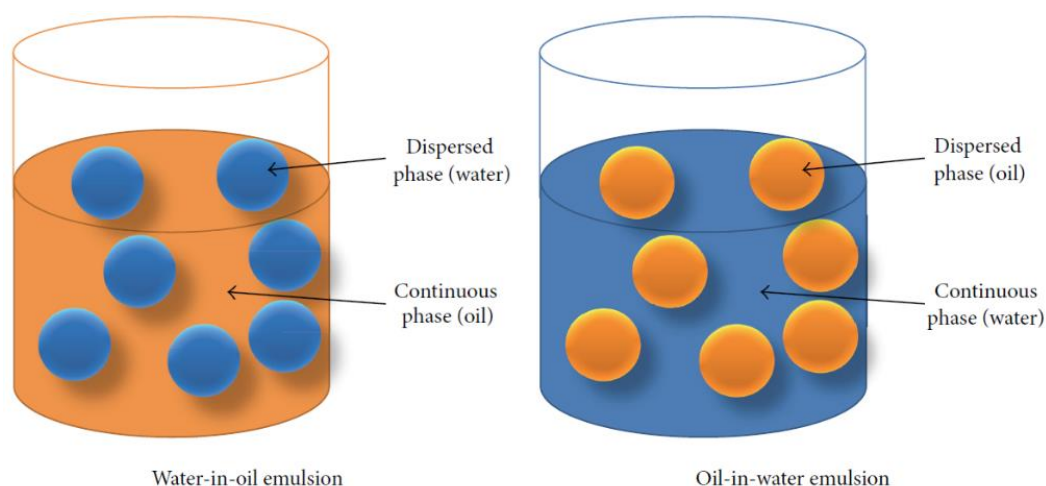
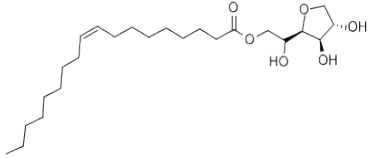
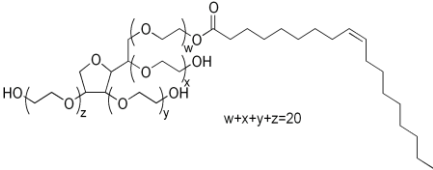
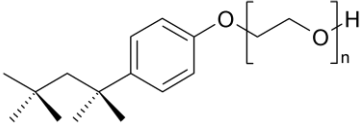


Figure 3.1 Schematic diagram of two-phase water-in-oil and oil-in-water emulsions (Yahaya Khan et al., 2014).

Surfactants

Generally, a surfactant is a substance that includes both polar and nonpolar groups in their molecules, which is used to lower the surface tension between water and oil molecules (Norazni et al., 2017). Therefore, to form a stable water/oil emulsion, it is crucial to find a suitable surfactant with appropriate hydrophilic-lipophilic balance (HLB) value and molecular structure. Within the scale of 20, hydrophilic surfactants have high HLB value, which tends to make stable oil-in-water emulsion due to the high attraction to polar liquids. In contrast, lipophilic surfactants tend to make stable water-in-oil emulsion because of low HLB and more attraction to nonpolar liquids (Dai et al., 1997). Meanwhile, the surfactant quantity in emulsion varies in the range of 0.5% to 2% of the total volume and a higher percentage will decrease the emulsion stability due to rapid coalescence (El-Din et al., 2013). Based on these characteristics, non-ionic surfactants of Span 80, Tween 80 and Triton X-100 are commonly used for preparing W/O emulsion and their chemical properties are shown in Table 3.1.

Table 3.1 Physiochemical properties of Span 80, Tween 80, Triton x-100 surfactant.

Chemical name	HLB	Chemical formula	Function	Chemical structure
Span 80 Sorbitan monooleate	4.3	$C_{24}H_{44}O_6$	Emulsifying agent	
Tween 80 Polyoxyethylene monooleate	15	$C_{64}H_{124}O_{26}$	Detergent	
Triton X-100 Polyoxyethylene octyl phenyl ether	13.4	$C_{14}H_{22}O(C_2H_4O)_n$	Wetting and spreading agent	

Water/diesel emulsions

The water/diesel (W/D) emulsion system has been intensively investigated in the past few years and many commercial applications were successfully produced for the reduction of exhaust air emission during fuel combustion (Zhao et al., 2006). The stability of W/D emulsion has been studied with different surfactants and mixing speed by researchers. Hasannuddin et al. (2014) reported that the increase of mixing speed and the decrease in water content could increase the emulsion stability. Abdurahman et al. (2016) studied W/D emulsions containing water concentrations of 5%, 20% and 40% with 3% Triton X-100 and mixing speed at 3000 rpm for 20 minutes. The result shows that 5% water gave the longest stable emulsion duration of 60 days, and 40% water had the worst stability of 30 days. A further investigation carried out by Ghannam et al. (2009) tested the emulsion stability with water concentrations from 10 to 50% (v/v), 0.2 – 5% of Triton X-

100 and mixing at 15,000 – 20,000 rpm for 2 –30 minutes. Under the condition of 0.2% surfactant, 15,000 rpm, and 2 minutes of mixing time, 10% W/D emulsion had the longest stable duration of 4 weeks. Meanwhile, higher water concentrations required more surfactant concentration and mixing time. Span 80 and Tween 80 were applied as surfactants in Badrana et al. (2011)'s research to generate W/D emulsion with 25% of demineralised water and tap water at 2000 rpm mixing speed for 15 minutes. The result showed that the emulsion with demineralised water gave 12 days stability and that with tap water was stable for 10 days. There are a few other researchers that reported successful production of W/D emulsion with salt, sugar or Span 20 and Tween 20, but the water content was very low ($\leq 10\%$ v/v) or the results did not provide enough data of agitation speed or stability of the emulsion, which are not representative.

3.1.2 Algae/diesel emulsion

Previous investigations on the potential of algae/diesel emulsion are limited. The first study was carried out by Scragg et al. (2003), who produced an emulsion consisting of *trans*-esterified rapeseed oil, a surfactant and a slurry of *Chlorella vulgaris*. The W/D emulsion was first prepared with 80% v/v of rapeseed ethyl ester, 20% v/v of water and 0.5% v/v of the surfactant Triton X-100 and it was stable for at least 14 days. 2 g per litre of dry algal biomass was then added into the W/D emulsion, which was stable enough for the engine test. The study followed by Al-lwayzy et al. (2014b) reported a stable algae/diesel emulsion containing 79.2% v/v of cottonseed biodiesel, 19.8% v/v water, 1% v/v Triton X-100 and 0.4 g per litre of dry algal biomass. More recently, Xu et al. (2016b) invented a novel surfactant package to prepare stable wet algal biomass slurry of *C. sorokiniana* and diesel emulsions. Each 1.5 mL of this package contained 0.45 mL of non-ionic Span80, 0.3 g of cationic CTAB, 0.6 mL of butanol and 0.45 mL of water and was premixed before adding into the mixture. The algae/diesel

emulsion consisted of 85% v/v diesel, 15% v/v surfactant package and 0.2 g algal biomass in 10 mL and mixed at high speed (2500 rpm) for 2 minutes. The result showed that the emulsion system can stay stable for several days without phase separation or algal cell settlement.

This chapter presents the investigation of the *C. sorokiniana* algal biomass production and the preparation of water/diesel emulsion and algae/diesel emulsion with different surfactants. Particular attention was paid to the impact of varying surfactant and algal biomass concentrations on the stability and viscosity of stable algae/diesel emulsions.

3.2 Material and methods

3.2.1 Algae characteristic and cultivation

Algae strain and culture medium

A wild freshwater type strain of microalgae *Chlorella sorokiniana* (UTEX1230) was selected and investigated in this research project, which was obtained from Culture Collection of Alga at the University of Texas (Austin, Texas, USA).

Four different culture media were used for culturing and maintaining *C. sorokiniana*: Tris Acetate Phosphate (TAP) (Raikova et al., 2016), Tris minimal (Tris-MIN) medium (Gorman et al., 1965) 10% Nitrogen TAP medium and TAP medium with glucose. The recipes of the culture media are shown in Table 3.2. Except Tris-MIN medium, the other culture media contain acetic acid as an extra carbon source for cell growth and Tris-MIN medium is for autotrophic growth only, which does not contain any organic carbon source and hydrochloric acid (HCl) was used to adjust the pH to 7.0 rather than acetic acid. According to the previous work by Xu et al. (2016b), a modified TAP medium is applied to enhance cellular

lipid accumulation under the nitrogen starvation condition. It contains only 10% nitrogen source of that in normal TAP medium, which is 0.75 mM instead of 7.5 mM. In order to increase the algal biomass production rate, 5 g/L of glucose was added in the TAP medium for the heterotrophic condition.

Table 3.2 Basic medium composition of TAP, 10%N TAP medium and TAP + Glucose medium.

Component	TAP Medium	10% N TAP Medium	TAP + Glucose Medium
NH ₄ Cl	7.5×10 ⁻³ M	7.5×10 ⁻⁴ M	7.5×10 ⁻³ M
CaCl ₂	4.5×10 ⁻⁴ M	4.5×10 ⁻⁴ M	4.5×10 ⁻⁴ M
MgSO ₄	8.3×10 ⁻⁴ M	8.3×10 ⁻⁴ M	8.3×10 ⁻⁴ M
K ₂ HPO ₄	2.5×10 ⁻⁴ M	2.5×10 ⁻⁴ M	2.5×10 ⁻⁴ M
KH ₂ PO ₄	1.7×10 ⁻⁴ M	1.7×10 ⁻⁴ M	1.7×10 ⁻⁴ M
Trace elements*	1 mL/L	1 mL/L	1 mL/L
Tris	2.42 g/L	2.42 g/L	2.42 g/L
Glacial Acetic Acid	to pH 7.0	to pH 7.0	to pH 7.0
Glucose	-	-	10 g/L

* For 1 L trace elements: EDTA·Na₂ 50g, H₃BO₄ 11.14g, ZnSO₄·7H₂O 22g, MnCl₂·4H₂O 5.1g, FeSO₄·7H₂O 5g, CoCl₂·6H₂O 1.6g, CuSO₄·4H₂O 1.6g, (NH₄)₆Mo₇O₂₄·4H₂O 1.1g.

Algae cultivation and growth condition

The master cell bank of *C. sorokiniana* culture were maintained in a BINDER KBW 240 (E5.1) Climate chamber (BINDER GmbH, Germany). 5 mL of algae cell stock culture were transferred from the master cell bank and inoculated to 250 mL flask with cotton plug containing 95 mL of the Tris-MIN medium at 29 ± 1 °C under continuous shaking (180 rpm). Constant light environment (intensity 30 μmol photons / [m²·s]) was provided by the cool white fluorescence lamps in a

Kuhner ISF-1-V incubator (Adolf Kühner AG, Switzerland). This is used as a working cell bank to maintain and provide the living algae cells for biomass production. For mixotrophic biomass production, algae cells were cultured in 5L shake flasks with 2L of TAP or 10% N TAP medium at 25 °C in a New Brunswick™ Innova® 44 incubator (Eppendorf Ltd., UK), which provided continuous light and constant shaking speed of 120 rpm. For heterotrophic production, 5L shake flasks were covered by Aluminium foil to prevent any light entering from the environment. Each flask contained 2L of TAP + glucose medium and placed in the ISF-1-V incubator shaker at 37 °C. Due to the small size of holders on the shaker, the flasks were stuck on the tray surface by using double sided tape and the shaker was operated at 100 rpm.

Evaluation of algal growth

During the cultivation, samples were taken regularly to monitor cell growth. The optical density was measured at 750 nm (OD 750 nm) wavelength by using UV/Vis spectrometer (Thermo Electron Co. UK). The calibration curve was generated to describe the relationship between biomass concentration and optical density (see Appendix A). Data were obtained for all culture conditions.

Two parameters were investigated: specific growth rate (μ) and doubling time (T_d). The maximum specific growth rate (μ) is calculated by:

$$\mu = \frac{\ln(OD_t/OD_0)}{\Delta t}$$

Equation 3.1

where OD_t is the optical density at time t (h). OD_0 is the optical density at time zero.

The doubling time (T_d) is calculated by:

$$T_d = \ln 2 / \mu$$

Equation 3.2

Where μ is the specific growth rate.

3.2.2 Algal biomass harvesting and determination of biomass

Harvesting process

The cell culture grown in 2L medium was harvested after reaching stationary phase. It was harvested via centrifugation of large volume broth (>100 mL) by using a Beckman Coulter Avanti[®] Centrifuge (Beckman Coulter, USA), JA-10 motor under 5000g centrifugal force and 4 °C for 20 minutes. The cell pellets were then resuspended in small volume (≤ 50 mL) of RO water and transferred into 50 mL Falcon[™] centrifuge tube. These algal suspensions were centrifuge again with 3220 g at 4 °C for 15 minutes via Eppendorf 5810R centrifuge (Eppendorf, 2012) and the supernatant removed. This washing step was repeated three time to remove any culture medium remained in the cell pellets. The concentrated cells were either freeze dried by FDS System LyoStar[™]3 (SP Scientific) or refrigerated at – 20 °C for further analysis.

Determination of growth standard curve

In order to determine the growth standard curve, the algal biomass cultured in TAP medium was centrifuged and resuspended with TAP medium in 12 mL of total volume. The new algae suspension was then diluted with TAP medium in seven dilution ratios and transferred into different Eppendorf tubes. The dilution ratios are shown in Table 3.3.

Table 3.3 Dilution rate for growth standard curve.

Dilution	Biomass volume (mL)	TAP medium (mL)
x1	5	0
x2	2.5	2.5
x4	1.25	3.75
x8	0.625	4.375
x10	0.5	4.5
x20	0.25	4.75
x50	0.1	4.9

Each dilution sample contained 5 mL algae suspension, which was separated into three 1.5 mL Eppendorf tubes. Each tube contained 1 mL suspension and another 2 mL were used for optical density test. Each sample was then centrifuged further with a Centrifuge 5424R (Scientific, 2016) for 15 minutes at 5000g. The Eppendorf tubes were weighed before use and after centrifugation (supernatant removed). The wet cell weight of each dilution can be calculated by:

$$m_{wet\ cell} = m_{tube\ and\ sediment} - m_{tube}$$

Equation 3.3

To determine the dry biomass weight, each tube with wet biomass pellet was weighed after drying in an oven (UM 100, Memmert, Germany) for 24 hours at 80°C. Afterwards, a graph of the wet and dry cell weight was plotted against the optical density of each sample. A calibration curve is shown in Appendix A.1.

Determination of the particle size of the biomass

The average diameter of *C. sorokiniana* was determined by using a Mastersizer 3000 (Malvern, UK). The cell sample was taken from the 10% N TAP medium algae culture and diluted to the concentration of OD 10 (wavelength of 750nm) with deionized water. The value of laser diffraction is required to achieve 10-15% for size distribution analysis performance after enough algae suspension was dropped into Hydro MV (large volume unit for controlling the particle sample dispersion) of the Mastersizer.

Determination of lipid production

To quantify the lipid content of algae cells, 100 mL of cell culture with TAP and 10% N TAP medium were obtained and the biomass was harvested by centrifugation at 5000g for 10 minutes and the cell pellet was then resuspended in 1 mL of 25% v/v DMSO (aq). The algae/DMSO solutions were diluted with dilution factor of 21 to prevent results outside of the standard curve range. After that, 25 μ L of Nile Red stock solution (50 μ g/ml of Nile Red in 100% acetone) was well mixed with 1 mL of the sample solutions and incubated at 37 °C for 10 minutes. Then, 121.8 μ L of each sample (three replicates) were added to a 96-Well Plate containing 178.2 μ L 25% v/v DMSO (aq) and the fluorescence intensity was measured at 540 - 700 nm and the excitation wavelength of 530 nm (Cooksey et al. 1987). To set a standard curve, Triolein was used for quantification and the preparation data is shown below.

Table 3.4 Dilution made for triolein standard curve.

Final Triolein conc. (µg/ ml)	Triolein from 100ug/ml stock (µL)	25% DMSO (Aq) (mL)
50	500	0.5
25	250	0.75
10	100	0.9
5	50	0.95
0	0	1

Determination of the heating value of the biomass

Higher heating value (HHV) and lower heating value (LHV) were investigated in this project. To determine the higher heating value of biomass, a bomb calorimeter (IKA[®] C1 compact calorimeter, Staufen, Germany) was used. There were three biomass samples for the test, which were biomass cultured in TAP medium, 10% N TAP medium and TAP + glucose medium. All of the samples were dried in an oven for 24 hours before the test. Around 0.5 g biomass sample was used in each test and the higher heating value was measured following the manufacturer's instruction. (dijkstra, 2015). The correlation between HHV and LHV can be described by using the equation:

$$LHV = HHV - 0.212 \times H - 0.0245 \times M - 0.008 \times Y$$

Equation 3.4

Where HHV = Higher heating value

H = Percent hydrogen

M = Percent moisture

Y = Percent oxygen (from an ultimate analysis which determines the amount of carbon, hydrogen, oxygen, nitrogen and sulphur present (i.e. includes Total Moisture (TM))

3.2.3 Preparation of algae/diesel emulsion

Preliminary experiment

Previous investigation of the preparation of stable algae/diesel emulsion, carried out by Xu et al. (2016b), has successfully increased the algal biomass content in the emulsion. In the report, five surfactants and co-surfactant were tested: Span80 (sorbitan monooleate), Tween80 (polyoxyethylene sorbitan mono-oleate), Triton X-100 (polyethylene glycol tertocetylphenyl ether), CTAB (cetyltrimethylammonium bromide) and butanol (co-surfactant). In order to continue improving the stability of the algae/diesel emulsion, the composition of the surfactant packages was firstly prepared following Xu's report and then examined. CTAB powder was obtained from G-Biosciences (US); Span 80, Triton X-100 and Tween 80 were obtained from Sigma-Aldrich Company Ltd. (Dorset, UK). Diesel was obtained from Haltermann Carless Ltd. (UK), which contains 5.3% of fatty acid methyl ester (FAME).

Algal biomass of *C. sorokiniana* was cultured in TAP medium, harvested and processed into algae powder according to the process described in Section 3.2.2. 0.1M CTAB aqueous solution was prepared from the CTAB powder to use for the emulsion preparation. Each combination of surfactants was blended with algae powder, water and fossil diesel to form a 10 mL final mixture, which contained ~ 0.2 g of algal biomass. Vortex (IKA VF2) was used to mix the mixture at the highest speed (2500 rpm) for at least 2 minutes until it became stable. The stability of each emulsion was visually observed, pictures were taken immediately after mixing, after 5-minute settling, after 10-minute settling, and after 1-hour settling. An optimisation of the composition of selected surfactant mixture was determined by considering the compromise between the amount of surfactants usage and an optimal stability of the emulsions.

Preparation of new combination of algae/diesel emulsions

Due to the high content of surfactant in the previous study, investigation of reduction of the surfactant usage in the algae/diesel emulsion was conducted. According to Scragg et al. (2003)'s research, Triton X-100 could be applied as single surfactant for blending algal biomass with diesel without any co-surfactant. Algal biomass was cultured in TAP + glucose medium and freeze dried for emulsion test. Fossil diesel without FAME was obtained from Petrochem Carless Ltd. (UK). Algae powder was blended with diesel in different concentrations of water content to form mixtures which contained 1-5% (v/v) algal biomass. The mixture was mixed in the 50 mL FalconTM and vortexed at high speed of 2500 rpm) until it became homogeneous emulsion.

Due to the fact that the commercial diesel in Europe normally contains up to 7% FAME (EN 590:2009 Standard), the effect of FAME content on the emulsion stability and exhaust emission in the IC engine combustion was investigated. The fossil diesel with FAME content of 5%, 10% and 20% (v/v) were prepared to form the algae/diesel emulsions in the experiments.

Characterisation of algae/diesel emulsions

The stability of emulsions was observed every hour until a clear phase separation occurred. Water/diesel and algae/diesel emulsions were characterized by visual observation and photo taken under the microscope. To prevent the blockage in the small holes of the engine injector, the viscosity of emulsions was examined before running the engine combustion test at 40 °C by using a Kinexus lab+ Rheometer (Malvern Panalytical Ltd, UK).

3.2.4 Combustion of algae/diesel emulsion

In a single combustion test, 90 mL of algae/diesel emulsion with 2.5% w/v biomass, 30% water content and 2% Triton X-100 surfactant was tested in a single cylinder diesel engine, the technical specifications of which are described in Chapter 2. The negative control consisted of pure diesel fuel and W/D emulsion containing 2% surfactant. The fuel delivery system shown in Figure 3.2 is a high pressure low volume fuel system (HPLVFS), designed and commissioned by Talibi (2015) for testing small volumes of fuel samples under the same injection pressure as maintained in the common rail.

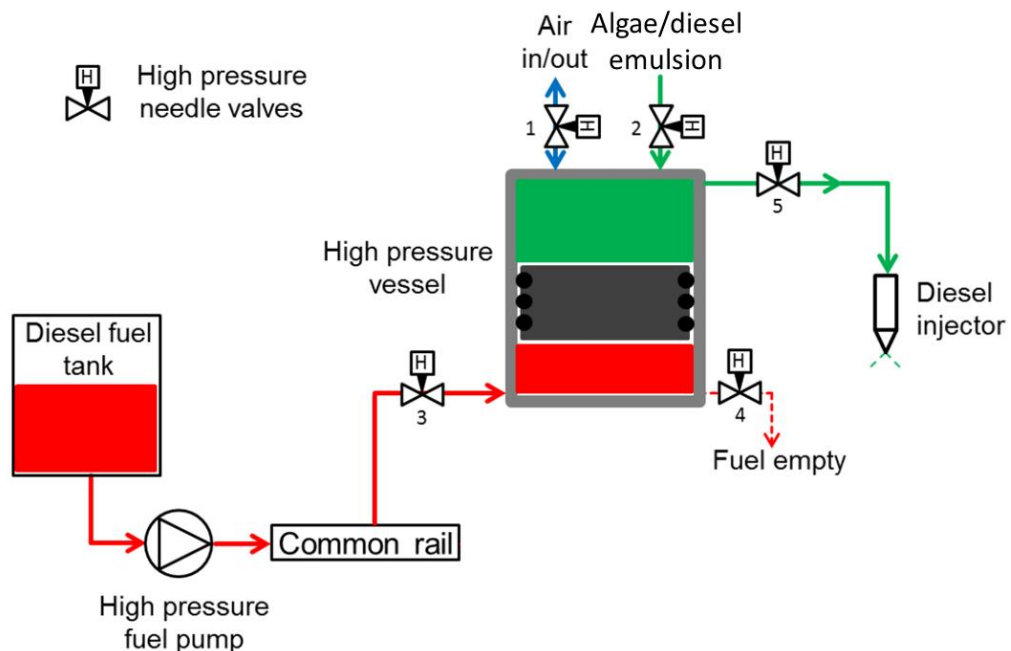


Figure 3.2 A sketch of the high pressure low volume fuel system in schematic form (Talibi, 2015).

The HPLVFS consisted of a stainless steel high pressure cylindrical vessel with a free moving piston inside the cylinder. The bottom chamber, which was isolated from the test fuel by the moving piston, was connected to the common rail system which provided high pressure diesel, fed by the high pressure fuel pump, with this injection pressure then transmitted by the free moving piston to the test fuel. The algae/diesel emulsion was filled into the test chamber of the HPLVFS and

pressurised to vent the air before the experiment. During the engine operation, the fuel system was pressurised to 500 bar and the emulsion was injected into the combustion chamber of the diesel engine via a solenoid valve diesel fuel injector, the inner configuration of which is shown in Figure 3.3.

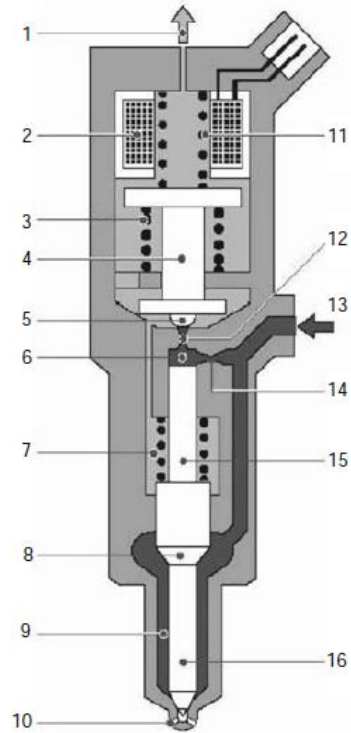


Figure 3.3 A solenoid valve fuel injector (functional principle). 1 Fuel return; 2 Solenoid coil; 3 Overlift spring; 4 Solenoid armature; 5 Valve ball; 6 Valve control chamber; 7 Nozzle spring; 8 Nozzle needle pressure shoulder; 9 Chamber volume; 10 Spray hole; 11 Solenoid valve spring; 12 Outlet throttle; 13 High pressure port; 14 Inlet throttle; 15 Valve piston (control piston); 16 Nozzle needle (Terentyev, 2019).

3.3 Results and discussion

3.3.1 Biomass production of *C. sorokiniana*

Algae cultivation

C. sorokiniana algae cells were grown in TAP medium and 10% TAP medium under autotrophic condition and TAP + glucose medium under heterotrophic condition in 2L shake flasks as described in section 2.1.1. Samples were taken and the OD_{750nm} was measured during cultivation until the cell growth became stationary. After harvesting of algal biomass, a standard growth curve was calculated to show the mathematical relationship between biomass concentration (g/L) in wet/dry weight and optical density (OD_{750nm}), which were plotted as shown in Appendix 1. The standard curves in both type of algal biomass showed a linear relationship between OD_{750nm} and biomass concentration ($R^2 > 0.99$), which suggest that it is reliable to use optical density to predict the biomass concentration and evaluate cell growth.

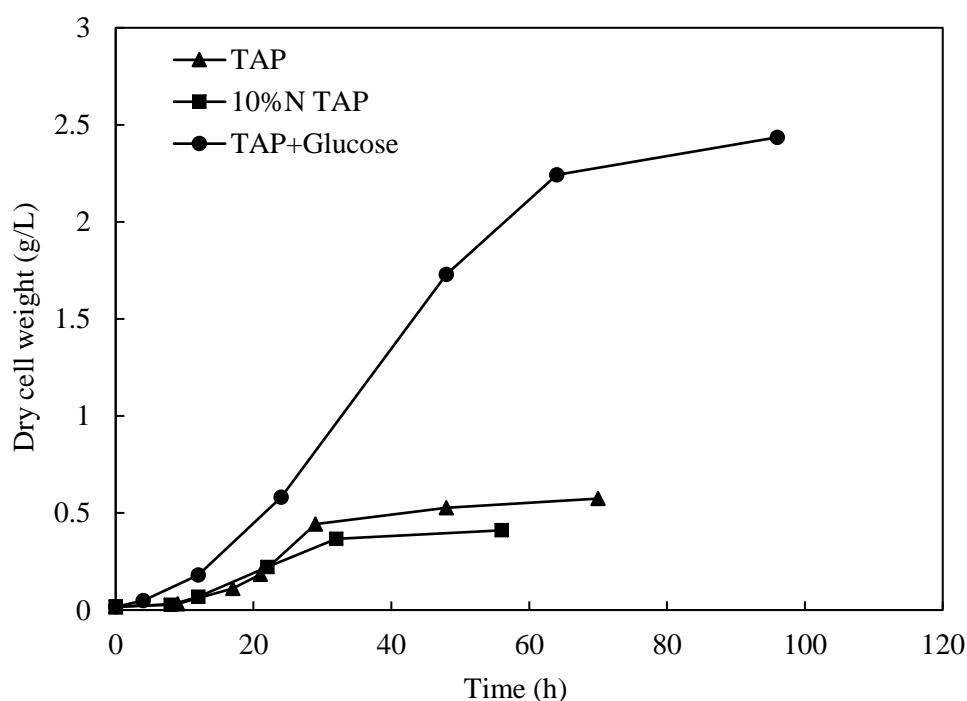


Figure 3.4 Dry cell weight of *C. sorokiniana* during cultivation in TAP medium, 10% N TAP medium and TAP + glucose medium.

Figure 3.4 shows the algae growth in three different culture media in 2L shake flasks. It can be seen that in TAP and 10% N TAP medium, cell growth had a clear lag phase, exponential phase and stationary phase, while in TAP + glucose medium a faster exponential phase occurred, and much higher cell concentration of 2.44 g/L (dry cell weight) was reached due to the extra carbon source. In the first 20 hours, the culture in complete nitrogen-containing TAP medium and nitrogen limited TAP medium (both contain acetate) had similar cell growth, however, the former reached a higher biomass yield (0.57 g/L) in the next few hours. It suggests that the limited nitrogen source in 10% N TAP may restrict the *C. sorokiniana* cell growth and reduce the cell growth rate. Moreover, the algae cells took shorter time to reach the stationary phase in TAP medium. This is most likely due to the fast consumption of nutrition under high cell growth rate.

Evaluation of algae growth rate

The specific growth rate (μ), cell doubling time (T_d) and the maximum biomass concentration after cultivation of *C. sorokiniana* in various media are shown in Table 3.5. These results indicate that large amount of algal biomass require a proportional amount of nitrogen for growth. Meanwhile, an extra carbon source, such as glucose, can extend the exponential phase for longer period during cultivation and significantly increase the cell growth rate.

Table 3.5 Specific growth rate, cell doubling time and maximum biomass concentration of biomass cultured in TAP and 10% N TAP and TAP + glucose medium.

	TAP medium	10% N TAP medium	TAP + glucose medium
Specific growth rate (μ, h⁻¹)	0.159	0.119	0.268
Cell doubling time (T_d, h)	2.532	2.821	2.009
Biomass concentration (g/L)	0.57	0.41	2.43

Algal biomass recovery

All the biomass was cultured in several 2L shake flasks and harvested via centrifugation according to the process described in section 2.1.2. Harvested cell pellets were then washed with RO water to remove any remaining ions from the culture medium. The water content of algal biomass was measured by weighing the biomass before and after freeze drying. Although the centrifugation removed the majority of water, the algae cell pellets still contained 64.8% (w/w) water content. Meanwhile, comparing the weight of the actual dried algal biomass with the estimated dry cell weight results, less than 5% of cells were lost during the whole harvesting processes.

3.3.2 Characterisation of *C. sorokiniana*

Determination the particle size of the biomass

According to a study by Momenikouchaksaraei (2013), the partial size of biomass will significantly impact the internal combustion efficiency. Therefore, it is necessary to investigate the *C. sorokiniana* cell diameter before running the combustion test. As can be seen in Figure 3.5, the average cell diameter of algae cell is around 3 μm , which was determined as described in section 3.2.2.

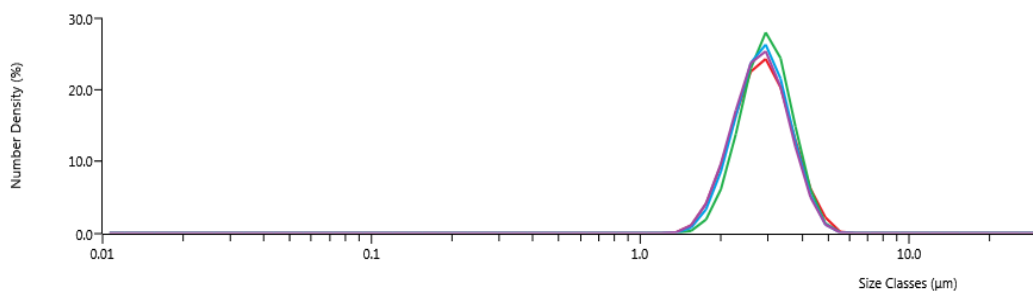


Figure 3.5 Average cell diameter of *C. sorokiniana* measured by Smartsizer 3000.

Determination of algae lipid production

A Nile red test was used to determine the lipid content inside the algae cell. The standard curve was generated to convert the fluorescence reading into lipid content and shown in the A.2. The result shows that the lipid content in the biomass cultured in TAP, 10% N TAP and TAP + glucose were 22.5, 21.4 and 18% (w/w) respectively. However, according to Xu et al. (2016b)'s report, cells cultured in 10% N TAP medium should contain more lipids than other conditions. A possible explanation is that the cells grown in 10% N-TAP may require more time during the stationary phase in order to accumulate the lipids.

Determination the heating value

For the preparation of the combustion test and estimation of the energy release in the IC engine, it is important to determine the heating value of the algal biomass. The HHV takes into account the latent heat of water vapour when heating and cooling fuel to 25°C. In comparison, lower heating value does not take into account the latent heat from the vaporisation of water in the same process. Due to the high temperature inside the engine, the lower heating value was used in the combustion results calculation.

The HHV of algal biomass cultured in different media were determined by using a bomb calorimeter. According to the correlation between HHV and LHV, the heating value of the water present depends on the hydrogen content of each type of sample. The elemental composition of algae biomass can be assumed as $C_{1.63}H_{1.63}O_{0.43}N_{0.15}P_{0.007}S_{0.003}$ (20% lipid content) (Azadi et al., 2015) and the percentage of each element was calculated with their molecular weight and listed in Table 3.6.

Table 3.6 Percentage of the elemental composition in *C. sorokiniana*.

Algae biomass	C	H	O	N	P	S
Molecular weight	12	1	16	14	31	32
Atom number	1	1.63	0.43	0.12	0.008	0.003
Mass	12	1.63	6.88	2.1	0.217	0.096
Total mass	22.923					
Percentage	52.35%	7.11%	30.01%	9.16%	0.95%	0.42%

Table 3.7 Higher and lower heating value of algal biomass cultured in TAP, 10% TAP and TAP+ glucose medium.

	TAP medium	10% N TAP medium	TAP + glucose medium
Higher Heating Value (HHV) (kJ/g)	23.2	21.2	18
Lower Heating Value (LHV) (kJ/g)	21.5	19.5	16.3

The results in Table 3.7 show that the average higher heating value of algal biomass cultured in 10% N TAP medium is 10% lower than in TAP medium and 15% higher than in TAP + glucose medium. This result is an agreement with the previous lipid content data, which suggests that higher lipid content in the algae cell produces more energy during combustion. During the engine operation, water delivered into the combustion chamber will remain in vapour form. Therefore, lower heating values are applied in the following chapters.

3.3.3 Preparation of stable algae/diesel emulsion

Preliminary experiments

Further investigation, built on Xu et al. (2016b)'s study, on the performance of the four surfactants (CTAB, Span 80, Triton X-100 and Tween 80) utilized in the blending of algal biomass and diesel was carried out in Xinyi Zhou's undergraduate research project under my supervision.

The algal biomass was cultured in TAP medium at 25 °C for 7 days and 0.7 ± 0.05 g/L of dry biomass powder was obtained after freeze drying. To demonstrate the performance of each surfactant in a water-oil mixture, all surfactants were tested separately. Photos were taken after 10 minutes settlement and it is clearly shown in Figure 3.6 that Span 80 has the best performance in emulsifying water into diesel among the four tested surfactants, which was in agreement with the theory that a surfactant with a low end HLB value (HLB value of Span 80 is at 4.3) is more likely to form a stable water-in-oil emulsion.

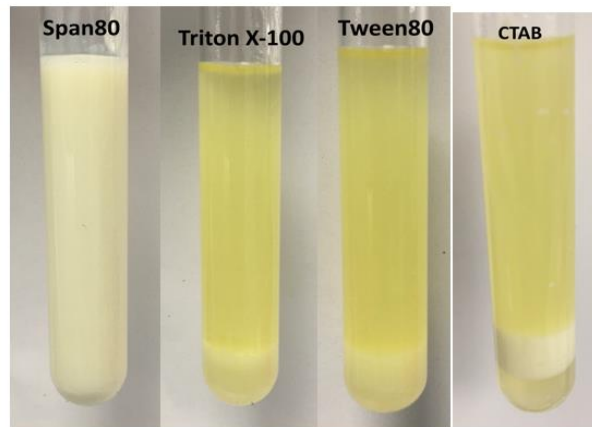


Figure 3.6 Comparison of the four tested surfactants for water/diesel blending (Span 80, Triton X-100, Tween 80 and CTAB, left to right).

Based on the W/O emulsion test, Span 80 was used alone to prepare algae/diesel emulsions and each 10 mL emulsion contained ~ 0.2 g algal biomass. As can be

seen from Figure 3.7 that algal cells started settling down within 10 minutes just after mixing, and most algal cells were settled down to the bottom of the test tube after one day. It suggests that the addition of algae cells disturbed the W/O emulsion system and significantly reduced the system stability.

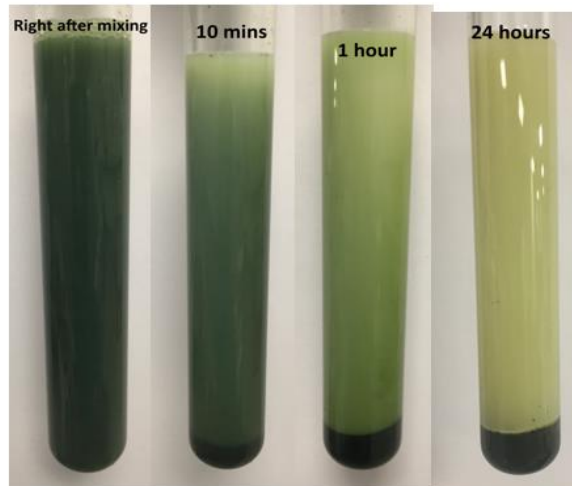


Figure 3.7 Use of Span 80 to prepare algal slurry/diesel emulsion. Pictures were taken right after mixing, after 10-minute, 1-hour and 24-hour settling (left to right).

According to Zhao et al. (2006), a combination of two surfactants (one with a low HLB value and one with a higher HLB value) would be more efficient than either single surfactant. Therefore, a ratio of 1:1 in the test surfactant mixtures was determined to blend Span 80 with CTAB, Tween 80 and Triton X-100 respectively. As shown in Figure 3.8, the combination of Span 80/Triton X-100 was the most suitable surfactant mixture for emulsifying stable algae/diesel emulsion.

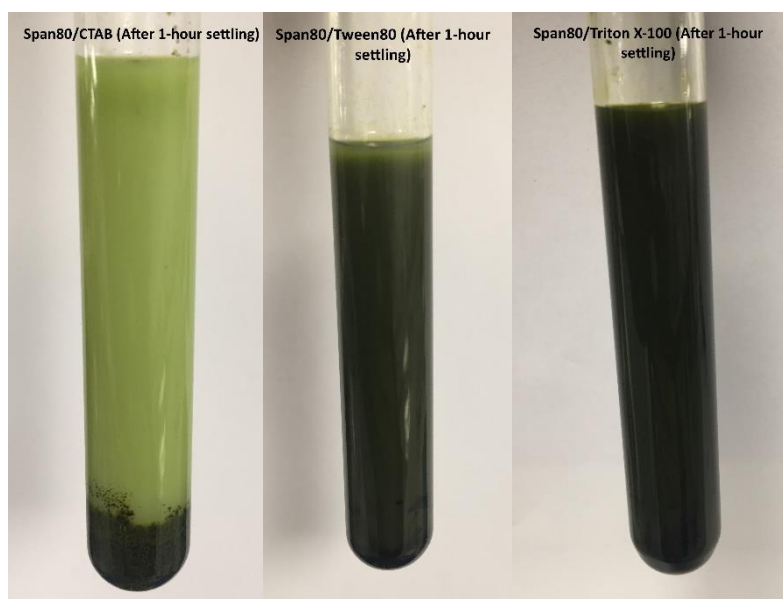


Figure 3.8 Three combinations of surfactant mixtures (Span 80/CTAB, Span 80/Tween 80, Span 80/Triton X-100) for preparing algal slurry/diesel emulsion. Pictures were taken after 1 hour settling.

In order to form a stable and homogeneous algae/diesel system, an optimisation of two surfactants, Span 80 and Triton X-100, was investigated. Meanwhile, *n*-butanol was also added to the system as a co-surfactant. For each combination of Span80, Triton X-100 and butanol, the algae/diesel emulsion was made to a final algal concentration of ~ 2% v/v dry biomass contained in 1 mL of algal slurry.

As shown in Table 3.8, the four combinations of surfactants highlighted in green could form very stable algae/diesel emulsions and there was no clear phase separation observed after 24-hour settling, which is shown in Figure 3.9. The other tested mixtures all exhibited water phase separation or cell settling within 1-hour or after 16-hour settlement. Moreover, comparing with other cases, relative stable emulsions were produced with the surfactants containing 0.2 mL butanol, which suggests that butanol as co-surfactant could help surfactants stabilising the emulsion system and the optimal amount of butanol would be between 0.1 mL and 0.2 mL (both end values included). Therefore, considering the requirement of

system stability, the optimised composition of the surfactant package should contain 0.4 mL of Span 80, 0.6 mL of Triton X-100 and 0.2 mL of n-Butanol.

Table 3.8 Optimization of the ratio of each chemical composition in the surfactant mixture Yellow: surfactant mixtures tested; Green: Surfactant mixtures formed stable emulsions after 24 hours settling.

10 mL: X mL diesel, 1 mL algal slurry, Y mL surfactant pack (Sp80/Triton X-100/n-Butanol)											
Span80 (0.2 mL/10 mL)		Triton X-100 (mL/10 mL)				Span80 (0.3 mL/10 mL)		Triton X-100 (mL/10 mL)			
		0.2	0.4	0.6	0.8			0.2	0.4	0.6	0.8
n-Butanol (mL/10 mL)	0.1	8.5	8.3	8.1	7.9	n-Butanol (mL/10 mL)	0.1	8.4	8.2	8.0	7.8
	0.2	8.4	8.2	8	7.8		0.2	8.3	8.1	7.9	7.7
	0.3	8.3	8.1	7.9	7.7		0.3	8.2	8	7.8	7.6
	0.4	8.2	8	7.8	7.6		0.4	8.1	7.9	7.7	7.5
	0.5	8.1	7.9	7.7	7.5		0.5	8	7.8	7.6	7.4
Span80 (0.4 mL/10 mL)		Triton X-100 (mL/10 mL)				Span80 (0.5 mL/10 mL)		Triton X-100 (mL/10 mL)			
		0.2	0.4	0.6	0.8			0.2	0.4	0.6	0.8
n-Butanol (mL/10 mL)	0.1	8.3	8.1	7.9	7.7	n-Butanol (mL/10 mL)	0.1	8.2	8.0	7.8	7.6
	0.2	8.2	8	7.8	7.6		0.2	8.1	7.9	7.7	7.5
	0.3	8.1	7.9	7.7	7.5		0.3	8	7.8	7.6	7.4
	0.4	8	7.8	7.6	7.4		0.4	7.9	7.7	7.5	7.3
	0.5	7.9	7.7	7.5	7.3		0.5	7.8	7.6	7.4	7.2

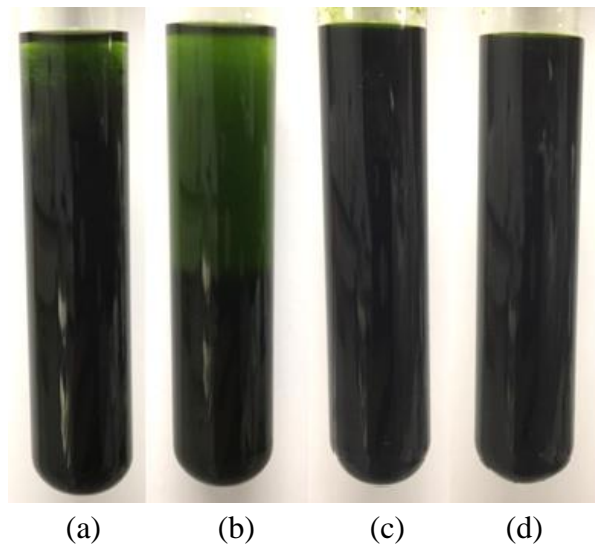


Figure 3.9 Algae/diesel emulsions prepared with highlighted surfactant mixtures after 24 hours settling. (a) 0.3 mL Span 80 + 0.6 mL Triton X-100; (b) 0.3 mL Span 80 + 0.8 mL Triton X-100 (c) 0.4 mL Span 80 + 0.6 mL Triton X-100 (d) 0.4 mL Span 80 + 0.8 mL Triton X-100.

Surfactant characterisation

Due to the low success rate of using new surfactant package found in the preliminary experiment, it was necessary to find a new surfactant or surfactant package for preparing a stable algae/diesel emulsion. Water/oil emulsion systems has been studied in the past decades and there were some in-depth research on the stability of water-in-diesel fuel emulsion. Ghannam and Selim (2009) investigated the stability of blending different water content in the emulsions and found that using small amount of Triton X-100 ($\leq 1\%$ v/v) can stabilise the low water content emulsion ($\leq 20\%$ v/v) for few days and large volume of water content would require higher surfactant concentration ($\sim 5\%$ v/v). Similar with the water/diesel emulsions, the surfactants are key to forming a stable algae/diesel emulsion. Recently, Al-lwayzy et al. (2014a) reported a research on utilising microalgae *Chlorella vulgaris* to create algae/diesel emulsion and found that 1% of Triton X-100 (v/v) used as surfactant gave a stable emulsion for at least two days with 20% water content (v/v). Therefore, initial tests were carried out by blending various volumes of RO water with the pure fossil diesel in the presence of Triton X-100 for algae/diesel emulsions.

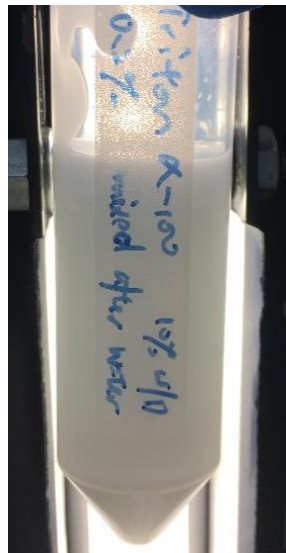


Figure 3.10 Water/diesel emulsion of 10% (v/v) water and 0.2% (v/v) Triton X-100 content. Picture was taken 5 minutes after mixing.

Figure 3.10 shows the results of using Triton X-100 to prepare a W/O emulsion. The mixture contained 30 mL sample in total, of which 3 mL (10%) was RO water and 0.06 mL (0.2%) was the surfactant and rest of the emulsion was pure fossil diesel (no FAME). After 3 minutes vortexing, the mixture became a highly homogeneous emulsion and was stable for at least 2 days. It was verified that Triton X-100 can be used as single surfactant for W/O emulsion, which is in agreement with the previous study of W/O emulsion.

Stability of algae/diesel emulsion

For the preparation of algae/diesel emulsion as a fuel source, stability is a critical parameter to evaluate the feasibility of combustion in the IC engine. The *C. sorokiniana* cells were cultured in TAP + glucose medium for seven days and harvested by centrifugation. The wet algal biomass was then washed with RO water to remove remaining ions from the culture media and freeze dried into powder. In the previous research by Xu et al. (2016b), a mixture of 0.5 g (~ 5% v/v) of dry algal biomass, 1.5 mL of surfactant package and 8.5 mL of diesel was selected for preparing the final emulsion. Therefore, 0.1g (1% w/v), 0.25g (2.5% w/v) and 0.5g (5% w/v) of algal biomass were added to 1 mL (10% v/v) of water and blended with 0.02 mL (0.2% v/v) Triton X-100 and pure diesel to make up a 10 mL mixture. High speed vortex was applied at least for 3 minutes until homogenous emulsions formed. Photos taken directly after the mixing are shown in Figure 3.11. The emulsions with three different algal biomass contents were stable for a day before a clear phase separation was observed, which is shorter than the time for a water/diesel emulsion. This suggests that the algae cells may affect the balance of W/O system and reduce the stability of the emulsion.

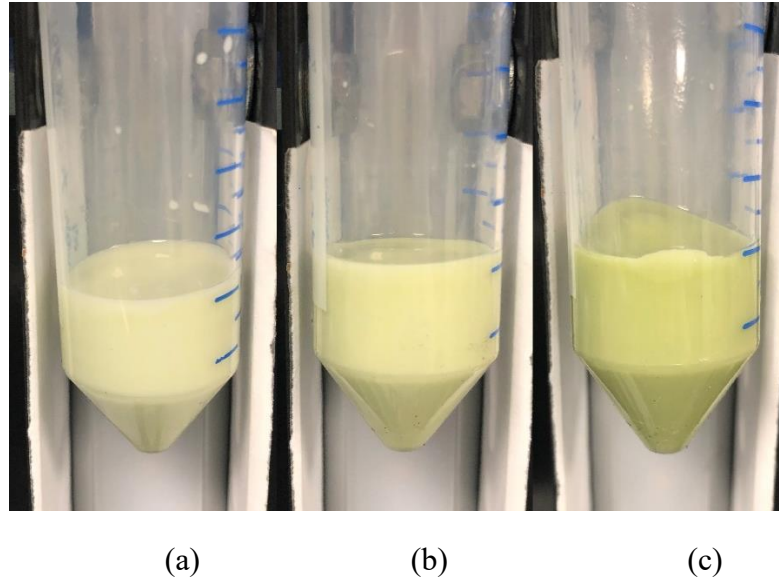
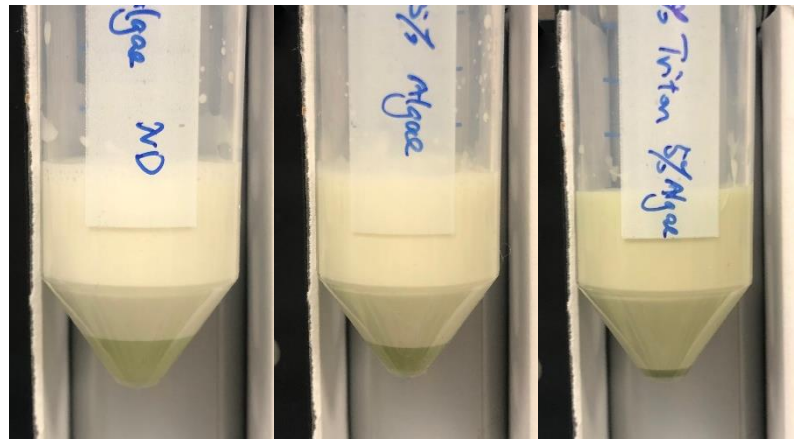


Figure 3.11 Photos of algae/diesel emulsions taken directly after mixing and containing (a) 1% (b) 2.5% and (c) 5% v/v biomass with 10% water concentration and 0.2% Triton X-100.

Although the algae/diesel emulsions were stable, the mixtures had extremely high viscosity and barely flowed in the tube. Since the viscosity can be reduced by replacing diesel with more water in the system, 20% and 30% (v/v) of water content were tested with 0.2% (v/v) Triton X-100 and 1%, 2.5% and 5% of algal biomass. Photos of the mixtures with 20% water content after high speed mixing and 2 hours settling are shown in Figure 3.12. It can be seen that all the emulsions were no longer stable and had water phase separated to varying degrees. It suggests that higher water content could accelerate the liquid phase separation and reduce the emulsion stability. Therefore, to maintain a stable and homogeneous emulsion system and prevent the separation of the water phase, the ratio of the surfactant needs to be increased. Meanwhile, the same phenomenon occurred in the 30% water content scenario and the stable time of the emulsions were reduced to around one hour (data not shown).



(a) (b) (c)
 Figure 3.12 Algae/diesel emulsion with 20% water content and (a) 1% (b) 2.5% (c) 5% algal biomass concentration after 2 hours settling period.

Table 3.9 Stability of algae/diesel emulsions with 2% (v/v) of Triton X-100.

Water content (v/v)	Algal biomass concentration (w/v)		
	1	2.5	5
20%	12 h ± 1 h	13 h ± 0.5 h	>13.5 h
30%	8 h ± 0.5 h	8.5 h ± 1 h	>9 h

In order to improve the stability, 2% (v/v) of Triton X-100 was then tested in the algae/diesel emulsions, which contained 20% and 30% of water and 1%, 2.5% and 5% of algal biomass. As can be seen from Table 3.9, the stability of algae cells in diesel suspension was significantly improved by increasing the surfactant concentration and the separation of water phase was delayed to at least 6 hours after mixing. Moreover, higher algal biomass content would also extend the stable period, but the improvement was not significant.

Viscosity of algae/diesel emulsion

According to Bukkarapu et al. (2018)'s report, high viscosity of fuel will cause excessive wear of engine and blockage of the fuel injector. Therefore, viscosity tests on algae/diesel emulsions containing 20% and 30% water were carried out by using the rheometer at 40 °C and the results are shown below.

Table 3.10 Viscosity of W/O and algae/diesel emulsions with 20% and 30% of water content and 2% of Triton X-100.

Algae content (w/v)	Viscosity (mPa·s)	
	20% water	30% water
0%	131.1	42.9
1%	117.1	39.2
2.5%	182.8	49.9
5%	280.2	62.7

As can be seen from Table 3.10, all the emulsions had high viscosity relative to pure fossil diesel (1.944 mPa·s). It is interesting to see that the emulsion with 1% biomass concentration reduced the viscosity comparing with water/diesel emulsion in both cases. This might be because small amounts of algal biomass reduced the resistance in the W/O system and increased the runniness of the emulsion. Meanwhile, with the same water content, increasing the algal biomass content significantly increased the emulsion viscosity. It suggests that large number of algae cells in the mixture could lead to aggregation and the bigger cell clusters increase the viscosity. Moreover, increasing of water content resulted in the reduction of emulsion viscosity, which is in agreement in the previous tests of W/O emulsion. Considering the requirement of system stability (stable >8 hours) as well as reducing viscosity of the emulsion, a mixture of 0.2 mL of Triton X-100, 3 mL of water containing 0.25 g of algal biomass and 6.8 mL diesel in every 10 mL was used for the FAME analysis.

Determination of FAME characterisation

To investigate the impact of FAME content on algae/diesel emulsion, mixtures of diesel and FAME were prepared in 5%, 10% and 20% (v/v) of FAME concentrations. 0.5 mL, 1 mL and 2 mL FAME were mixed with pure fossil diesel in every 10 mL and vortexed at high speed (2500 rpm) for 2 minutes. It can be seen from Figure 3.13, there was no clear effect on introducing FAME into diesel and all the mixtures were stable and homogenous. However, the viscosity results of three mixtures shown in Figure 3.14 present a small but increasing trend with increase of FAME concentration. It might due to the higher viscosity and impurity of FAME relative to pure diesel, which will increase the total viscosity of FAME diesel mixture. (Graboski et al., 1998).

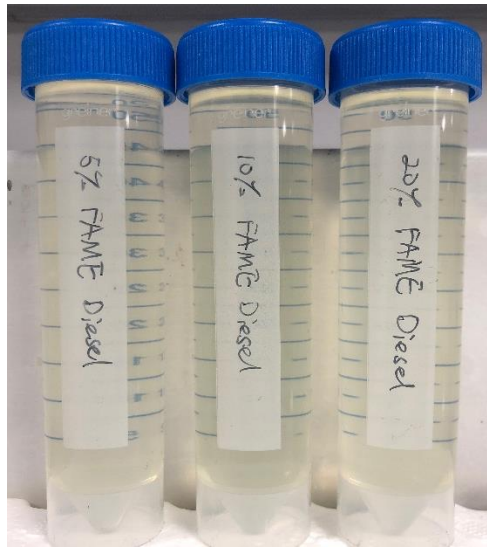


Figure 3.13 Diesel mixtures with 5%, 10% and 20% (v/v) FAME concentration.

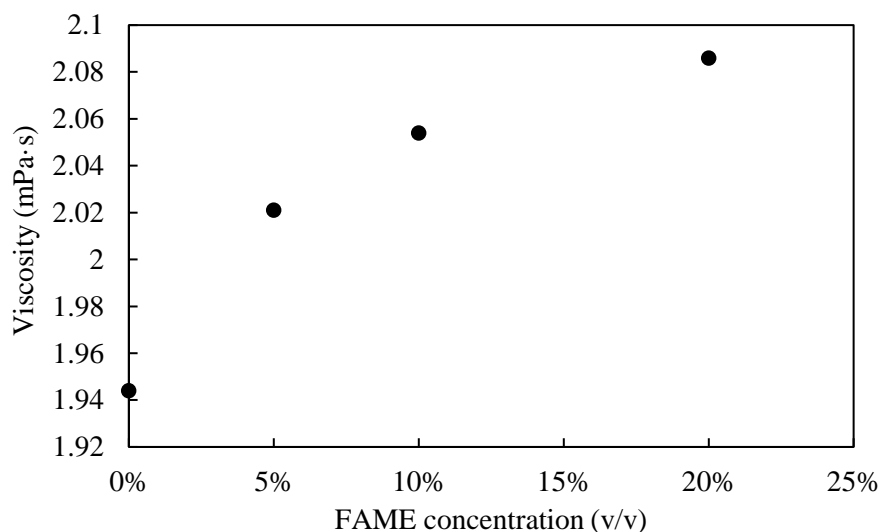


Figure 3.14 The diesel viscosity with varying FAME concentration.

Table 3.11 The viscosity of emulsions containing 30% water and 2.5% algae and 2% surfactant Triton X-100.

Name	Stability	Viscosity (mPa·s)
Algae/diesel	8.5 ± 1 h	49.9
Algae/ FAME 5 diesel	8.5 ± 0.5 h	50.8
Algae/ FAME 10 diesel	8.75 ± 1 h	49.7
Algae/ FAME 20 diesel	8.5 ± 1 h	49.8

Next the impact of FAME content on stability of algae/FAME diesel emulsions was investigated. For each 10 mL algae/FAME diesel emulsion to be prepared, 0.2 mL Triton X-100 and 2.5g dry algae was added to 3 mL water and then mixed with 6.8 mL FAME diesel. The stabilities and viscosities of algae/FAME 5 diesel emulsion, algae/FAME 10 diesel emulsion and algae/FAME 20 diesel emulsion are shown in Table 3.11. The viscosity data was collected directly after 3 minutes of high speed mixing and the stability is measured by observing water phase

separation after mixing. As can be seen from Table 3.11, there was no clear impact of adding FAME into mixtures on the emulsion stability in all cases. However, a small increase of viscosity in algae/FAME 5 diesel mixture was observed, which suggests that the preparation of emulsion might contain human errors and further testing is required.

The stable emulsions of algae/diesel and algae/FAME diesel were observed under microscope and photos were taken and shown in Figure 3.15. It can be seen from the pictures (a) to (c) that with the biomass concentration increasing, the algae cell aggregation (black shadows in green circle) became more pronounced and even reached a size of nearly 100 μm . This might be the reason of increasing of the emulsion viscosity and suggesting that the emulsions require more powerful mixing method to prevent the cell aggregation for viscosity reduction. Moreover, introducing FAME into algae/diesel mixture would not affect the algae cell distribution in the emulsion. However, there were more air bubbles (black circle) observed in the algae/FAME 20 diesel emulsion (f). Based on the previous viscosity study, it suggests that more air was captured during the high-speed mixing and there is no direct connection with the changing of FAME concentration.

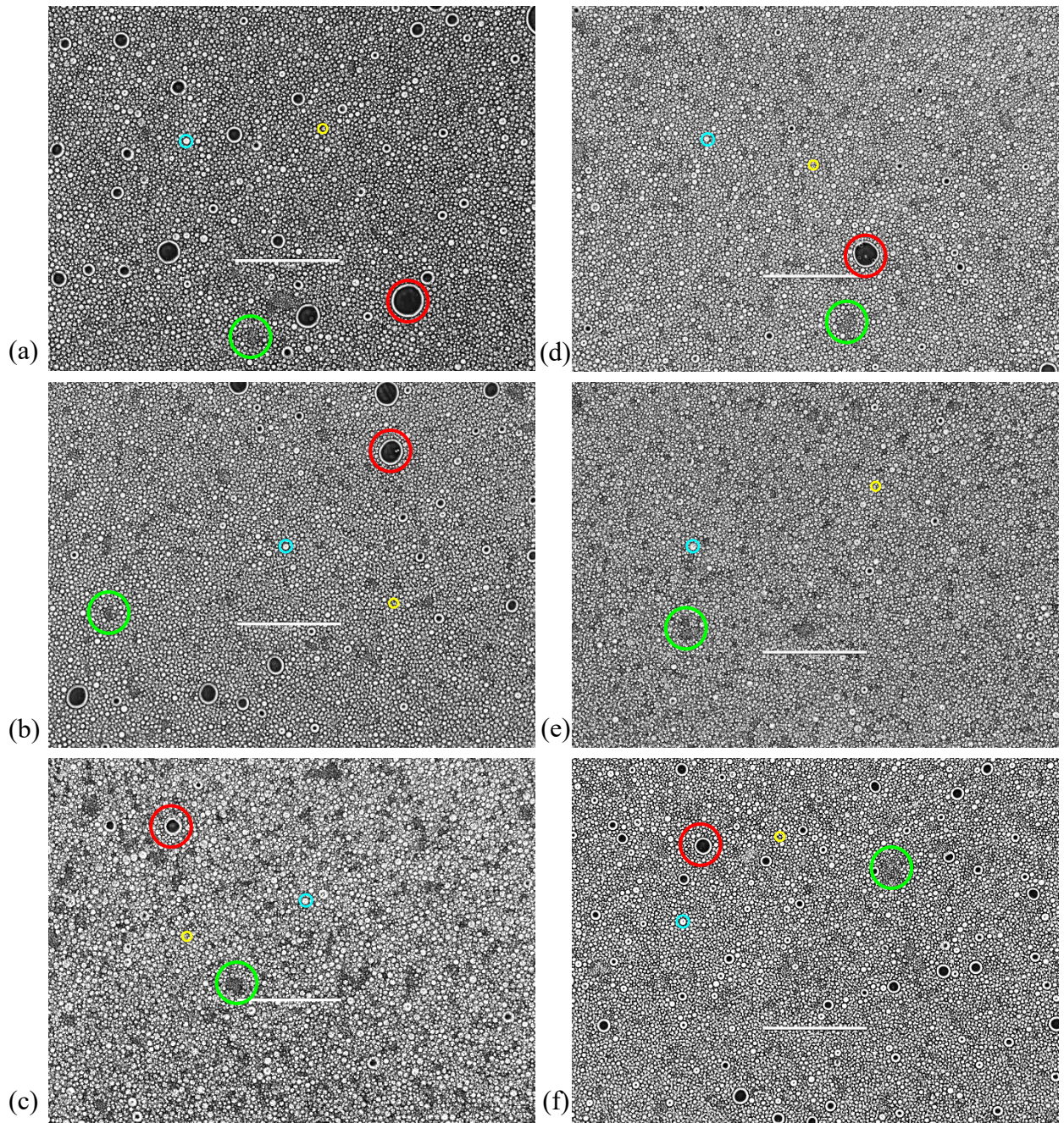


Figure 3.15 Microscopic observations of stable emulsions. With 30% (v/v) water content and (a) 1% (w/v) algal biomass content; (b) 2.5% (w/v) algal biomass content; (c) 5% (w/v) algal biomass content. With 30% (v/v) water content, 2.5% (w/v) algal biomass content and (d) algae/FAME 5 diesel; (e) algae/FAME 10 diesel; (f) algae/FAME 20 diesel. The white bars show the 200 μm of actual scale in the image. Circles represent algae cells (green), air bubble (red), water (blue) and diesel (yellow).

3.3.4 Combustion of algae/diesel emulsion

The single combustion test of algae/diesel emulsion was conducted to verify the possibility of using algae/diesel emulsion as an alternative fuel in a modern direct injection diesel engine. However, the experiment was only continued for 5 minutes as the injector failed a few seconds following the start of delivery of the algae emulsion at 500 bar to the fuel injector. The pressure data during the successful period of combustion is shown in Figure 3.16.

As can be seen from Figure 3.16, initially stable combustion commenced after the starting of fuel injection, with a peak in-cylinder pressure of around 47.8 bar achieved during each combustion cycle prior to 0.5 s. However, after a small decrease of in-cylinder pressure, no combustion took place at 0.7 s despite the control signal sent to the injector. It was tentatively suggested that this initial period of stable combustion was in fact that of pure fossil diesel remaining within the injector internal volume following previous running of the engine. Moreover, it can be seen from Figure 3.17 that although the combustion was restarted during the period of 0.8 s to 1.3 s, peak in-cylinder pressure declined gradually over the course of several combustion cycles, suggesting a gradual (but rapid) decrease in injector operation, rather than an abrupt and rapid sudden failure. As shown in Figure 3.3 the correct operation of a solenoid valve requires fuel flow and balancing of pressure across very small diameter orifices, which may limit the particle size of the algae emulsion to go through. Meanwhile, the observation of excess fuel drained from the fuel system following the combustion test showed that the emulsions had not remained stable under injection pressures, and thus it is tentatively suggested that the algae cells within the emulsions may have agglomerated and gradually blocked the injector internal passages, resulting in failure of the injector.

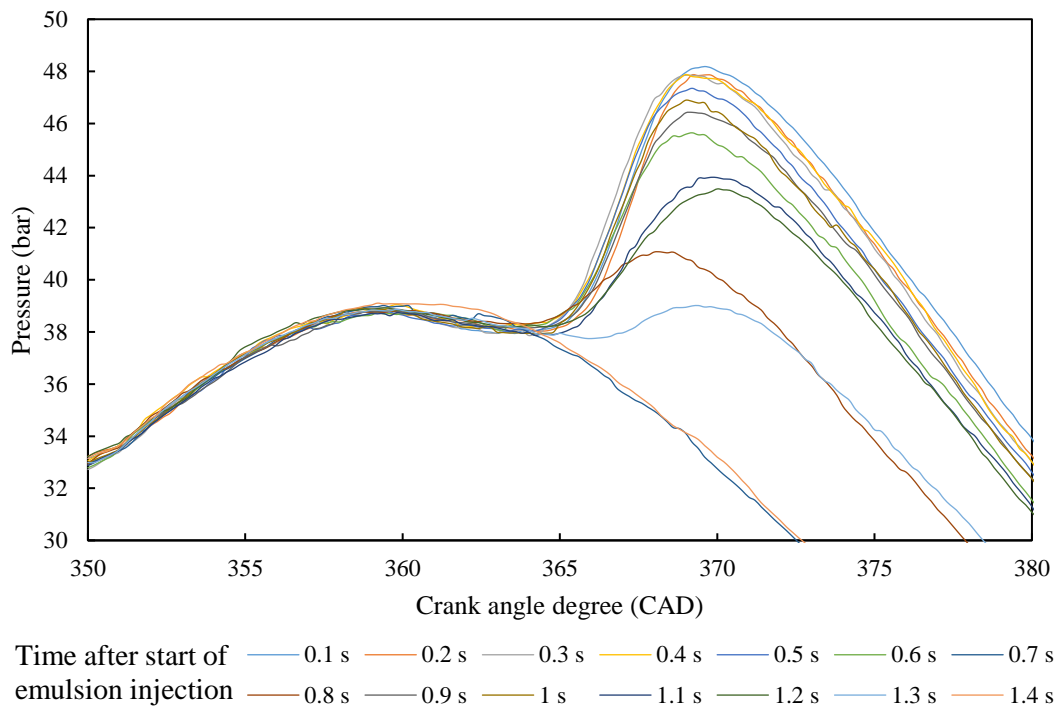


Figure 3.16 In-cylinder pressures during direct injection of algae/diesel emulsion at 500 bar.

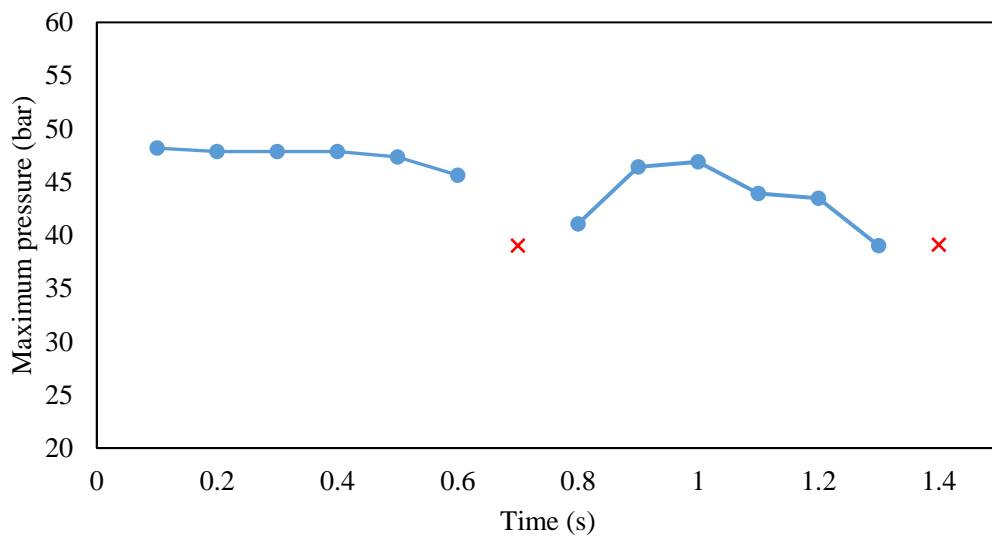


Figure 3.17 Maximum in-cylinder pressures achieved during direct injection of algae/diesel emulsion at 500 bar. Red crosses indicated no combustion was taken place.

3.4 Conclusion

The algae strain of *C. sorokiniana* was selected to produce algal biomass and the characteristics of water/diesel and algae/diesel emulsions were investigated in this chapter. The algae cells cultivated in TAP + glucose medium for 4 days reached highest biomass concentration of 2.43 g/L but had the lowest LHV of 16.1 kJ/g. The cells cultured in TAP medium had moderate growth rate but highest LHV of 21.3 kJ/g. Due to the large amount of algal biomass required for the experiments, TAP + glucose medium was selected to produce algal biomass for preparing algae/diesel emulsions.

The preliminary experiments of preparing algae/diesel emulsion were based on Xu et al. (2016b)'s research and further the performance of four surfactants (CTAB, Span 80, Triton X-100 and Tween 80) on emulsion stability was tested. Their experiments optimised a novel surfactant package consisting of 0.4 mL of Span 80, 0.6 mL of Triton X-100 and 0.2 mL of n-Butanol, which successfully stabilised the algae/diesel emulsion for 24 hours. Each 10 mL emulsion contained 7.8 mL diesel (5.3% FAME), 1.2 mL surfactant package and 1 mL algae slurry (~ 2% v/v dry biomass). Due to the low success rate of producing stable emulsions with this surfactant combination in this work, further study was carried out.

According to Ghannam and Selim (2009)'s research, the effect of surfactant Triton X-100 concentration on the stability and viscosity of W/D emulsion and algae/diesel emulsion was investigated. The results showed that a W/D emulsion with 10% v/v water content and 0.2% v/v surfactant after 3 minutes vortexing was stable for at least 2 days. Based on this result and considering the stability and viscosity of the algae/diesel emulsion, 2.5% v/v algal biomass was added into the water/diesel mixture, which contained 2% surfactant and 30% water. The final emulsion could stay stable for around 8.5 hours with relative low viscosity of 49.9

mPa·s.

In order to investigate the impact of FAME content on the combustion emissions, 5%, 10% and 20% v/v FAME was mixed with pure diesel and then algae/FAME diesel emulsions formed. Although the increase of FAME content had a small increasing impact on viscosity of water/FAME diesel emulsions, there were no clear effects on the stability and viscosity of algae/FAME diesel emulsions.

The experiment on the combustion of algae/diesel emulsion was not successful as the injector failed a few seconds following the start of delivery of the algae emulsion. The emulsion did not remain stable under high pressure of the common rail system in the modern diesel engine and suggesting an agglomeration of algae cells result in the failure of the injector.

Chapter 4 Life Cycle Assessment

4.1 Introduction

Life Cycle Assessment (LCA) is an essential environmental management tool that has been developed since the 1960s. The life cycle refers to the defined boundary of a product or process from the acquisition of raw materials, production, utilisation and disposal, which is the process from the cradle to the grave. As defined by ISO 14040 (Standardization, 2006), life cycle assessment can be used to quantify the environmental factors and potential impacts associated with a product (or service) by compiling a data record of inputs and outputs from the system, evaluating the potential environmental impacts associated with these inputs and outputs, and interpreting the results of the data record and environmental impact analysis based on the objectives of the life cycle assessment study. It helps identify the process hotspots that must be improved to minimise the overall impact.

As an ideal third-generation biofuel feedstock, microalgae have been intensely investigated from the biomass production to the energy utilisation. However, comparing with other biofuel production processes, microalgae biofuels are not environmentally competitive due to the high energy consumption for harvesting and production (Lardon et al., 2009). Since the energy used in these processes produced most of the environmental burden, the integrated LCA of energy flow based on the microalgae biofuel production process will help determine the environmental impact of each process step (Bradley et al., 2015). The results of the analysis differ depending on the assumptions of the properties of algae cells (e.g. lipid content), methods of algae cultivation, allocation and lipid extraction, and the selection of unit process technologies (Shi et al., 2019).

Several researchers have studied the microalgae cultivation and biodiesel production process by using the LCA approach. A recent review conducted by Ketzer et al. (2018) summarised 16 such studies and reported a large variation of 0.01 to 3.35 for the net energy ratio (NER) dependent on the different assumptions made, such as biomass productivity, lipid content and operation processes, etc. Lardon et al. (2009) investigated the energetic balance and the potential environmental impacts of the whole algal biodiesel process. The research confirmed the potential of microalgae as an energy source but the optimisation of wet lipid extraction is required to reduce the energy consumption. Orfield et al. (2015) presented a reduction of the global warming potential (GWP) in the algal biomass cultivation process with heterotrophic condition and sugarcane as the feedstock. Jez et al. (2017) reported an LCA for the comparison between oil production from microalgae and terrestrial oilseed crops. The results show that the microalgae oil production process had the most substantial environmental impact due to high electricity consumption. Focusing on the downstream process, O'Connell et al. (2013) conducted a life cycle analysis on emissions associated with harvesting, dewatering, extraction, reaction, and product purification stages of algae biodiesel production. The results indicated that 96 % of total emission was contributed from the spray dryer in the drying process. They found that a combination of mechanical and thermal dewatering techniques gives a substantial reduction (91%) of the total emission. Sander et al. (2010) showed the dewatering process consumes the most energy resources and produces the most GHG emissions. The application of a filter press process resulted in a significant reduction of 156.61 kg CO₂-equivalent per MJ of algae biodiesel relative to the centrifugation process.

This chapter conducts a life cycle assessment for evaluating the environmental impact of the downstream process of dry algae powder production and the

aspiration of algal biomass suspension in the intake air of a direct injection diesel engine (Chapter 2) on global warming potential (GWP), NO_x emissions and water consumption.

4.2 Goals and scoping

The goal of this study was to produce a harvesting to combustion LCA of algal biomass by using the data from the experiments in the Chapter 2 while elaborating on major standards used (ISO 14040 and 14044) (Finkbeiner et al., 2006). The results were evaluated by comparing with the base case study of biodiesel production carried out by Passell et al. (2013). The production of 1 MJ energy during the combustion in a CI engine was defined as a reference unit (functional unit).

Based on the combustion tests, two scenarios were examined in the LCA study: in the first scenario four cases examined the harvesting processes of algal biomass and combustion processes with varying biomass concentration and in the second scenario three cases were conducted to examine the impact of varying aspiration flowrate of algal biomass on the engine combustion.

4.2.1 Impact assessment method

Three impact categories as shown in Table 4.1 were considered in this analysis. The global warming potential is a measurement based on the Intergovernmental Panel on Climate Change (IPCC) characterisation factors, representing the impact of GHG on global warming. Due to the fact that CO₂ contributes the most of GHG, CO₂-equivalents is defined as the basic unit for measuring the greenhouse effect. NO_x is measured for evaluating the process impact of exhaust emissions on human health and the water consumption measures the usage of freshwater throughout the

life cycle. All the results were counted of all the direct and indirect consumed or generated sources from the processes involved in this life cycle assessment. The NER was not included in this study because it is difficult to determine the contribution of the commercial diesel production in the analysis.

Table 4.1 Impact categories considered in the analysis.

Impact category	Unit of measure
GWP	kg CO ₂ -equivalents
NO _x (oxide of nitrogen)	kg NO _x
Water consumption	m ³

4.2.2 System boundaries

This study includes the harvesting of algal biomass and combustion processes of aspirated algal biomass in the CI engine, which was investigated in Chapter 2. The system includes biomass harvesting and dewatering, spray drying, preparation of algae suspension and the aspiration combustion of algae suspension in a diesel engine. Figure 4.1 shows the life cycle stages and all the process units in the system. The transportation of materials and construction of process facilities were excluded in this analysis.

4.2.3 System description

Two scenarios of aspiration combustion of algal biomass are based on four cases with biomass concentrations of 5%, 7.5%, 10% and 20% (constant aspiration flowrate of 40 mL/min) and three cases with aspiration injection flowrates of 40, 49.2 and 56 mL/min (constant biomass concentration of 5%). In all the cases, algal biomass was harvested from a 105 m³ culture broth and dewatered via five centrifuges using a liquid pump to transport the algal broth. The concentrated biomass slurry was then heat-dried by using a spray dryer to obtain dry biomass powder. The details of preparing biomass suspensions in four different concentrations and the combustion processes of each case are described in Chapter

2. In addition, in this LCA model, all the wastewater produced during the algae powder production process is sent to the treatment plant.

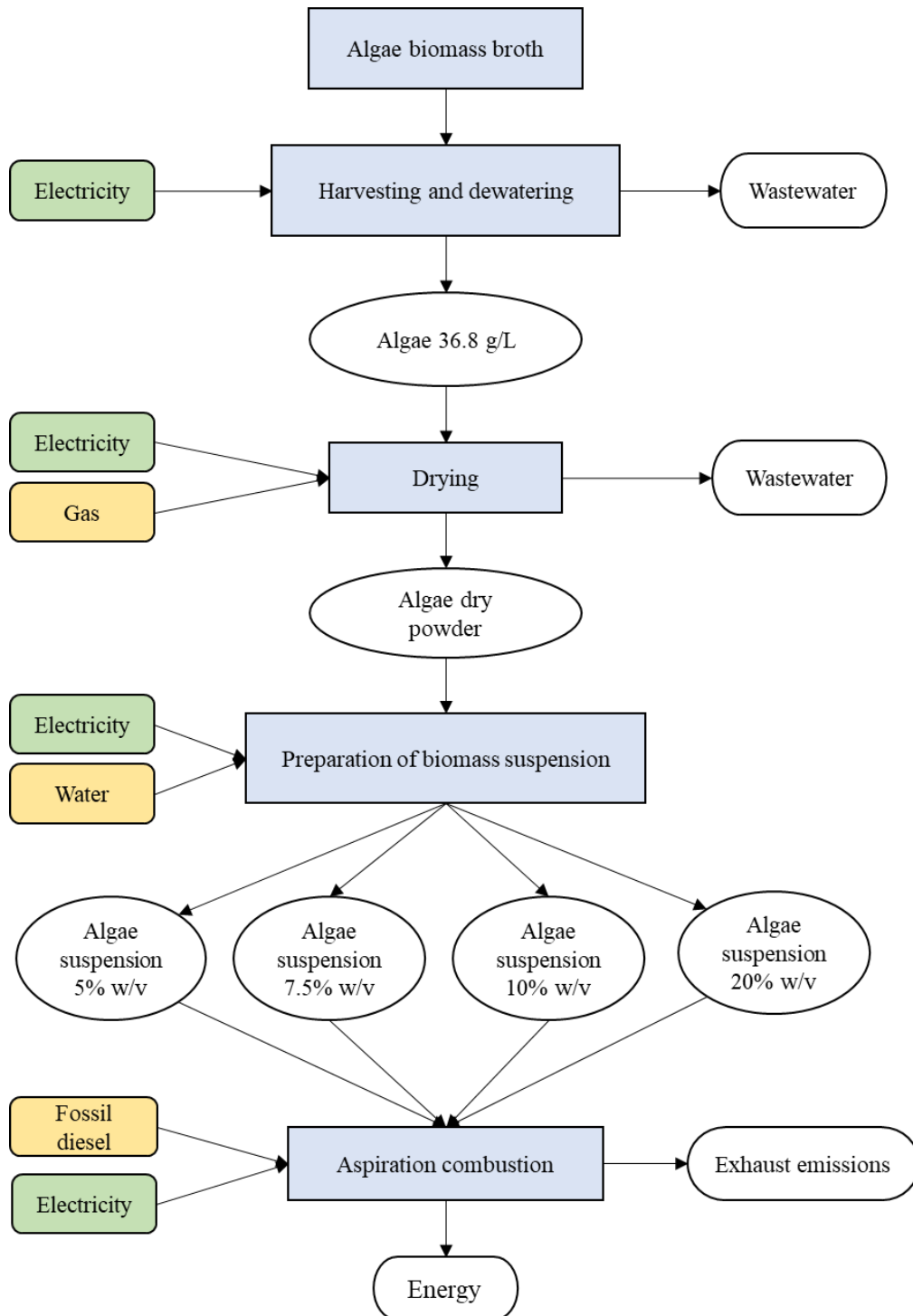


Figure 4.1 System boundaries depicting the unit processes considered in the LCA study.

4.3 Data sources

The biomass production and harvesting data after cell cultivation was obtained from the Chinese Academy of Tropical Agricultural Sciences (CATAS) (<http://www.catas.cn/EN/index.html>), a national institution engaged in tropical agricultural research and development based in China. CATAS produces algae of *C. sorokiniana* at the 105 m³ open pond facility in Haikou, China. The data of the preparation of biomass suspension and aspiration combustion of algal biomass was obtained from the experiments undertaken in this project and described in Chapter 2. The Ecoinvent Life Cycle Inventory, the European Life Cycle Database (ELCD) and the U.S. Life Cycle Inventory (USLCI) database were used for input materials and modelling the biomass harvesting and secondary processes.

4.3.1 Dry algal biomass powder production data

The LCA study was initialled from the dewatering process of algal biomass production after cell cultivation, the volume of culture broth and the biomass concentration before and after centrifugation are shown in Table 4.2.

Table 4.2 Input data of algae culture broth and biomass concentration.

Cultivation data	Value	Unit
Cultivation volume	105	m ³
Harvest biomass concentration	0.368	g/L
Concentration after centrifugation	36.8	g/L

In the dewatering process, five centrifuges (11 kW each) and one 0.5kW pump were employed. Meanwhile, the spray dryer is operated by electricity and natural gas, which the consumption of each energy source is 1.46 kWh and 1.16 m³ gas per kg of dry biomass powder produced. The final product of algae powder contains 3% of water content and the properties and assumptions (Azadi et al., 2015) are shown in Table 4.3.

Table 4.3 Properties of dry algae powder.

Properties	Value	Unit
Density	0.63	g/mL
Lower heating value (LHV)	23.64	kJ/g
<i>Assumptions</i>		
Volume occupied in suspension	1.1	mL/g
Carbon content	52.35	% w/w
Hydrogen content	7.11	% w/w
Oxygen content	30.01	% w/w
Element composition	C ₁ H _{1.63} O _{0.43} N _{0.15}	

4.3.2 Combustion and exhaust emissions data

The engine combustion and exhaust gas emissions data were obtained from the engine tests described in Chapter 2. All the equations and calculations for the input data of the combustion process in the LCA study is shown in Appendix B.

Property of the fossil diesel

The fossil diesel with no FAME content was collected from Haltermann Carless (UK) and the specifications are shown in Table 4.4. Details of the diesel properties can be found in the data sheets in Appendix C.

Table 4.4 Specifications of fossil diesel with no FAME content.

Properties	Value	Unit
Density (15°C)	0.8347	g/mL
Net calorific value	43.18	kJ/g
Carbon content	86.99	% w/w
Hydrogen content	13.01	% w/w

Aspiration combustion of algal biomass

In order to quantify the diesel consumption during combustion, the injection duration of diesel in each test was recorded and the injection flowrate was calculated and shown in Table 4.5.

Table 4.5 Injection duration and flowrate of fossil diesel in combustion tests.

	Biomass concentration				Aspiration flowrate (mL/min)		
	with 40mL/min				With biomass concentration 5%		
	5%	7.50%	10%	20%	40	49.2	56
Injection duration (µs)	775	778	794	772	775	783	792
Injection flowrate (mL/min)	13.34	13.4	13.72	13.28	13.34	16.88	17.10

Because the exhaust analyser condensed the water vapour from the total exhaust gases before processing the gas sample, the actual value of each exhaust gas should be recalculated and adjusted under water-containing conditions. The final data input of the air exhaust gases from the aspiration combustion in the diesel engine is shown in Table 4.6.

Table 4.6 Data input of air exhaust gases in the aspiration combustion process.

Condition	CO (g/min)	CO₂ (g/min)	NO_x (g/min)
Biomass concentration 5%	0.333	29.921	0.054
Biomass concentration 7.5%	0.266	30.170	0.060
Biomass concentration 10%	0.345	27.106	0.051
Biomass concentration 20%	0.361	30.910	0.065
Flowrate 40mL/min	0.333	29.921	0.054
Flowrate 49.2mL/min	0.402	30.663	0.035
Flowrate 56mL/min	0.519	36.355	0.017

4.4 Life cycle inventory

The Life Cycle Inventory (LCI) consists of the material and energy input and output for all the downstream processes of dry algae powder production and the aspiration combustion of algae suspension. The SimaPro 8.5.2 (PRéConsultants, 2019) LCA software was used as a tool for modelling the data and ReCiPe midpoint (E) methodology was used for evaluating and delivering the results. The LCI data of two scenarios (7 cases) are summarised in Table 4.7 and the assumptions for these scenarios in the LCA study are described below.

General assumptions

- The assumption of 5% dry biomass lost during the process is applied on harvesting and dewatering, drying and combustion processes.
- The assumption of elements of the biomass and fossil diesel involved in the combustion process are carbon, hydrogen, oxygen and nitrogen.
- The electrical requirements in all processes are modelled using the GB medium voltage electricity and the diesel combusted in the aspiration combustion process is using the diesel in Europe without Switzerland from the Ecoinvent database.
- The RO water consumed in preparing of algae suspension process is modelled using the de-ionised water/reverse osmosis water from ground water from the ELCD.
- Because the spray dryer is operating with the support of electricity and natural gas, the data of combustion of natural gas in the industrial equipment is collected from the USLCI database.
- Co-location is assumed for all processes in this study and thus the impacts associated with the material transportation and construction of any infrastructure have been excluded.

- The comparison data of the biodiesel production process from Passell et al. (2013)'s study is only considering the impacts of downstream and combustion processes.

Table 4.7 Life cycle inventory data.

Processes inputs/outputs	Value	Unit
Centrifugation		
Inputs (kg ⁻¹ Dry biomass powder)		
Algal biomass culture broth	2.92	m ³
Electricity	4.72	kWh
Outputs (kg ⁻¹ Dry biomass powder)		
Concentrated algal biomass	27.64	kg
Drying		
Inputs (kg ⁻¹ Dry biomass powder)		
Concentrated algal biomass	27.64	kg
Electricity	1.46	kWh
Natural gas	1.16	m ³
Outputs (kg ⁻¹ Dry biomass powder)		
Dry biomass powder	1	kg
Blending		
<i>5% algal biomass suspension</i>		
Inputs (MJ ⁻¹ energy produced in the combustion)		
Dry biomass powder	0.0167	kg
De-ionised water	0.3050	kg
Electricity	0.0808	kWh
Outputs (MJ ⁻¹ energy produced in the combustion)		
5% algal biomass suspension	0.3217	kg
<i>7.5% algal biomass suspension</i>		
Inputs (MJ ⁻¹ energy produced in the combustion)		
Dry biomass powder	0.0244	kg
De-ionised water	0.2882	kg
Electricity	0.1181	kWh

Outputs (MJ ⁻¹ energy produced in the combustion)		
7.5% algal biomass suspension	0.3126	kg
<i>10% algal biomass suspension</i>		
Inputs (MJ ⁻¹ energy produced in the combustion)		
Dry biomass powder	0.0319	kg
De-ionised water	0.2747	kg
Electricity	0.1549	kWh
Outputs (MJ ⁻¹ energy produced in the combustion)		
10% algal biomass suspension	0.3066	kg
<i>20% algal biomass suspension</i>		
Inputs (MJ ⁻¹ energy produced in the combustion)		
Dry biomass powder	0.0629	kg
De-ionised water	0.2359	kg
Electricity	0.3051	kWh
Outputs (MJ ⁻¹ energy produced in the combustion)		
20% algal biomass suspension	0.2989	kg
Combustion		
Inputs (MJ ⁻¹ energy produced in the combustion)		
<i>5% algal biomass suspension with 40 mL/min flowrate</i>		
5% algal biomass suspension	0.3217	kg
Fossil Diesel	0.0948	kg
<i>7.5% algal biomass suspension with 40 mL/min flowrate</i>		
7.5% algal biomass suspension	0.3126	kg
Fossil Diesel	0.0928	kg
<i>10% algal biomass suspension with 40 mL/min flowrate</i>		
10% algal biomass suspension	0.3066	kg
Fossil Diesel	0.0934	kg
<i>20% algal biomass suspension with 40 mL/min flowrate</i>		
20% algal biomass suspension	0.2989	kg
Fossil Diesel	0.0891	kg
<i>5% algal biomass suspension with 49.2 mL/min flowrate</i>		
5% algal biomass suspension	0.3988	kg
Fossil Diesel	0.1209	kg

5% algal biomass suspension with 56 mL/min flowrate

5% algal biomass suspension

0.4502 kg

Fossil Diesel

0.1214 kg

Outputs (MJ⁻¹ energy produced in the combustion)

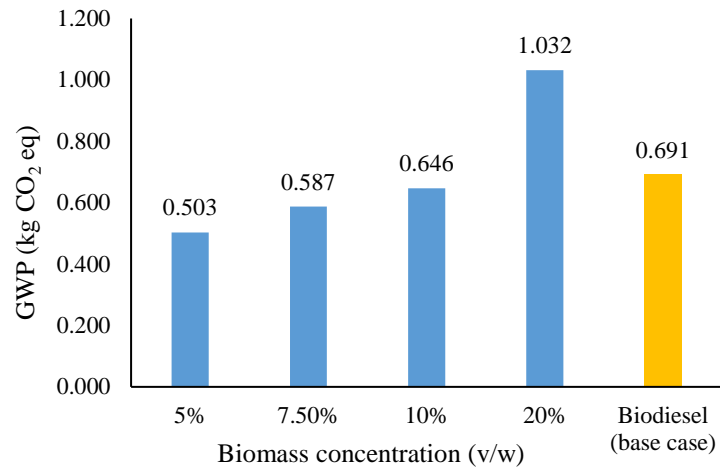
Energy

1 MJ

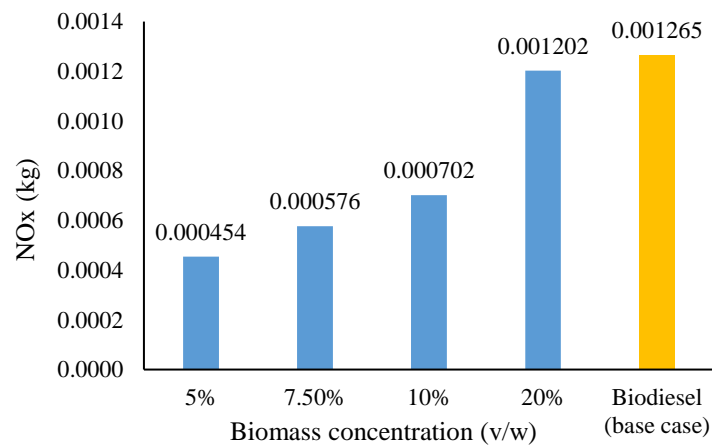
4.5 Life cycle impact assessment and discussion

4.5.1 Scenario with varying biomass concentrations

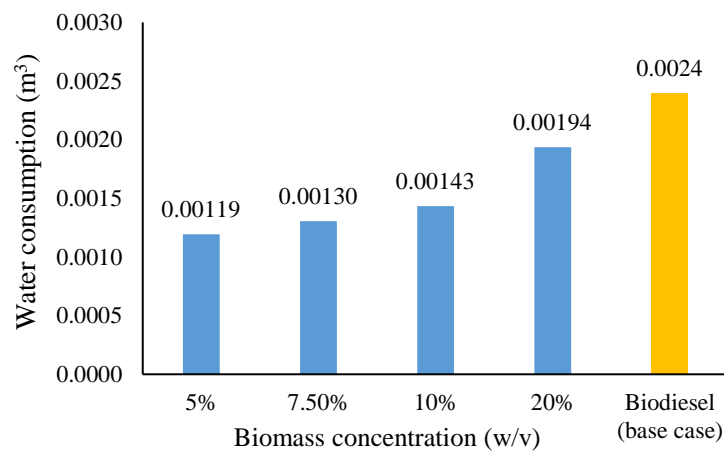
The environmental impacts of the scenarios analysis with 5%, 7.5%, 10% and 20% biomass concentrations were investigated and the results are shown in Figure 4.2. As can be seen from Figure 4.2 an increase in biomass concentration leads to a proportional increase in the values of all impact categories. The GWP produced in the cases of biomass concentrations lower than 20% are lower than the base case of biodiesel and the case of 20% biomass concentration produced much more CO₂-equivalents (0.341 kg) relative to reference biodiesel case to generate 1 MJ of energy. It suggests that the concentration of algal biomass significantly affect the GWP and a reduction of GWP is achieved by using the aspiration combustion of algal biomass with 5-7.5% concentration. Meanwhile, a reduction of NO_x produced in all the aspiration combustion cases is presented relative to the base case of biodiesel. The case of 20% biomass concentration produced the most NO_x, which still has 5% reduction relative to biodiesel. This suggests that this novel technique of utilising the energy from algal biomass can sufficiently reduce the formation of NO_x, which is a benefit to human health. Moreover, the water consumptions of all the cases are also reduced compared with the reference biodiesel case. This could be due to the fact that the processes in the aspiration combustion do not contain steps of lipid extraction and lipid conversion, thus lowering the freshwater requirement through the whole processes. However, the preparation of algae suspension requires RO water to avoid side effects on the diesel engine, which could potentially increase the energy usage of the downstream process.



(a)



(b)



(c)

Figure 4.2 Comparison of three impact categories: (a) GWP; (b) NO_x; (c) water consumption of algal biomass suspension combusted using different biomass concentrations per functional unit (1MJ of energy released in the diesel engine).

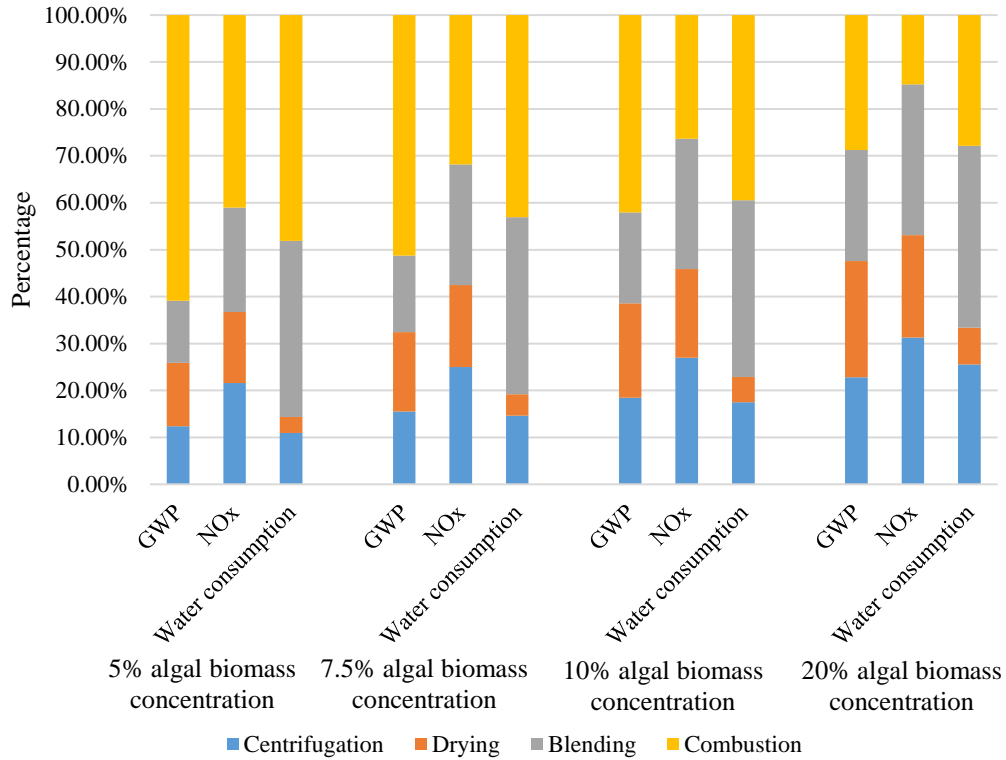
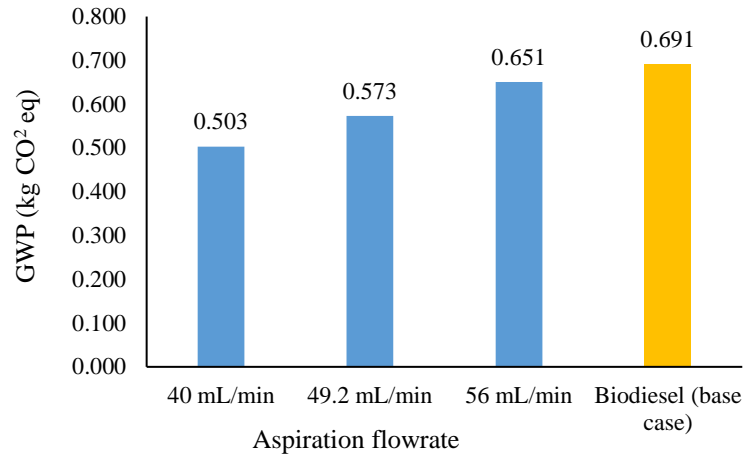


Figure 4.3 Contribution analysis of the main process of algal biomass preparation and combustion using different biomass concentrations per functional unit (1MJ of energy released in the diesel engine).

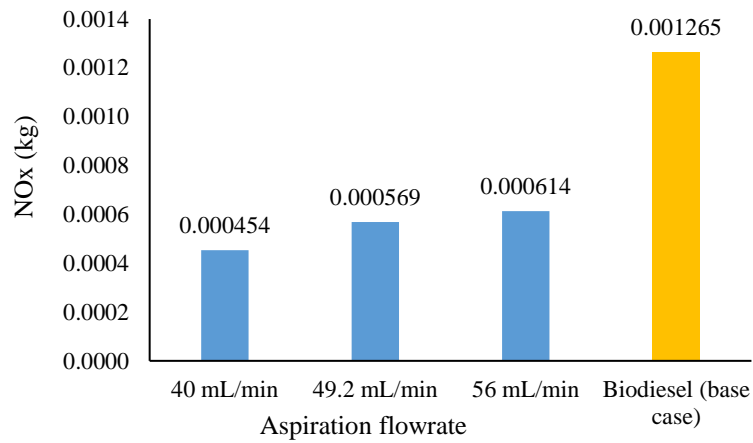
A contribution analysis was conducted to evaluate the environmental contribution of each process on the impact categories. As can be seen from Figure 4.3, the impact of downstream processes including harvesting, drying and blending (preparation of algae suspension) increase with increase of algal biomass concentration. It suggests that producing more biomass requires more energy consumption, which leads to increase of the total impact of GWP, NO_x and water consumption. Furthermore, the combustion process with 20% biomass concentration has the highest amount of CO₂ production. However, it only contributes 28.77% of the total GWP. This indicates that the GWP impact of producing the biomass suspension is larger than the combustion. In addition, the impact of water consumption in the combustion process is also observed, which is because the production of the fossil diesel combusted in the diesel engine requires use of water resource.

4.5.2 Scenario with varying biomass aspiration flowrate

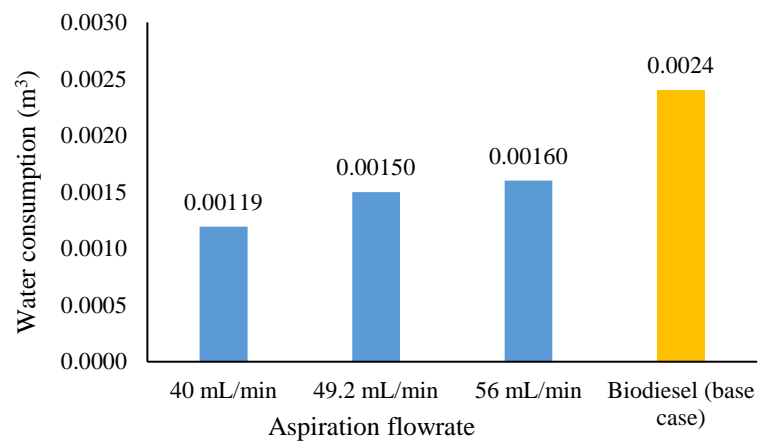
Another scenario analysis including three cases with the aspiration flowrate of 40, 49.2 and 56 mL/min was conducted and shown in Figure 4.4. Although an increase of aspiration flowrate leads to a proportional increase of the impact on GWP, NO_x and water consumption in three cases, all of them have lower environmental impact across all categories relative to the reference base case of biodiesel. The case with the aspiration flowrate of 56 mL/min has a similar but still has 5.8% reduction on GWP impact than the base case of biodiesel, which indicates that the higher aspiration flowrate increase the GWP impact, but the whole process still have a better control on the GHG emissions than the conventional biodiesel process. Meanwhile, significant improvement is seen in the environmental impact for all cases in this scenario, in which the NO_x is more than 50% lower than the biodiesel case. This suggests that the increase of aspiration flowrate has a small impact on NO_x compared with the benefit of NO_x reduction from the whole processes of aspiration combustion of algal biomass. Moreover, a significant increase (26%) of the water consumption is observed when the aspiration flowrate increases from 40 to 49.2 mL/min and reaches 0.0016 m³ at a flowrate of 56 mL/min. However, it is still much lower than the water consumption (0.0024 m³) in the reference case. It may imply that the biomass concentration is not changed in this scenario and therefore, the increase of water consumption is located in the external source supplied for the processes.



(a)



(b)



(c)

Figure 4.4 Comparison of three impact categories: (a) GWP; (b) NO_x; (c) water consumption of algal biomass suspension combusted using different aspiration flowrate per functional unit (1MJ of energy released in the diesel engine).

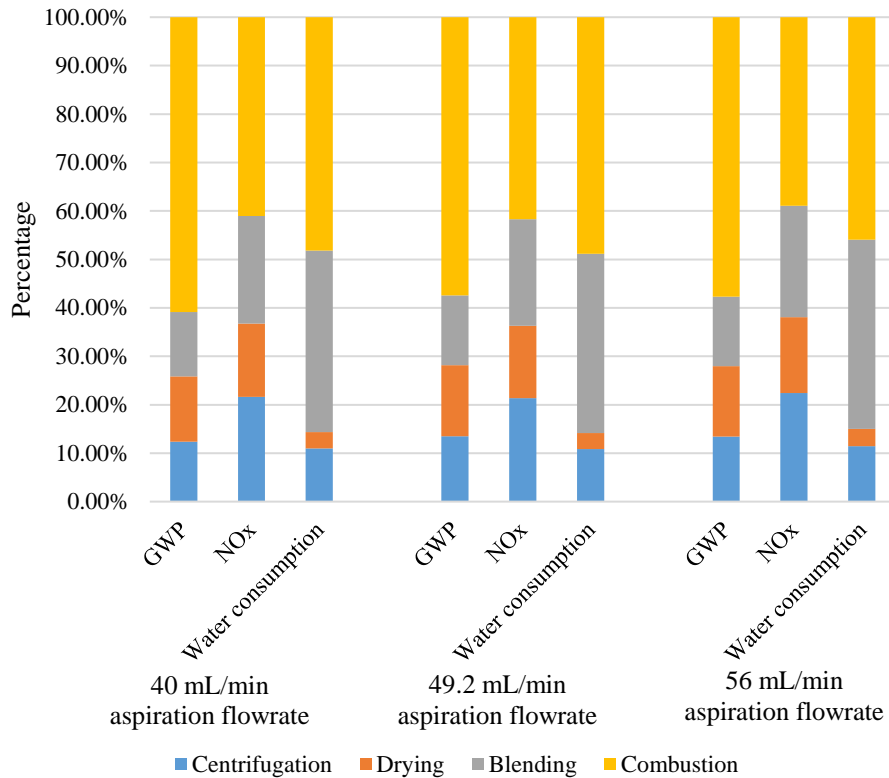


Figure 4.5 Contribution analysis of the main process of algal biomass preparation and combustion using different aspiration flowrate per functional unit (1MJ of energy released in the diesel engine).

The contribution analysis shown in Figure 4.5 for the environmental impact of the processes in the three cases with varying aspiration flowrate was carried out. It can be seen that there is no major effect of changing flowrate on all impact categories. However, considering the increase of the total amount of impact category values (Figure 4.4) with increasing flow rate, each process has almost the same contribution. This indicates that changing of the aspiration flowrate has a larger influence on the total environmental impact but a small impact on each individual process stage. However, in case of using the highest aspiration flow rate there is a small reduction in the impact of the combustion process on NO_x and water consumption on the total contribution compared with the other two cases. It suggests that the increase of the aspiration flowrate requires producing more biomass suspension, which in turn will increase the proportion of the biomass

production and suspension preparation process on the environmental impact categories.

Overall, both of the scenarios and the reference case of biodiesel are small scale processes, which means that the total environmental impacts are theoretically much lower for an industrial process. Most of the LCA study includes the algal biomass cultivation process, which contributes significantly to energy consumption and emissions on all impact categories. A predicted commercial scale model (future case) of algal biodiesel production and combustion was also described in the Passell et al. (2013)'s study, which shows that the total environmental impact on GWP, NO_x and water consumption from the large-scale downstream process and combustion in the diesel engine are 0.115 kg CO₂ equivalent, 0.00007 kg and 0.00016 m³. The huge difference of values between small scale and industrial scale process shows the importance of scaling up in the improvement of the process emissions reduction and environmental sustainability. Additionally, the flowrate of fossil diesel injection in the combustion process from the previous engine test may vary depending on the engine conditions, which have a minor impact on the input of fossil diesel and exhaust emissions.

4.6 Conclusion

This study demonstrates the effect of utilising algal biomass directly in the diesel engine from an environmental perspective. The environmental impacts of aspiration combustion of algal biomass with varying biomass concentration and aspiration flowrate were evaluated and compared. With the increase of biomass concentrations and aspiration flowrates, both of the scenarios show a proportional increase in all environmental impact categories of GWP, NO_x and water consumption. Comparing with the reference base case of algal biodiesel, the case of 20% biomass concentration produced an extra 0.341 kg CO₂ equivalent, which

reaches the largest level of all the cases. Meanwhile, all the cases show a substantial reduction of total NO_x and water consumption for all process stages relative to the reference case. The contribution analysis shows that changing of biomass concentration has a more significant impact than changing the aspiration flowrate on the process contribution. Although the combustion process produces the highest GHG emissions and consumes the largest water resources in the case of 5% biomass concentration, the downstream processes including dry algae powder production and preparing of algal suspension contribute more environmental impact than the combustion in the cases with higher biomass concentration.

In general, this new approach for utilising the energy from algal biomass in diesel engine has better results on controlling the NO_x emission and water consumption relative to the small scale case of algal biodiesel production and combustion. However, comparing with the commercial scale biodiesel process, there is still a substantial gap to reach a similar level of environmental impact. Meanwhile, considering the energy release result in the diesel engine from Chapter 2, a trade-off between energy contribution from the combustion and the total environmental impact has to be investigated. In order to achieve a better energy release and less environmental impact, the case of aspiration combustion with 10% biomass concentration is a good target for future analysis. Furthermore, higher lipid content and the LHV of the algal biomass is also an important factor that is likely to further reduce the environmental impact and improve the sustainability of this approach.

Chapter 5 Conclusion and future work

5.1 General conclusion

Despite recent advances, numerous challenges remain to achieve the industrial scale of producing biodiesel derived from algal biomass. In order to reduce the operating cost and environmental impact of the downstream process, alternative routes of utilising algal biomass directly for energy production have been investigated and their impact on the environment and human health was evaluated in this project.

Chapter 2 presents a novel approach of direct aspiration of algal biomass slurry in the air intake of a diesel engine. For the past decades, combustion of solid fuel such as coal dust has been investigated in a CI engine (Piriou et al., 2013). Inspired by the previous research, this is the first study to demonstrate the feasibility of delivering algae suspension directly through the air intake into a modern diesel engine for energy production. The engine was operated at 1200 rpm with constant SOI of 5 CAD BTDC and two control variables, the concentration of biomass suspension and aspiration flowrate, were tested in the experiments.

The results indicate a positive contribution of the aspirated algae biomass to useful work output at algal biomass suspension concentrations of more than 7.5% w/v. However, with the presence of the algal cells, a reduced IMEP relative to an equivalent aspiration flowrate of water only was observed at lower algal biomass concentrations (5% w/v). From the perspective of exhaust emissions, all the engine combustion with the aspiration of water (with and without algae) reduced NO_x emission levels relative to reference diesel. Meanwhile, the NO_x level increased with increasing biomass concentration and decreased with increasing aspiration flowrate. Moreover, the present of algae cells contribute additional carbon source

to increase the CO₂ emission level but also increases levels of incomplete combustion. In general, the study proved the possibility of increasing the total engine output by aspirating algal biomass into the engine but this approach leads to a decrease of the thermal efficiency in the engine combustion.

In Chapter 3, a study of biomass production and property characterization of microalgae *C. sorokiniana* was firstly addressed. Due to the requirement for a large amount of algal biomass in the experiment, the algae cells cultivated in TAP + glucose medium was selected, which could reach the highest biomass concentration of 2.43 g/L after 4 days of cultivation with LHV of 16.1 kJ/g. Followed by the preliminary experiments of preparing algae/diesel emulsion based on earlier research by Xu et al. (2016b), a novel surfactant package was optimised, which contains 0.4 mL of Span 80, 0.6 mL of Triton X-100 and 0.2 mL of n-Butanol. The algae/diesel emulsion sample was the prepared with 7.8 mL diesel (5.3% FAME), 1.2 mL surfactant package and 1 mL algae slurry (~ 2% v/v dry biomass) that formed a stable emulsion for 24 hours. However, this algae/diesel emulsion was not suitable for the engine test due to the low success rate to obtain stable emulsions.

According to Ghannam and Selim (2009)'s research, further investigation of the effect of surfactant Triton X-100 concentration on the stability and viscosity of W/D emulsion and algae/diesel emulsion was carried out. Based on the results from the stable W/D emulsion (10% v/v water content and 0.2% v/v surfactant), the final algae/diesel emulsion was created with 2.5% v/v algal biomass, 2% surfactant and 30% water considering its stability and viscosity. It was stable for 8.5 hours with the relatively low viscosity of 49.9 mPa·s. The analysis of the impact of FAME content on the W/D and algae/diesel emulsions indicated that there is a small increase of viscosity on W/D emulsion but no impact on

algae/diesel emulsion. The single combustion test of the algae/diesel emulsion was not successful due to the injector failure caused by phase separation of the emulsion under high pressure of the common rail system in the modern diesel engine. Overall, the algae/diesel emulsion has the potential to become a novel fuel source for energy production. However, it still requires further study on the stability of the emulsion under a high-pressure environment.

Following the aspiration combustion test of algae suspension in Chapter 2, a life cycle analysis was established in Chapter 4 to evaluate the environmental impact of the process including dry algae powder production and the aspiration combustion in a diesel engine. Two scenarios involving the processes with varying biomass concentration and varying aspiration flowrate were examined and compared with the reference base case of biodiesel carried out by Passell et al. (2013). Both of the scenarios in the life cycle impact assessment show a proportional increase in GWP, NO_x and water consumption with the increase of biomass concentration and aspiration flowrates. The GWP reaches the highest level in the case of 20% biomass concentration, which produced extra 0.341 kg CO₂ equivalent comparing with the reference case. Meanwhile, it is interesting to see that all the cases show a substantial reduction of total NO_x and water consumption relative to the reference case. The contribution analysis suggests a more significant influence on the environment by changing the biomass concentration than changing the aspiration flowrate and the downstream process increases the proportion of total impact with the increase of biomass concentration.

Through the LCA of the novel approach (Chapter 2), it shows a better environmental control relative to small scale biodiesel production and combustion. It has potential to reach the same reduced level as the large scale conventional

biodiesel process without the additional drying process of algal biomass. Moreover, a future study on balance between the energy release from combustion and the environmental impact is required.

As a summary, the results presented from this project show the potential of directly using algal biomass for energy production without conventional biodiesel production. However, there are many issues such as the delivery system of algae suspension and stability of algae/diesel emulsion that need to be further studied in the future.

5.2 Future work

5.2.1 Short-term experiments

Due to the time constraints, further experiments need to be carried out in order to better understand the approach of utilising algal biomass without complete dewatering in a diesel engine, including the energy release and combustion emissions of algae/diesel emulsion and the LCA comparison between these two approaches.

First, for the aspiration of algal biomass, the particulate matters and hydrocarbons in the exhaust gas emissions should be measured in the future experiment. Meanwhile, it is necessary to redesign the air intake on the diesel engine. The current intake pipe and manifold on the engine have connected all cylinders and have many blind corners, which may accumulate the algae suspension in the engine manifold. In order to avoid this problem and reduce the biomass lost before combustion, a smooth pipe with a straight connection between one cylinder and the spray nozzle should be applied. Meanwhile, the spray system used in the study was simply modified from a spray gun, which did not provide the smallest liquid droplets of algae suspension during the experiment. Therefore, a better delivery system for the algal suspension is required.

Secondly, the production system for algal biomass could be further improved. The current cultivation equipment is a 5 L shake flask, which has limited volume for cell culture and lowed the oxygen transfer rate in the culture media at low shaking speed. As proved by the characterisation of algae growth condition in Section 3.3.1, the algae cells cultivated under heterotrophic condition with extra carbon source gave the highest biomass concentration. Thus, the bioreactor system can be used for rapid algal biomass production as it has a larger volume, better agitation and

control of the cultivation conditions. Moreover, the stability of the algae/diesel emulsion could be further investigated. There are many surfactants, such as Triton X-100, Span 80, Span 20, etc., that have been studied for creating W/O emulsion and the viscosity of the W/D and algae/diesel emulsion has potential to be reduced by using other surfactant packages. In order to utilise the algal/diesel emulsion in a modern direct injection diesel engine, a study on the stability of the emulsion under high-pressure environment should be performed.

Finally, since the LCA study is carried out based on the data of energy release and exhaust emissions from the combustion experiment, the comparison of aspiration combustion of algae suspension and combustion of algae/diesel emulsion can be examined. Meanwhile, the sensitivity analysis could be evaluated with different lipid content of algal biomass, which requires more data from the biomass production and characterisation. Furthermore, the measurements using ultimate and proximate analysis of algal biomass should be carried out to determine the biomass composition and properties. Hence, the feasibility of scaling up of these two approaches will be demonstrated from the perspective of total environmental impact and human health.

5.2.2 Long-term prospect

The research conducted in this study has confirmed the feasibility of using algal biomass directly in a diesel engine for energy generation and the reduction of the total environmental impact. In the future, stationary power generation nearby the algae cultivation would be a good approach to produce energy by directly using algal biomass in engine combustion. Alternatively, using algal biomass in the indirect combustion system for heating/power generation is also feasible and their advantages relative to the use in a diesel engine can be further investigated (Zhao

et al., 2016). As the algae cells can be grown in wastewater (Komolafe et al., 2014), the aspiration combustion of algal biomass can be applied to an industrial symbiosis and circular economy concept (Martin, 2013), which aims to use the waste of one industry as feedstock for another. In this case, growing microalgae for the wastewater treatment and then generate energy for another industrial facilities. Alternatively, algae/diesel emulsion can be used in industrial settings such as mining site, where the algae can be cultivated in waste treatment water and then harvested and prepared with diesel as stable emulsion for supplying a diesel blend for the industrial vehicles. In addition, the downstream process in the future will not include the drying process, which can simplify the pre-treatment of algal biomass and results in a reduction of total energy consumption and environmental impact. In view of integrated algal biorefineries, high value products from algal cells can be firstly extracted followed by the utilisation of residual biomass in engines, and this approach will help to improve the economic viability of algae cultivation and use (Bleakley et al., 2017).

With the continued exploration in this field, microalgae could become a truly competitive energy resource and make a significant contribution to cleaner energy production.

Reference

- Abdurahman, N. H., Rosli, Y. M., Azhari, N. H. & Abdul Adam, A. 2016. The Potential of a Water-in-Diesel Emulsion for Increased Engine Performance and as an Environmentally Friendly Fuel. *MATEC Web Conf.*, 70, 01003.
- Al-Lwayzy, S., Yusaf, T. & Al-Juboori, R. 2014a. Biofuels from the Fresh Water Microalgae *Chlorella vulgaris* (FWM-CV) for Diesel Engines. *Energies*, 7, 1829.
- Al-Lwayzy, S., Yusaf, T. F. & Al-Juboori, R. 2014b. Biofuels from the Fresh Water Microalgae *Chlorella vulgaris* (FWM-CV) for Diesel Engines. *Energies*, 7, 1829-18513390.
- Annamalai, K. & Puri, I. K. 2006. *Combustion science and engineering*, CRC press.
- Arai, M. Physics behind diesel sprays. Proc. of ICLASS, 12th Triennial International Conference on Liquid Atomization and Spray Systems, Heidelberg, Germany, Sept, 2012.
- Asif Faiz, C. S. W. a. M. P. W. 1996. *Air pollution from motor vehicles*, The World Bank.
- Aslan, S. & Kapdan, I. K. 2006. Batch kinetics of nitrogen and phosphorus removal from synthetic wastewater by algae. *Ecological engineering*, 28, 64-70.
- Azadi, P., Brownbridge, G., Mosbach, S., Inderwildi, O. & Kraft, M. 2015. Simulation and life cycle assessment of algae gasification process in dual fluidized bed gasifiers. *Green Chemistry*, 17, 1793-1801.
- Badrana, O., Emeishb, S., Abu-Zaidc, M., Abu-Rahmaa, T., Al-Hasana, M. & Al-Ragheba, M. 2011. Impact of emulsified water/diesel mixture on engine performance and environment. *Int. J. of Thermal & Environmental Engineering*, 3, 1-7.
- Banani, R., Youssef, S., Bezzarga, M. & Abderrabba, M. 2015. Waste frying oil with high levels of free fatty acids as one of the prominent sources of biodiesel production. *J. Mater. Environ. Sci*, 6, 1178-1185.
- Barros, A. I., Gonçalves, A. L., Simões, M. & Pires, J. C. M. 2015. Harvesting techniques applied to microalgae: A review. *Renewable and Sustainable Energy Reviews*, 41, 1489-1500.
- Béchet, Q., Laviale, M., Arsapin, N., Bonnefond, H. & Bernard, O. 2017. Modeling the impact of high temperatures on microalgal viability and photosynthetic activity. *Biotechnology for biofuels*, 10, 136.
- Belousov, E. V. 2006. *Creation and perfecting of solid propellant reciprocating engines of internal combustion*, XIIT.
- Bittle, J., Knight, B. & Jacobs, T. 2010. Investigation into the use of ignition delay as an indicator of low-temperature diesel combustion attainment. *Combustion Science and Technology*, 183, 138-153.

- Bleakley, S. & Hayes, M. 2017. Algal Proteins: Extraction, Application, and Challenges Concerning Production. *Foods (Basel, Switzerland)*, 6, 33.
- Bligh, E. G. & Dyer, W. J. 1959. A rapid method of total lipid extraction and purification. *Canadian journal of biochemistry and physiology*, 37, 911-917.
- Borowitzka, M. A. 1992. Algal biotechnology products and processes—matching science and economics. *Journal of applied phycology*, 4, 267-279.
- Bradley, T., Maga, D. & Antón, S. 2015. Unified approach to Life Cycle Assessment between three unique algae biofuel facilities. *Applied Energy*, 154, 1052-1061.
- Brennan, L. & Owende, P. 2010. Biofuels from microalgae—a review of technologies for production, processing, and extractions of biofuels and co-products. *Renewable and sustainable energy reviews*, 14, 557-577.
- Bukkarapu, K., Srinivas Rahul, T., Kundla, S. & Vishnu Vardhan, G. 2018. *Effects of blending on the properties of diesel and palm biodiesel*.
- Caton, J. & Rosegay, K. 1983. A review and comparison of reciprocating engine operation using solid fuels. *SAE transactions*, 1108-1124.
- Che, R., Ding, K., Huang, L., Zhao, P., Xu, J.-W., Li, T., Ma, H. & Yu, X. 2016. Enhancing biomass and oil accumulation of *Monoraphidium* sp. FXY-10 by combined fulvic acid and two-step cultivation. *Journal of the Taiwan Institute of Chemical Engineers*, 67, 161-165.
- Cheirsilp, B. & Torpee, S. 2012. Enhanced growth and lipid production of microalgae under mixotrophic culture condition: Effect of light intensity, glucose concentration and fed-batch cultivation. *Bioresource Technology*, 110, 510-516.
- Chen, C.-Y., Yeh, K.-L., Aisyah, R., Lee, D.-J. & Chang, J.-S. 2011. Cultivation, photobioreactor design and harvesting of microalgae for biodiesel production: A critical review. *Bioresource Technology*, 102, 71-81.
- Chen, Z., Wang, L., Qiu, S. & Ge, S. 2018. Determination of microalgal lipid content and fatty acid for biofuel production. *BioMed research international*, 2018.
- Chew, K. W., Chia, S. R., Show, P. L., Yap, Y. J., Ling, T. C. & Chang, J.-S. 2018. Effects of water culture medium, cultivation systems and growth modes for microalgae cultivation: A review. *Journal of the Taiwan Institute of Chemical Engineers*, 91, 332-344.
- Chi, Z., Zheng, Y., Jiang, A. & Chen, S. 2011. Lipid production by culturing oleaginous yeast and algae with food waste and municipal wastewater in an integrated process. *Applied Biochemistry and Biotechnology*, 165, 442-453.
- Chia, S. R., Ong, H. C., Chew, K. W., Show, P. L., Phang, S.-M., Ling, T. C., Nagarajan, D., Lee, D.-J. & Chang, J.-S. 2018. Sustainable approaches for algae utilisation in bioenergy production. *Renewable Energy*, 129, 838-852.

- Chisti, Y. 2007. Biodiesel from microalgae. *Biotechnology Advances*, 25, 294-306.
- Chojnacka, K. & Marquez-Rocha, F.-J. 2004. Kinetic and stoichiometric relationships of the energy and carbon metabolism in the culture of microalgae. *Biotechnology*, 3, 21-34.
- Concas, A., Lutz, G. A., Pisu, M. & Cao, G. 2012. Experimental analysis and novel modeling of semi-batch photobioreactors operated with *Chlorella vulgaris* and fed with 100% (v/v) CO₂. *Chemical Engineering Journal*, 213, 203-213.
- Dai, L., Li, W. & Hou, X. 1997. Effect of the molecular structure of mixed nonionic surfactants on the temperature of miniemulsion formation. *Colloids and Surfaces A: Physicochemical and Engineering Aspects*, 125, 27-32.
- Daliry, S., Hallajani, A., Mohammadi Roshandeh, J., Nouri, H. & Golzary, A. 2017. Investigation of optimal condition for *Chlorella vulgaris* microalgae growth. *Global Journal of Environmental Science and Management*, 3, 217-230.
- Dieselhub. 2019. *INDIRECT INJECTION VS DIRECT INJECTION* [Online]. Available: <http://www.dieselhub.com/tech/idi-vs-di.html> [Accessed 06 October 2019].
- Dijkstra 2015. ika-calorimeter.
- Dragone, G., Fernandes, B. D., Vicente, A. A. & Teixeira, J. A. 2010. Third generation biofuels from microalgae.
- Dryer, F. L. 1977. Water addition to practical combustion systems—Concepts and applications. *Symposium (International) on Combustion*, 16, 279-295.
- Duan, Y. & Shi, F. 2014. Bioreactor design for algal growth as a sustainable energy source. *Reactor and Process Design in Sustainable Energy Technology*. Elsevier.
- Eere. 2019. *A field of algae raceway ponds*. [Online]. U.S. Department of Energy's Office of Energy Efficiency and Renewable Energy Available: <https://www.energy.gov/eere/bioenergy/algal-production> [Accessed 31st August 2019].
- El-Din, M. N., El-Hamouly, S. H., Mohamed, H., Mishrif, M. R. & Ragab, A. M. 2013. Water-in-diesel fuel nanoemulsions: Preparation, stability and physical properties. *Egyptian Journal of Petroleum*, 22, 517-530.
- Entwistle, J. 2015. Algae-powered architecture. *INGENIA*.
- Fingas, M. & Fieldhouse, B. 2004. Formation of water-in-oil emulsions and application to oil spill modelling. *Journal of Hazardous Materials*, 107, 37-50.
- Finkbeiner, M., Inaba, A., Tan, R., Christiansen, K. & Klüppel, H.-J. 2006. The new international standards for life cycle assessment: ISO 14040 and ISO 14044. *The international journal of life cycle assessment*, 11, 80-85.
- Garg, S., Wang, L. & Schenk, P. M. 2015. Flotation separation of marine microalgae from

- aqueous medium. *Separation and Purification Technology*, 156, 636-641.
- Ghannam, M. T. & Selim, M. Y. E. 2009. Stability Behavior of Water-in-Diesel Fuel Emulsion. *Petroleum Science and Technology*, 27, 396-411.
- Goh, B. H. H., Ong, H. C., Cheah, M. Y., Chen, W.-H., Yu, K. L. & Mahlia, T. M. I. 2019. Sustainability of direct biodiesel synthesis from microalgae biomass: A critical review. *Renewable and Sustainable Energy Reviews*, 107, 59-74.
- Gorman, D. S. & Levine, R. P. 1965. Cytochrome f and plastocyanin: their sequence in the photosynthetic electron transport chain of *Chlamydomonas reinhardtii*. *Proceedings of the National Academy of Sciences of the United States of America*, 54, 1665-1669.
- Graboski, M. S. & McCormick, R. L. 1998. Combustion of fat and vegetable oil derived fuels in diesel engines. *Progress in Energy and Combustion Science*, 24, 125-164.
- Halim, R., Danquah, M. K. & Webley, P. A. 2012a. Extraction of oil from microalgae for biodiesel production: a review. *Biotechnology advances*, 30, 709-732.
- Halim, R., Gladman, B., Danquah, M. K. & Webley, P. A. 2011. Oil extraction from microalgae for biodiesel production. *Bioresource technology*, 102, 178-185.
- Halim, R., Harun, R., Danquah, M. K. & Webley, P. A. 2012b. Microalgal cell disruption for biofuel development. *Applied Energy*, 91, 116-121.
- Hasannuddin, A. K., Ahmad, M. I., Zahari, M., Mohd, S. S., Aiman, A. B., Aizam, S. A. & Wira, J. Y. 2014. Stability Studies of Water-in-Diesel Emulsion. *Applied Mechanics and Materials*, 663, 54-57.
- Hebbar, G. S. 2014. NOx from Diesel Engine Emission and Control Strategies-A Review. *International Journal of Mechanical Engineering and Robotics Research*, 3, 471.
- Hellier, P., Ladommatos, N., Allan, R., Payne, M. & Rogerson, J. 2012a. The impact of saturated and unsaturated fuel molecules on diesel combustion and exhaust emissions. *SAE International Journal of Fuels and Lubricants*, 5, 106-122.
- Hellier, P., Ladommatos, N., Allan, R. & Rogerson, J. 2012b. The Influence of Fatty Acid Ester Alcohol Moiety Molecular Structure on Diesel Combustion and Emissions. *Energy & Fuels*, 26 (3) pp. 1912-1927. (2012).
- Heywood, J. B. 1988. *Internal Combustion Engine Fundamentals*, McGraw-Hill.
- Huang, G., Chen, F., Wei, D., Zhang, X. & Chen, G. 2010. Biodiesel production by microalgal biotechnology. *Applied energy*, 87, 38-46.
- Ifc, I. F. C. 2017. *Converting Biomass to Energy: A Guide for Developers and Investors* [Online]. Available: <http://documents.worldbank.org/curated/en/451461502956339912/pdf/118738-WP-BioMass-report-06-2017-PUBLIC.pdf> [Accessed 04 August 2019].

- Imtenan, S., Varman, M., Masjuki, H. H., Kalam, M. A., Sajjad, H., Arbab, M. I. & Rizwanul Fattah, I. M. 2014. Impact of low temperature combustion attaining strategies on diesel engine emissions for diesel and biodiesels: A review. *Energy Conversion and Management*, 80, 329-356.
- Inagaki, K., Fuyuto, T., Nishikawa, K., Nakakita, K. & Sakata, I. 2006. Dual-fuel PCI combustion controlled by in-cylinder stratification of ignitability. SAE Technical Paper.
- Islam, M. A., Heimann, K. & Brown, R. J. 2017. Microalgae biodiesel: Current status and future needs for engine performance and emissions. *Renewable and Sustainable Energy Reviews*, 79, 1160-1170.
- Jez, S., Spinelli, D., Fierro, A., Dibenedetto, A., Aresta, M., Busi, E. & Basosi, R. 2017. Comparative life cycle assessment study on environmental impact of oil production from micro-algae and terrestrial oilseed crops. *Bioresource technology*, 239, 266-275.
- Juneja, A., Ceballos, R. & Murthy, G. 2013. Effects of environmental factors and nutrient availability on the biochemical composition of algae for biofuels production: a review. *Energies*, 6, 4607-4638.
- Kamimoto, T. & Kobayashi, H. 1991. Combustion processes in diesel engines. *Progress in Energy and Combustion Science*, 17, 163-189.
- Kamo, R., Kakwani, R. M., Valdmanis, E. & Woods, M. E. 1988. Thermal ignition combustion system. Google Patents.
- Kapadia, H., Brahmabhatt, H., Dabhi, Y. & Chourasia, S. 2019. Investigation of emulsion and effect on emission in CI engine by using diesel and bio-diesel fuel: A review. *Egyptian Journal of Petroleum*.
- Ketzer, F., Skarka, J. & Rösch, C. 2018. Critical Review of Microalgae LCA Studies for Bioenergy Production. *BioEnergy Research*, 11, 95-105.
- Khan, M. I., Shin, J. H. & Kim, J. D. 2018. The promising future of microalgae: current status, challenges, and optimization of a sustainable and renewable industry for biofuels, feed, and other products. *Microbial cell factories*, 17, 36.
- Kilian, O., Benemann, C. S. E., Niyogi, K. K. & Vick, B. 2011. High-efficiency homologous recombination in the oil-producing alga *Nannochloropsis* sp. *Proceedings of the National Academy of Sciences*, 108, 21265-21269.
- Kim, J., Yoo, G., Lee, H., Lim, J., Kim, K., Kim, C. W., Park, M. S. & Yang, J.-W. 2013. Methods of downstream processing for the production of biodiesel from microalgae. *Biotechnology advances*, 31, 862-876.
- Klinthong, W., Yang, Y.-H., Huang, C.-H. & Tan, C.-S. 2015. A review: microalgae and their applications in CO₂ capture and renewable energy. *Aerosol Air Qual Res*, 15,

- Komolafe, O., Orta, S. B. V., Monje-Ramirez, I., Noguez, I. Y., Harvey, A. P. & Ledesma, M. T. O. 2014. Biodiesel production from indigenous microalgae grown in wastewater. *Bioresource technology*, 154, 297-304.
- Krichnavaruk, S., Loataweesup, W., Powtongsook, S. & Pavasant, P. 2005. Optimal growth conditions and the cultivation of *Chaetoceros calcitrans* in airlift photobioreactor. *Chemical Engineering Journal*, 105, 91-98.
- Krzemińska, I., Pawlik-Skowrońska, B., Trzcińska, M. & Tys, J. 2014. Influence of photoperiods on the growth rate and biomass productivity of green microalgae. *Bioprocess and biosystems engineering*, 37, 735-741.
- Laamanen, C. A., Ross, G. M. & Scott, J. A. 2016. Flotation harvesting of microalgae. *Renewable and Sustainable Energy Reviews*, 58, 75-86.
- Lam, M. K. & Lee, K. T. 2012. Microalgae biofuels: A critical review of issues, problems and the way forward. *Biotechnology Advances*, 30, 673-690.
- Lam, M. K., Lee, K. T. & Mohamed, A. R. 2010. Homogeneous, heterogeneous and enzymatic catalysis for transesterification of high free fatty acid oil (waste cooking oil) to biodiesel: a review. *Biotechnology advances*, 28, 500-518.
- Lardon, L., Hélias, A., Sialve, B., Steyer, J.-P. & Bernard, O. 2009. Life-cycle assessment of biodiesel production from microalgae. ACS Publications.
- Lee, A. K., Lewis, D. M. & Ashman, P. J. 2012. Disruption of microalgal cells for the extraction of lipids for biofuels: processes and specific energy requirements. *Biomass and bioenergy*, 46, 89-101.
- Lemões, J. S., Sobrinho, R. C. A., Farias, S. P., De Moura, R. R., Primel, E. G., Abreu, P. C., Martins, A. F. & D'oca, M. G. M. 2016. Sustainable production of biodiesel from microalgae by direct transesterification. *Sustainable Chemistry and Pharmacy*, 3, 33-38.
- Li, Y., Ghasemi Naghdi, F., Garg, S., Adarme-Vega, T. C., Thurecht, K. J., Ghafor, W. A., Tannock, S. & Schenk, P. M. 2014. A comparative study: the impact of different lipid extraction methods on current microalgal lipid research. *Microbial cell factories*, 13, 14-14.
- Liang, K., Zhang, Q. & Cong, W. 2012. Enzyme-assisted aqueous extraction of lipid from microalgae. *Journal of agricultural and food chemistry*, 60, 11771-11776.
- Liau, B.-C., Shen, C.-T., Liang, F.-P., Hong, S.-E., Hsu, S.-L., Jong, T.-T. & Chang, C.-M. J. 2010. Supercritical fluids extraction and anti-solvent purification of carotenoids from microalgae and associated bioactivity. *The Journal of Supercritical Fluids*, 55, 169-175.
- Lim, D. K. & Schenk, P. M. 2017. Microalgae selection and improvement as oil crops:

- GM vs non-GM strain engineering. *AIMS Bioeng*, 4, 151-161.
- Liu, Y. 2006. Effects of Salinity on the Growth and Toxin Production of a Harmful Algal Species, *Microcystis aeruginosa*. *Microcystis Aeruginosa, SJWP*, 1.
- Martin, M. 2013. *Industrial symbiosis in the biofuel industry: Quantification of the environmental performance and identification of synergies*. Linköping University Electronic Press.
- Mata, T. M., Martins, A. A. & Caetano, N. S. 2010. Microalgae for biodiesel production and other applications: A review. *Renewable and Sustainable Energy Reviews*, 14, 217-232.
- Momenikouchaksaraei, M. 2013. *Fundamental Study of Single Biomass Particle Combustion*. Videnbasen for Aalborg UniversitetVBN, Aalborg UniversitetAalborg University, Det Teknisk-Naturvidenskabelige FakultetThe Faculty of Engineering and Science.
- Natarajan, R., Ang, W. M. R., Chen, X., Voigtmann, M. & Lau, R. 2014. Lipid releasing characteristics of microalgae species through continuous ultrasonication. *Bioresource technology*, 158, 7-11.
- Norazni, S. A., Yahya, W. J., Ithnin, A. M., Abd Kadir, H., Abd Razak, I. F., Bahar, N. D., Sugeng, D. A. & Ramlan, N. A. 2017. Stability behavior of non-surfactant water-in-diesel emulsion fuel using microscopic observation. *MATEC Web Conf.*, 90, 01059.
- O'connell, D., Savelski, M. & Slater, C. S. 2013. Life cycle assessment of dewatering routes for algae derived biodiesel processes. *Clean Technologies and Environmental Policy*, 15, 567-577.
- Oh, H.-M., Lee, S. J., Park, M.-H., Kim, H.-S., Kim, H.-C., Yoon, J.-H., Kwon, G.-S. & Yoon, B.-D. 2001. Harvesting of *Chlorella vulgaris* using a bioflocculant from *Paenibacillus* sp. AM49. *Biotechnology Letters*, 23, 1229-1234.
- Orfield, N. D., Levine, R. B., Keoleian, G. A., Miller, S. A. & Savage, P. E. 2015. Growing algae for biodiesel on direct sunlight or sugars: a comparative life cycle assessment. *ACS Sustainable Chemistry & Engineering*, 3, 386-395.
- Park, J.-Y., Oh, Y.-K., Lee, J.-S., Lee, K., Jeong, M.-J. & Choi, S.-A. 2014. Acid-catalyzed hot-water extraction of lipids from *Chlorella vulgaris*. *Bioresource technology*, 153, 408-412.
- Passell, H., Dhaliwal, H., Reno, M., Wu, B., Amotz, A. B., Ivry, E., Gay, M., Czartoski, T., Laurin, L. & Ayer, N. 2013. Algae biodiesel life cycle assessment using current commercial data. *Journal of environmental management*, 129, 103-111.
- PetrušEvski, B., Bolier, G., Van Breemen, A. N. & Alaerts, G. J. 1995. Tangential flow filtration: A method to concentrate freshwater algae. *Water Research*, 29, 1419-

1424.

- Piriou, B., Vaitilingom, G., Veyssi re, B., Cuq, B. & Rouau, X. 2013. Potential direct use of solid biomass in internal combustion engines. *Progress in Energy and Combustion Science*, 39, 169-188.
- Pr consultants 2019. SimaPro 8.5.2. The Netherlands: PR  Consultants.
- Raikova, S., Smith-Baedorf, H., Bransgrove, R., Barlow, O., Santomauro, F., Wagner, J. L., Allen, M. J., Bryan, C. G., Sapsford, D. & Chuck, C. J. 2016. Assessing hydrothermal liquefaction for the production of bio-oil and enhanced metal recovery from microalgae cultivated on acid mine drainage. *Fuel Processing Technology*, 142, 219-227.
- Ranjith Kumar, R., Hanumantha Rao, P. & Arumugam, M. 2015. Lipid extraction methods from microalgae: a comprehensive review. *Frontiers in Energy Research*, 2, 61.
- Rawat, I., Kumar, R. R., Mutanda, T. & Bux, F. 2011. Dual role of microalgae: phycoremediation of domestic wastewater and biomass production for sustainable biofuels production. *Applied energy*, 88, 3411-3424.
- Ren, T. 2014. Primary factors affecting growth of microalgae optimal light exposure duration and frequency.
- Re ito lu,  . A., Altini ik, K. & Keskin, A. 2015. The pollutant emissions from diesel-engine vehicles and exhaust aftertreatment systems. *Clean Technologies and Environmental Policy*, 17, 15-27.
- Reskilab 2019. Moss Bioreactor culture of *Physcomitrella patens*. University of Freiburg.
- Samec, N., Dibble, R. W., Chen, J. Y. & Pagon, A. 2000. Reduction of NOx and soot emission by water injection during combustion in a diesel engine. SAE Technical Paper.
- Sander, K. & Murthy, G. S. 2010. Life cycle analysis of algae biodiesel. *The International Journal of Life Cycle Assessment*, 15, 704-714.
- Sayre, R. 2010. Microalgae: The Potential for Carbon Capture. *BioScience*, 60, 722-727.
- Scientific, F. 2016. *Eppendorf™ 5424/5424R Microcentrifuges* [Online]. Available: <https://www.fishersci.com/shop/products/eppendorf-5424-5424r-microcentrifuges-14/p-3070405> [Accessed 07/08].
- Scragg, A. H., Morrison, J. & Shales, S. W. 2003. The use of a fuel containing *Chlorella vulgaris* in a diesel engine. *Enzyme and Microbial Technology*, 33, 884-889.
- Shah, J. H., Deokar, A., Patel, K., Panchal, K. & Mehta, A. V. A comprehensive overview on various method of harvesting microalgae according to Indian perspective. International Conference on Multidisciplinary Research & Practice. International Conference on Multidisciplinary Research & Practice, 2014. 313-17.

- Sheehan, J., Dunahay, T., Benemann, J. & Roessler, P. 1998. Look back at the US department of energy's aquatic species program: biodiesel from algae; close-out report. National Renewable Energy Lab., Golden, CO.(US).
- Shi, R., Handler, R. M. & Shonnard, D. R. 2019. Life cycle assessment of novel technologies for algae harvesting and oil extraction in the renewable diesel pathway. *Algal Research*, 37, 248-259.
- Shi, W., Zhu, L., Chen, Q., Lu, J., Pan, G., Hu, L. & Yi, Q. 2017. Synergy of flocculation and flotation for microalgae harvesting using aluminium electrolysis. *Bioresource Technology*, 233, 127-133.
- Shu, C.-H. & Tsai, C.-C. 2016. Enhancing oil accumulation of a mixed culture of *Chlorella* sp. and *Saccharomyces cerevisiae* using fish waste hydrolysate. *Journal of the Taiwan Institute of Chemical Engineers*, 67, 377-384.
- Singh, R. N. & Sharma, S. 2012. Development of suitable photobioreactor for algae production – A review. *Renewable and Sustainable Energy Reviews*, 16, 2347-2353.
- Singh, S. & Singh, P. 2015. Effect of temperature and light on the growth of algae species: a review. *Renewable and Sustainable Energy Reviews*, 50, 431-444.
- Soehngen, E. 1976. Development of Coal-Burning Diesel Engines in Germany.
- Soloiu, V., Lewis, J., Yoshihara, Y. & Nishiwaki, K. 2011. Combustion characteristics of a charcoal slurry in a direct injection diesel engine and the impact on the injection system performance. *Energy*, 36, 4353-4371.
- Spiden, E. M., Yap, B. H., Hill, D. R., Kentish, S. E., Scales, P. J. & Martin, G. J. 2013. Quantitative evaluation of the ease of rupture of industrially promising microalgae by high pressure homogenization. *Bioresource technology*, 140, 165-171.
- Standardization, I. O. F. 2006. *Environmental Management: Life Cycle Assessment; Principles and Framework*, ISO.
- Stone, R. 1999. Introduction to internal combustion engines.
- Suali, E. & Sarbatly, R. 2012. Conversion of microalgae to biofuel. *Renewable and Sustainable Energy Reviews*, 16, 4316-4342.
- Taher, H., Al-Zuhair, S., Al-Marzouqi, A. H., Haik, Y. & Farid, M. M. 2011. A review of enzymatic transesterification of microalgal oil-based biodiesel using supercritical technology. *Enzyme research*, 2011.
- Talibi, M. 2015. *Co-combustion of diesel and gaseous fuels with exhaust emissions analysis and in-cylinder gas sampling*. PhD Thesis, UCL (University College London).
- Tan, X. B., Lam, M. K., Uemura, Y., Lim, J. W., Wong, C. Y. & Lee, K. T. 2018.

- Cultivation of microalgae for biodiesel production: A review on upstream and downstream processing. *Chinese Journal of Chemical Engineering*, 26, 17-30.
- Tataiah, K. & Wood, C. D. 1980. Performance of Coal Slurry Fuel in a Diesel Engine. SAE International.
- Terentyev, A. 2019. *The diesel injection system* [Online]. Available: <https://en.ppt-online.org/183412> [Accessed 06 October 2019].
- Tesfa, B., Mishra, R., Gu, F. & Ball, A. D. 2012. Water injection effects on the performance and emission characteristics of a CI engine operating with biodiesel. *Renewable Energy*, 37, 333-344.
- Ting, H., Haifeng, L., Shanshan, M., Zhang, Y., Zhidan, L. & Na, D. 2017. Progress in microalgae cultivation photobioreactors and applications in wastewater treatment: A review. *International Journal of Agricultural and Biological Engineering*, 10, 1-29.
- Tracy Jr, E. 1957. Feasibility Study of the Use of Powdered Coal as a Fuel for Diesel Engines. SwRI Report.
- Tree, D. R. & Svensson, K. I. 2007. Soot processes in compression ignition engines. *Progress in Energy and Combustion Science*, 33, 272-309.
- Vandamme, D., Foubert, I. & Muylaert, K. 2013. Flocculation as a low-cost method for harvesting microalgae for bulk biomass production. *Trends in Biotechnology*, 31, 233-239.
- Venkata Subhash, G., Rangappa, M., Raninga, S., Prasad, V., Dasgupta, S. & Raja Krishna Kumar, G. 2019. Electromagnetic stratagem to control predator population in algal open pond cultivation. *Algal Research*, 37, 133-137.
- Wang, S.-K., Stiles, A. R., Guo, C. & Liu, C.-Z. 2015. Harvesting microalgae by magnetic separation: A review. *Algal Research*, 9, 178-185.
- Westbrook, C. K. 2000. Chemical kinetics of hydrocarbon ignition in practical combustion systems. *Proceedings of the Combustion Institute*, 28, 1563-1577.
- Wilson, R. 2007. Clean coal diesel demonstration project-final report. DOE/NETL-2007/1287.
- Xu, H., Miao, X. & Wu, Q. 2006. High quality biodiesel production from a microalga *Chlorella protothecoides* by heterotrophic growth in fermenters. *Journal of Biotechnology*, 126, 499-507.
- Xu, Y.-J., Li, G.-X. & Sun, Z.-Y. 2016a. Development of biodiesel industry in China: Upon the terms of production and consumption. *Renewable and Sustainable Energy Reviews*, 54, 318-330.
- Xu, Y., Hellier, P., Purton, S., Baganz, F. & Ladommatos, N. 2016b. Algal biomass and

- diesel emulsions: An alternative approach for utilizing the energy content of microalgal biomass in diesel engines. *Applied Energy*, 172, 80-95.
- Yahaya Khan, M., Abdul Karim, Z., Hagos, F. Y., Aziz, A. R. A. & Tan, I. M. 2014. Current trends in water-in-diesel emulsion as a fuel. *The Scientific World Journal*, 2014.
- Zhang, X., Yan, S., Tyagi, R. D., Drogui, P. & Surampalli, R. Y. 2016. Ultrasonication aided biodiesel production from one-step and two-step transesterification of sludge derived lipid. *Energy*, 94, 401-408.
- Zhao, B., Su, Y., Liu, D., Zhang, H., Liu, W. & Cui, G. 2016. SO₂/NO_x emissions and ash formation from algae biomass combustion: Process characteristics and mechanisms. *Energy*, 113, 821-830.
- Zhao, D.-Z., Wang, Y.-P. & Liu, J.-H. 2006. Preparation and Application of Diesel Microemulsion. *Petroleum Science and Technology*, 24, 1017-1025.
- Zhu, L. 2015. Microalgal culture strategies for biofuel production: a review. *Biofuels, Bioproducts and Biorefining*, 9, 801-814.
- Zhu, L., Nugroho, Y., Shakeel, S., Li, Z., Martinkauppi, B. & Hiltunen, E. 2017. Using microalgae to produce liquid transportation biodiesel: what is next? *Renewable and Sustainable Energy Reviews*, 78, 391-400.
- Zhu, S., Hu, B., Akehurst, S., Copeland, C., Lewis, A., Yuan, H., Kennedy, I., Bernards, J. & Branney, C. 2019. A review of water injection applied on the internal combustion engine. *Energy Conversion and Management*, 184, 139-158.
- Zuorro, A., Maffei, G. & Lavecchia, R. 2016. Optimization of enzyme-assisted lipid extraction from *Nannochloropsis* microalgae. *Journal of the Taiwan Institute of Chemical Engineers*, 67, 106-114.

Appendix A

A.1 Evaluation of algal growth

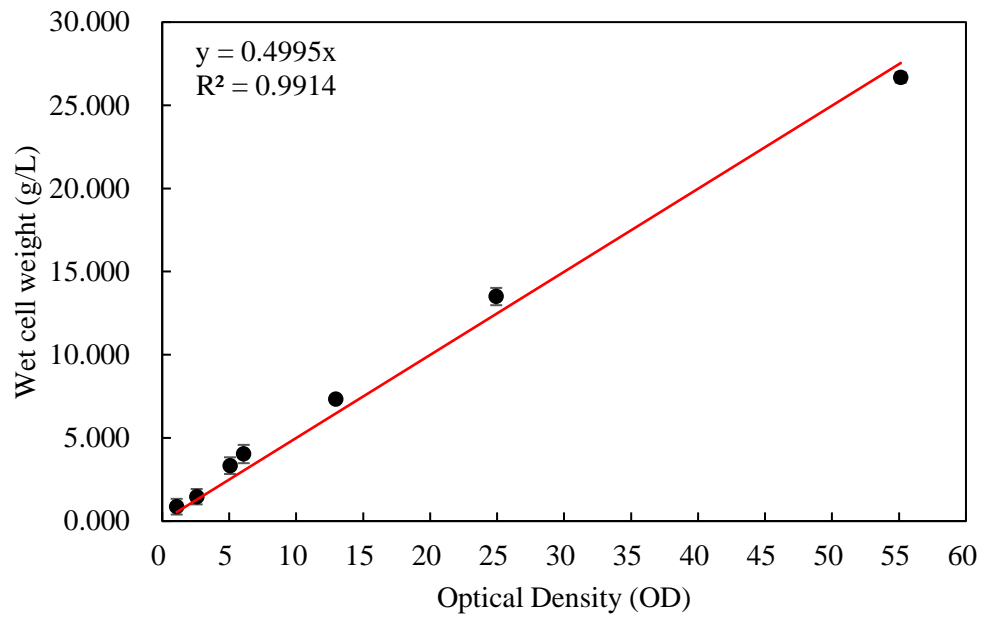


Figure A.1 The biomass concentration (g/L) in wet weight versus optical density (OD_{750nm}).

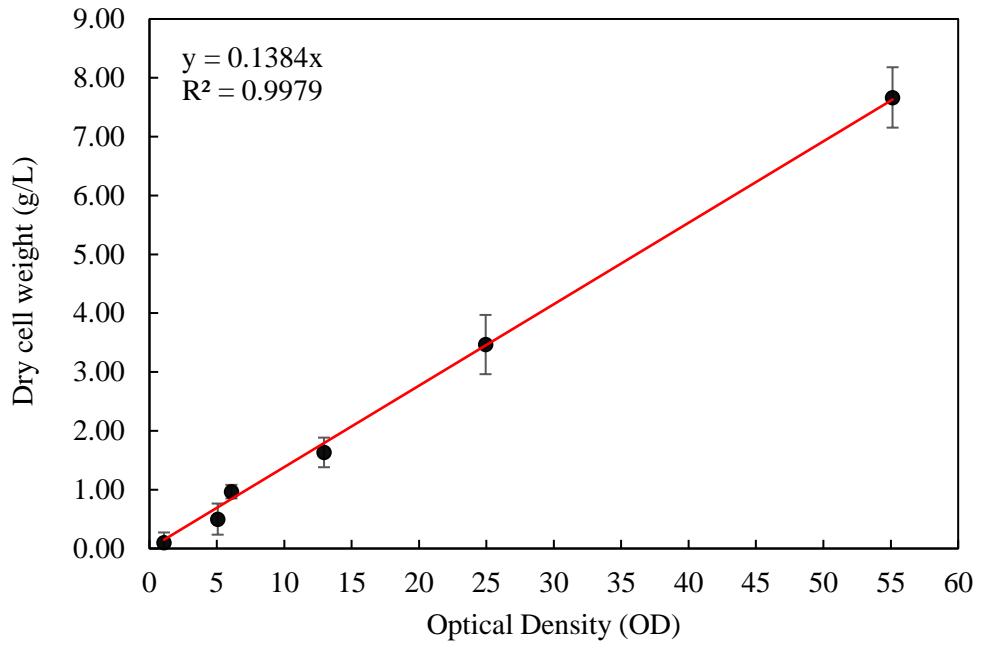


Figure A.2 The biomass concentration (g/L) in dry weight versus optical density (OD_{750nm}).

A.2 Determination of lipid production.

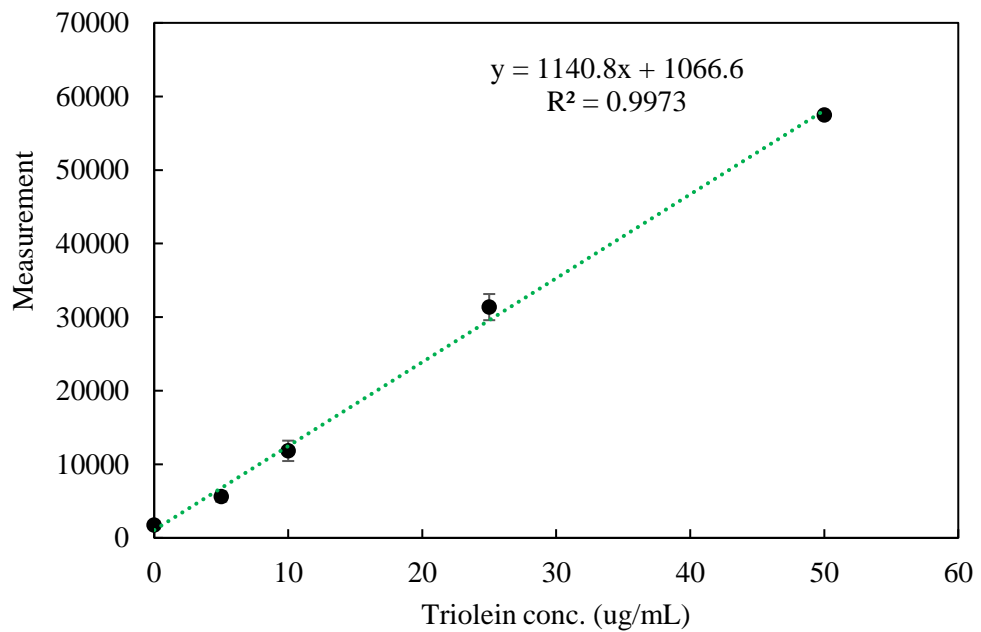


Figure A.3 The calibration curve of Nile Red test.

Appendix B

B.1 Assumptions for the LCA study

It was assumed that the air intake temperature was 40 °C and the temperature at measuring point of exhaust gases was 25 °C. The water content in the exhaust gas is assumed as vapour phase.

Table B.1 General assumptions.

Descriptions	Assumptions
Elemental composition of algal biomass	$C_1H_{1.63}O_{0.43}N_{0.15}$
Atomic C/H ratio of fossil diesel (no FAME)	1.783
Gas molar volume at 25 °C, $V_{m\ 25\ ^\circ C}$ (L/mol)	24.465
Gas molar volume at 40 °C, $V_{m\ 40\ ^\circ C}$ (L/mol)	25.696
Cylinder volume (m ³)	0.0005
Intake air volume (m ³ /min)	0.27
Operating numbers of cylinder	1

To calculate amount of substance in the exhaust gas calculation, the molar mass of each element is shown below.

Table B.2 Molar mass of elements.

Elements	Molar Mass (g/mol)
C	12
H	1
O	16
N	14
CO	28
CO ₂	44
NO _x *	31.1
H ₂ O	18
Air	29

* Assuming the NO_x contains 90% of NO and 10% of NO₂ (Hebbbar, 2014).

B.2 Calculations and data in combustion process

B.2.1 Calculations of injection flowrate of fossil diesel

The previously determined experimental correlation between injection duration and injection flowrate of fossil diesel can be described as:

$$\text{Injection flowrate} = -1.6 \times 10^{-5} \cdot t + 0.0448 \cdot t - 11.7672$$

Equation B.1

Where t is the injection duration under engine speed of 1200 rpm.

The injection duration of fossil diesel in the reference diesel only cases are recorded, and the injection flowrates are calculated and shown below.

Table B.3 Injection duration and injection flowrate of fossil diesel for the reference diesel only condition.

	Biomass concentrations with 40mL/min				Aspiration flowrates (mL/min) With biomass concentration 5%		
	5%	7.50%	10%	20%	40	49.2	56
Injection duration (μs)	762	767	777	762	762	771	766
Injection flowrate (mL/min)	13.08	13.18	13.38	13.08	13.08	13.26	13.16

B.2.2 Calculations of the power out from the combustion process

The correlation between the Indicated Power (IP) and the IMEP is described below.

$$\text{Indicated Power, } IP = p_{imep} V_s n N z \text{ J/min}$$

Equation B.2

Where p_{imep} is the indicated mean effective pressure ($IMEP \times 10^5 \text{ N/m}^2$);

V_s is the cylinder volume (0.0005 m^3 , 0.5 litre/cylinder);

N is the engine speed in rpm (1200 rpm);

n is the number of cylinders in the engine (1 cylinder);

$z = 1$ for 2-stroke engine;

$z = 0.5$ for 4-stroke engine (use 0.5 in this study).

The indicated mean effective pressure (IMEP) was recorded during the combustion and indicated power from each case are calculated and shown in Table B.4.

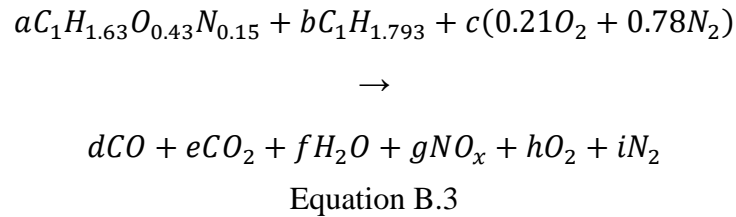
Table B.4 IMEP measured in the combustion process.

	Biomass concentrations				Aspiration flowrates (mL/min)		
	with 40mL/min				With biomass concentration 5%		
	5%	7.50%	10%	20%	40	49.2	56
IMEP (bar)	3.917	4.021	4.088	4.151	3.917	3.886	3.918
Indicated Power (kJ/min)	117.51	120.63	122.65	124.53	116.59	117.51	117.55

B.3 Adjustment of exhaust emissions data from combustion process

B.3.1 The combustion equation:

The combustion of algal biomass and diesel in air (assuming only contains O₂ and N₂) can be described by Equation B.3 below:



B.3.2 Balancing the atoms in the combustion equation

Based on the law of conservation of mass, the number of atoms in the reactant is equal to the number of atoms in the product after combustion reaction. Therefore, each type of atoms such as C, H, O and N atoms follows the law and then can be calculated individually. Every atomic balance is described by one mathematical equation as shown below:

The balance of carbon atoms

Consider the combustion reaction given by Equation B.3. The balance of carbon atoms is described by the following equation:

$$a + b = d + e$$

Equation B.4

The balance of hydrogen atoms

The balance of hydrogen atoms in Equation B.3 is described by:

$$1.63a + 1.793b = 2f$$

Equation B.5

The balance of oxygen atoms

the balance of oxygen atoms in Equation B.3 is described by:

$$0.43a + 0.21 \cdot 2c = d + 2e + f + g \cdot (0.9 + 0.1 \cdot 2) + 2h$$

Equation B.6

The balance of nitrogen atoms

The balance of nitrogen atoms in Equation B.3 is described by:

$$0.15a + 0.78 \cdot 2c = g + 2i$$

Equation B.7

B.3.3 Calculation of the molar fraction of atoms

a is the mole of carbon source input from algal biomass and b is the mole of carbon source input from fossil diesel. Due to the results of the combined material input from algae suspension and fossil diesel and the output of exhaust gases recorded during the combustion, the molar ratio of CO and CO₂ and CO and NO_x can be defined as α and β respectively. In addition, the flowrate of intake air is 0.27 m³/min, which is equal to 10.5075 mol/min. Therefore, based on the balance equations in section B.3.2, the molar number of each atom can be presented as:

$$c = 10.5075$$

Equation B.8

$$d = \frac{1 + \alpha}{a + b}$$

Equation B.9

$$e = \alpha \cdot d = \alpha \cdot \frac{1 + \alpha}{a + b}$$

Equation B.10

$$f = \frac{1.63a + 1.793b}{2} = 0.815a + 0.8965b$$

Equation B.11

$$g = \beta \cdot d = \beta \cdot \frac{1 + \alpha}{a + b}$$

Equation B.12

$$h = 2.421575 - \frac{(1 + 2\alpha + 1.1\beta)(1 + \alpha)}{2(a + b)} - 0.4075a - 0.44825b$$

Equation B.13

$$i = 0.075a - \beta \cdot \frac{1 + \alpha}{2(a + b)} + 8.19585$$

Equation B.14

Thus, the total mole of exhaust gas is:

$$mol_{exhaust} = mol_{water\ input} + d + 2e + f + 1.1g + 2h$$

Equation B.15

Where $mol_{water\ input}$ is the amount of water input from algae suspension in mole.

The adjusted exhaust gas emissions can be calculated by:

$$ppm_{adjusted} = 10^6 \times \frac{ppm_{original}}{1 + \frac{mol_{total\ water\ output}}{mol_{exhaust}}}$$

Equation B.16

Where $\text{ppm}_{\text{original}}$ is the original data collected from the exhaust analyser,
 $\text{mol}_{\text{total}}$ water output is the mole of total water content in the exhaust
emission and can be calculated by using the Equation B.17.

$$\text{mol}_{\text{total water output}} = \text{mol}_{\text{water input}} + f$$

Equation B.17

To calculate the mass balance the values in ppm need to be converted to g/m^3 .
Therefore, the equation of the conversion can be described as:

$$\text{mg}/\text{m}^3 = \text{ppm} \times \frac{M}{V_{m\ 25\ ^\circ\text{C}}}$$

Equation B.18

The original exhaust emission data is shown in Table B.5 and the adjusted exhaust
emission data is shown in Table B.6.

Table B.5 Original exhaust emission data on a dry basis.

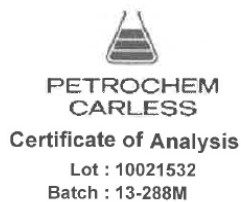
Condition	CO (ppm)	CO₂ (ppm)	NO_x (ppm)
Biomass concentration 5%	1073.814	61453.356	158.372
Biomass concentration 7.5%	858.071	62044.904	175.072
Biomass concentration 10%	1114.986	55806.370	149.428
Biomass concentration 20%	1173.699	63892.635	191.084
Flowrate 40mL/min	1073.814	61453.356	158.372
Flowrate 49.2mL/min	1284.761	62293.383	101.648
Flowrate 56mL/min	1640.083	73069.473	47.905

Table B.6 Adjusted exhaust emission data on a wet basis.

Conditions	CO		CO ₂		NO _x	
	ppm	g/m ³	ppm	g/m ³	ppm	g/m ³
Biomass concentration 5%	882.151	1.010	50484.650	90.796	130.105	0.165
Biomass concentration 7.5%	705.585	0.808	51019.001	91.757	143.960	0.183
Biomass concentration 10%	917.050	1.050	45899.437	82.550	122.901	0.156
Biomass concentration 20%	971.217	1.112	52870.106	95.086	158.119	0.201
Flowrate 40mL/min	882.151	1.010	50484.650	90.796	130.105	0.165
Flowrate 49.2mL/min	1021.500	1.169	49528.829	89.077	80.819	0.103
Flowrate 56mL/min	1283.915	1.469	57201.344	102.876	37.502	0.048

Appendix C

Petrochem Carless Ltd
 Head Office - Cedar Court
 Guildford Road, Fetcham
 Leatherhead
 Surrey, KT22 9RX
 Telephone 44 (0) 1372 360000
 Fax 44 (0) 1372 380400
 A member of H+C+S Group



Petrochem Carless BVBA
 Orteliuskaai 2-4/Bus 26
 2000 Antwerp
 Belgium
 Telephone + 323 2059370
 Fax + 323 2263126
 A member of H+C+S Group

Customer Name University College London
Customer No 357440
Consignee University College London
Delivery Address Mechanical Engineering Dept,
 4th Floor Roberts Building,
 Torrington Place, London WC1E
PCL Order Reference 436708
Customer Reference TBC
Customer Item Code
Customer Description

Product Name Carcal RF-06-03 (Marked)
Product Number 47244
Certificate No 20052368
Certificate Date 03/03/2014
Approval Date 11/12/2013
Approved By: Nicholas Hiett
Checked by Stuart Calver
Approval Status Released For Sale
Spec No 47244 v 11

Method	Description	Min	Max	Results	Unit
ASTM D4052	Density at 15°C	0.833	0.837	0.8347	g/mL
Appearance					
VISUAL	Marker			PASS	
Distillation					
ASTM D86	I.B.Pt.			202.5	°C
ASTM D86	10 % Recovered at			226.5	°C
ASTM D86	50 % Recovered at	245		268.0	°C
ASTM D86	90 % Recovered at			327.5	°C
ASTM D86	95 % Recovered at	345	350	346.5	°C
ASTM D86	F.B.Pt.		370	350.5	°C
Engine Tests					
ASTM D613	Cetane Number	52.0	54.0	52.8	Units
FIA					
ASTM D1319	Aromatics			19.1	% vol
ASTM D1319	Olefins			4.8	% vol
General Properties					
ASTM D93	Flash Point, Pensky Closed	55		84.5	°C
IP 391	Polycyclic Aromatic Hydrocarbons (PCA)	3.0	6.0	4.9	% mass
ASTM D974	Strong Acid Number		0.02	0	mg KOH/g
ASTM D2274	Oxidation Stability		2.5	0.1	mg/100mL
ASTM D130	Copper Corrosion, 3hrs at 100°C			1A	
ASTM D445	Viscosity at 40°C	2.3	3.3	2.715	mm ² /s
ASTM D5453	Sulphur		10	<1.0	mg/kg
ISO 12156-1	Lubricity at 60°C		400	391	µm
ASTM D4530	Carbon Residue (on 10% Dist. Res)		0.20	<0.1	% m/m
ASTM D482	Ash		0.01	<0.001	% mass
EN 116	Cold Filter Plug Pt.		-5	-16	°C
IP 438	Water Content		200	40	mg/kg
EN 14078	Fatty Acid Methyl Ester (FAME) Content			NONE	% v/v

Figure C.1 Certificate of analysis for the fossil diesel fuel used in the experiments presented in this thesis (page 1 of 2).

Petrochem Carless Ltd
 Head Office - Cedar Court
 Guildford Road, Fetcham
 Leatherhead
 Surrey, KT22 9RX
 Telephone 44 (0) 1372 360000
 Fax 44 (0) 1372 380400
 A member of H•C•S Group



**PETROCHEM
 CARLESS**
Certificate of Analysis
 Lot : 10021532
 Batch : 13-288M

Petrochem Carless BVBA
 Orteliuskaai 2-4/Bus 26
 2000 Antwerp
 Belgium
 Telephone + 323 2059370
 Fax + 323 2263126
 A member of H•C•S Group

Customer Name University College London
Customer No 357440
Consignee University College London
Delivery Address Mechanical Engineering Dept,
 4th Floor Roberts Building,
 Torrington Place, London WC1E
PCL Order Reference 436708
Customer Reference TBC
Customer Item Code
Customer Description

Product Name Carcal RF-06-03 (Marked)
Product Number 47244
Certificate No 20052368
Certificate Date 03/03/2014
Approval Date 11/12/2013
Approved By: Nicholas Hiett
Checked by Stuart Calver
Approval Status Released For Sale
Spec No 47244 v 11

Method	Description	Min	Max	Results	Unit
To Be Recorded					
ASTM D2500	Cloud Point			-11	°C
IP 12	Gross Heat of Combustion			45.94	MJ/kg
IP 12	Net Calorific Value			43.18	MJ/kg
IP 12 / CALCULATION	Net Calorific Value			18564	Btu/lb
ELEMENTAL ANALYSIS	Oxygen Content			<0.04	% m/m
ASTM D5291	Carbon Content			86.99	% m/m
ASTM D5291	Hydrogen Content			13.01	% m/m
CALCULATION	Atomic H/C Ratio			1.783	Ratio
CALCULATION	Atomic O/C Ratio			<0.0003	Ratio
CALCULATION	C/H Mass Ratio			6.69	Ratio
IP 391	Aromatics: Total			29.0	% m/m
ASTM D2709	Water & Sediment			0	% vol
CALCULATION	Carbon Weight Fraction			0.8699	Units

Additional Details

Figure C.2 Certificate of analysis for the fossil diesel fuel used in the experiments presented in this thesis (page 2 of 2).

APPENDICES

1. SME BIODIESEL SPECIFICATION SHEET



Certificate of Analysis

Fuel Blend No:	CAF-G16/810	Contact:	Christopher Ogbunuzor
Fuel Type:	SME	Order No:	Pro Forma
Customer:	UCL	Date:	13/07/2017

Test	Method	Unit	Limit		Result
			Min	Max	
Appearance	Visual		Report		C&B
Density @ 15°C	EN ISO 12185	kg/L	Report		0.8854
Cloud Point	EN ISO 23015	°C	Report		0
CFPP	EN 116	°C	Report		-2
Acid Value	EN 14104	mgKOH/g	-	0.50	0.12
Flash Point	EN ISO 2719	°C	93	-	151
Sulfur	EN ISO 20846	mg/kg	-	15.0	1.6
Viscosity at 40°C	EN ISO 3104	mm ² /s	1.900	6.000	4.101
Water Content	EN ISO 12937	mg/kg	-	500	200
Ester Content	EN 14103	% m/m	Report		97.1
Free Glycerol	EN 14105	% m/m	-	0.02	0.17
Total Glycerol	EN 14105	% m/m	-	0.24	0.00
Iodine value	EN 14111	g Iodine/100g	Report		130
Methanol	EN 14110	% m/m	-	0.20	0.04
Oxidation Stability	EN 15751	h	3.0	-	7.9
C12:0	EN ISO 5508	% m/m	Report		<0.1
C14:0	EN ISO 5508	% m/m	Report		0.1
C16:0	EN ISO 5508	% m/m	Report		10.3
C16:1	EN ISO 5508	% m/m	Report		0.1
C18:0	EN ISO 5508	% m/m	Report		4.0
C18:1	EN ISO 5508	% m/m	Report		23.7
C18:2	EN ISO 5508	% m/m	Report		53.4
C18:3	EN ISO 5508	% m/m	Report		6.1
C20:0	EN ISO 5508	% m/m	Report		0.4
C20:1	EN ISO 5508	% m/m	Report		0.2
C22:0	EN ISO 5508	% m/m	Report		0.4
C22:1	EN ISO 5508	% m/m	Report		<0.1

Figure C.3 Certificate of analysis for the FAME used in the experiments presented in this thesis (page 1 of 2).

Certificate of Analysis

Fuel Blend No: CAF-G16/810 **Contact:** Christopher Ogbunuzor
Fuel Type: SME **Order No:** Pro Forma
Customer: UCL **Date:** 13/07/2017

Test	Method	Unit	Limit		Result
			Min	Max	
Distillation (Evaporated)					
E250	EN ISO 3104	% v/v	Report		0.8
E350	EN ISO 3104	% v/v	Report		97.5
IBP	EN ISO 3104	°C	Report		171.0
10% Volume Evaporated	EN ISO 3104	°C	Report		332.8
20% Volume Evaporated	EN ISO 3104	°C	Report		333.2
30% Volume Evaporated	EN ISO 3104	°C	Report		333.7
40% Volume Evaporated	EN ISO 3104	°C	Report		334.1
50% Volume Evaporated	EN ISO 3104	°C	Report		334.8
60% Volume Evaporated	EN ISO 3104	°C	Report		335.7
70% Volume Evaporated	EN ISO 3104	°C	Report		336.9
80% Volume Evaporated	EN ISO 3104	°C	Report		339.0
90% Volume Evaporated	EN ISO 3104	°C	-	360.0	345.8
95% Volume Evaporated	EN ISO 3104	°C	Report		347.4
FBP	EN ISO 3104	°C	Report		347.4
Residue	EN ISO 3104	% v/v	Report		2.5

Sample Received Condition: Good (No Seal)
Date Sample Received: 29/12/2016

Notes:

Date: 13/07/2017
 Authorised by: A. Trusty
Junior Fuels Formulation Scientist

Coryton Advanced Fuels Ltd
 The Manorway
 Stanford-le-Hope
 Essex SS17 9LN, UK

Tel: +44 (0)1375 665707
 Fax: + 44 (0)1375 678904
 Email: admin@corytonfuels.co.uk
 Website: www.corytonfuels.co.uk

Figure C.4 Certificate of analysis for the FAME used in the experiments presented in this thesis (page 2 of 2).